Synaptic plasticity in the lateral habenula controls neuronal output : implications in physiology and drug addiction

Kristina Valentinova

16.09.2016

Université Pierre et Marie Curie

Ecole doctorale n°138

« Cerveau Cognition Comportement »

Doctoral thesis title:

Synaptic plasticity in the lateral habenula controls neuronal output: implications in physiology and drug addiction

Presented by Kristina Valentinova

Directed by Dr. Manuel Mameli

Team « Synapses and pathophysiology of reward »

Institut du Fer à Moulin

Members of the jury:

Dr. Philippe Faure – président

Pr. Jaideep Bains –rapporteur

Pr. Camilla Bellone – rapporteur

Pr. Mark Ungless – examinateur

Dr. Vivien Chevaleyre –examinateur

Dr. Manuel Mameli – directeur de thèse

Abstract

The capacity of the brain to anticipate and seek future rewards or alternatively escape aversive events allows individuals to adapt to their environment. A considerable research effort has focused on unraveling the cellular and synaptic mechanisms within the meso-cortico-limbic system underlying motivational processing both in physiological conditions and in pathologies such as addiction and depression. However, only recently we begin to understand the circuit substrates capable to control midbrain monoaminergic nuclei and their contribution to motivated behaviors.

The Lateral Habenula (LHb) has emerged in the last decade, as a major player encoding stimuli with motivational value and in controlling monoaminergic systems. The wiring of this epithalamic structure subserves discrete features of motivated behaviors, including preference and avoidance. Recent advances have also demonstrated that aberrant modifications in LHb function trigger negative emotional states in disorders including depression and addiction, highlighting the LHb as an important brain target for therapeutic intervention for these pathological states.

In my thesis work I first sought to investigate how modulation of synaptic transmission in the LHb controls neuronal activity, especially focusing on the role of metabotropic glutamate receptors. In a second study, I expanded my work examining how drug experience changes synaptic transmission in a precise habenular circuit that we discovered to be crucial for depressive states during cocaine withdrawal.

In an initial data set, we found that, in the LHb, metabotropic glutamate receptor 1 activation drives a PKC-dependent long term depression of excitatory (eLTD) and inhibitory (iLTD) synaptic transmission. Despite the common induction, eLTD and iLTD diverged in their expression mechanism. While eLTD required endocannabinoid-dependent reduction of glutamate release, iLTD expressed postsynaptically through a decrease of β2-containing $GABA_A$ receptors function. Further, eLTD and iLTD bidirectionally controlled LHb neuronal output.

In a second study, we showed that chronic cocaine exposure leads to a persistent and projection-specific increase of excitatory synaptic transmission onto LHb neurons. This form of synaptic potentiation required membrane insertion of GluA1-containing AMPA

receptors and a reduction in potassium channels function ultimately leading to increased LHb neuronal excitability both *in vitro* and *in vivo*. These cocaine-driven adaptations within the LHb were instrumental for depressive-like states emerging after drug withdrawal.

Altogether this work demonstrates how synaptic plasticity in the LHb affects neuronal output and thereby contributes to behaviors associated with the pathology of motivation.

Résumé

La survie des individus dépend de leur capacité d'anticiper la survenue d'une récompense ou d'un danger leur permettant ainsi de s'adapter à leur environnement. De considérables efforts ont été réalisés pour identifier les mécanismes cellulaires et synaptiques ayant lieu au niveau du circuit de la récompense afin d'avoir une meilleure compréhension des processus sous tendant des états motivationnels physiologiques et pathologiques tels que l'addiction et la dépression. Pour autant, ce n'est que récemment qu'on commence à comprendre les circuits capables de contrôler les systèmes monoaminergiques mésencéphaliques et leurs contributions aux comportements motivés.

Dans les dernières décennies l'habénula latérale (LHb) a émergé comme un acteur majeur capable d'encoder des stimuli de valeur motivationnelle et de contrôler les systèmes monoaminergiques. La connectivité de cette structure épithalamique joue un rôle clé dans différents aspects des comportements motivationnels, comme l'approche et la fuite. Des avancées récentes ont aussi démontré que des altérations de la fonction de la LHb entrainent des états émotionnels négatifs caractéristiques de la dépression et l'addiction. Ces observations suggèrent que la LHb pourrait s'avérer une cible importante pour le traitement de ces pathologies.

Au cours de mon travail de thèse, j'ai d'abord cherché à comprendre comment moduler la transmission synaptique au niveau de la LHb pouvait contrôler son activité. Pour répondre à cette question, je me suis focalisée sur le rôle des récepteurs métabotropiques au glutamate (mGluRs). Dans une seconde étude, j'ai examiné les mécanismes par lesquels les drogues d'abus modifient la transmission synaptique des neurones de la LHb. Ces modifications se produisent spécifiquement dans les neurones LHb se projetant vers le noyau tegmental rostral (RMT) et sont nécessaires pour l'émergence des états dépressifs.

Dans un premier temps, nous avons démontré qu'au niveau de la LHb les mGluRs de type I sont capables d'induire une dépression à long terme de la transmission synaptique excitatrice (eLTD) et inhibitrice (iLTD). Ces deux formes de plasticité dépendent de la signalisation PKC, mais requièrent des mécanismes d'expression

différents. Tandis que eLTD réduit la probabilité de libération du glutamate via l'activation de récepteurs présynaptiques aux endocannabinoides (CB1), iLTD s'exprime par la réduction de la fonction des récepteurs $GABA_A$ postsynaptiques contenant la sous-unité β2. De plus, eLTD and iLTD exercent un contrôle bidirectionnel sur la décharge des neurones de la LHb.

Dans un second temps, nous avons mis en évidence qu'une exposition chronique à la cocaïne produit une augmentation persistante de la transmission excitatrice au niveau des neurones de la LHb ciblant le RMTg. Cette forme de potentialisation synaptique nécessite l'insertion membranaire de récepteurs contenant la sous-unité GluA1, ainsi que la réduction de conductances potassiques entrainant une hyperexcitabilité neuronale *in vitro* et *in vivo* dans la LHb. Ces modifications sont nécessaires pour l'établissement d'états dépressifs émergeant lors de la période de sevrage à la cocaïne.

En conclusion, ce travail a contribué à la compréhension de mécanismes de plasticité synaptique ayant lieu au niveau de la LHb et leurs répercussions pour son activité contrôlant ainsi des comportements motivationnels.

Acknowledgements

I would like to thank in first place the amazing lovable people in the lab. Starting with my advisor and dear friend Manuel. I thank you for your time, attention and help during all these years, for the countless days and nights you spent to guide me through my experience as a young scientist, for the discussions and fights, for the sharing and advices. I thank you for the inspiration and love for science that you are building in me with your example every single day. I thank you for making my experience in the lab an amazing adventure, overcoming difficulties and frustration and learning how to enjoy the good moments, for making me laugh when I am desperate and for showing me that there is a way out even in the most difficult moments. Thank you for being always available for me and the others in the lab. Thank you for supporting my downs and helping me get over them. Thank you for creating a positive and motivated environment where trust, mutual respect and enthusiasm are the driving forces. Thank you for challenging me and believing in me. And I thank you for all the great fun we had in the lab and outside, for all the celebrations and…… although I can continue thanking you for many other things most importantly I want to thank you for proving me that when you have positive attitude, enthusiasm and persistence everything is possible!

I want to thank also Salvatore, Frank and Anna... you guys are not only colleagues and friends for me, but my bigger brothers and sister. I have not enough words to express how much I enjoyed having you around and how grateful I am for all the amazing time we spent together. I thank you so much for all the fun and enjoyable moments we shared, for all the laughing, for all the dinners, celebrations and birrettas, for all the foosball games, for the Italian and Dutch lessons, for the adventures in Sardinia, Sizel Montpellier and Copenhagen. I thank you also for being so understanding, caring and attentive, for listening and giving me your precious advices when I most need them. I thank you for being so creative and funny, for all the jokes you make, for being so positive and pleasant, I always enjoy your company. I thank you for sharing with me your knowledge and experience, for all the discussions we had, for your constructive feedback, for sharing your ideas, for being so much passionate and implicated in our work, you keep me motivated and make my days happier.

Finally, I want to thank all of you Manuel, Salvatore, Anna and Frank for keeping this unique family ambiance alive every day.

With all my love and respect a big THANK YOU!!!!!

I also want to thank many people from the IFM institute with who I shared countless nice moments: Tamar, Quentin, Martin, Sana, Marie, Ferran, Jessica, Emily, Enrica, Assunta, Nicolas, Benoit, Mariano, Alfredo, Sebastian for all the enjoyable moments we spent together, sharing work space, but also knowledge and ideas, for creating friendly and convivial ambiance in the institute and for all the parties and celebrations. I thank Jean-Christophe, Sabine, Nicolas and Corentin for helpful discussions and advices. I want to thank also Jean-Antoine and Fiona for making the effort to keep this institute a dynamic and friendly place.

I want to thank my friend Silvana, who has been side by side with me throughout all these years (8!!!) I spent in Paris. I want to thank you for sharing all these precious moments and being around when I most needed you. You are very very special friend.

Finally, I want to thank my family, mom, dad and sis, the people who are always around me even thousands of kilometers away, for their endless love, understanding and support throughout my life. I feel lucky and extremely grateful to have such a loving and caring family. I love you!

Contents

ABSTRACT **1**

RESUME **3**

ACKNOWLEDGEMENTS **5**

TABLE OF FIGURES **8**

LIST OF ABBREVIATIONS **9**

INTRODUCTION **13**

THE CIRCUITS OF MOTIVATION - IS IT ALL ABOUT DOPAMINE? **16**

NEUROBIOLOGICAL SUBSTRATES OF AVERSION **18**

THE LATERAL HABENULA: A CONTROL STATION OF AVERSION **20**

PHYLOGENY AND ANATOMY OF THE LHB 20
INPUTS TO THE LHB 22
OUTPUT CONNECTIVITY OF THE LHB 24
FUNCTION OF THE LHB IN REWARD AND AVERSION ENCODING 25
ROLE OF LHB OUTPUT FOR AVERSION PROCESSING 29
ROLE OF INPUTS TO THE LHB FOR AVERSION PROCESSING 32

DYSFUNCTION OF THE LHB: IMPLICATIONS IN DEPRESSION AND ADDICTION **37**

LHB IN DEPRESSION 37
LHB IN ADDICTION 38

PROPERTIES OF LATERAL HABENULA NEURONS **42**

CELL MORPHOLOGY AND ELECTROPHYSIOLOGY 42
FAST EXCITATORY TRANSMISSION VIA IONOTROPIC GLUTAMATE RECEPTORS 44
FAST INHIBITORY SYNAPTIC TRANSMISSION VIA IONOTROPIC $GABA_A$ RECEPTORS 47
MODULATION OF FAST EXCITATORY AND INHIBITORY TRANSMISSION: ROLE OF MGLURS 49

SYNAPTIC PLASTICITY IN THE LHB: A CELLULAR SUBSTRATE FOR MOTIVATED STATES IN DISEASE **52**

CELLULAR MECHANISMS IN THE LHB IN DEPRESSION 52
CELLULAR MECHANISMS IN THE LHB IN ADDICTION 53

CONTEXT AND OBJECTIVES FOR THE STUDIES **56**

I. MGLUR-LTD AT EXCITATORY AND INHIBITORY SYNAPSES CONTROLS LATERAL HABENULA OUTPUT 56
II. COCAINE-EVOKED NEGATIVE SYMPTOMS REQUIRE AMPA RECEPTOR TRAFFICKING IN THE LATERAL HABENULA 100

DISCUSSION **111**

WHICH INPUTS UNDERGO MGLUR-ELTD AND ILTD? 111
IS THERE ANY OUTPUT-SPECIFICITY FOR MGLUR-ELTD AND ILTD? 113
WHAT IS THE BEHAVIORAL RELEVANCE OF MGLUR-LTD IN THE LHB? 113
INDUCTION MECHANISMS AND CIRCUIT SPECIFICITY OF COCAINE-EVOKED PLASTICITY IN THE LHB 116
SYNAPTIC ADAPTATIONS AFTER COCAINE WITHDRAWAL 117

DISTINCT SYNAPTIC ADAPTATIONS CONVERGE TO INCREASE LHB NEURONAL AND BEHAVIORAL OUTPUT 119
CONCLUDING REMARKS 120

ADDITIONAL PUBLICATIONS AND CONTRIBUTIONS 123

REFERENCE LIST 125

Table of figures

Figure 1 Simplified schematic of the meso-cortico-limbic and associated circuits in the rodent brain 15
Figure 2 Cell-type specific modulation in the VTA for distinct motivational states 19
Figure 3 Anatomical localization of the habenular complex 20
Figure 4 Comparative analysis of human and rat LHb and LHb subnuclear organization 22
Figure 5 Afferents and their territorial distribution within the LHb 23
Figure 6 LHb efferents and territorial distribution of their cell bodies throughout the LHb 25
Figure 7 LHb function in aversion encoding and negative prediction error 28
Figure 8 Contribution of LHb output to motivated behaviors 31
Figure 9 Contribution of inputs to the LHb to different motivational states 36
Figure 10 Acute effects of psychostimulants in the LHb 41
Figure 11 AMPA receptors trafficking and channel properties 45
Figure 12 Excitatory and inhibitory synapses in the LHb 49
Figure 13 mGluR1/5 signaling and mechanisms of long term depression 51
Figure 14 GqPCR model of inhibitory LTD 112
Figure 15 Input and cell type-specific model for mGluR-LTD in the LHb 115
Figure 16 Effects of cocaine withdrawal in the LHb 118

List of abbreviations

5HT	5-hydroxytriptamine
AHP	afterhyperpolarization
AMPA	α-amino-3-hydroxy-5methyl-4-isoxazolepropionic acid
AP	action potential
BNST	bed nucleus of the stria terminalis
Ca^{2+}	calcium ion
CaMKII	calcium calmoduline-dependent protein kinase type II
cAMP	cyclic adenosine monophosphate
CB1	cannabinoid receptor type 1
ChR2	channel rhodopsin 2
CNS	central nervous system
D1R	dopamine type 1 receptor
D2R	dopamine type 2 receptor
DAT	dopamine transporter
DBB	diagonal band of Broca
DBS	deep brain stimulation
eLTD	long term depression of excitatory transmission
EPCS	excitatory postsynaptic current
EPN	entopeduncular nucleus
fMRI	functional magnetic resonance imaging
FST	forced swim test
GABA	γ-aminobutyric acid
$GABA_A$ R	γ-aminobutyric acid type A receptor

$GABA_B R$ γ-aminobutyric acid type B receptor

GAD67 glutamate decarboxylase

GIRK G-protein inwardly-rectifying potassium channel

GluA1-4 glutamate AMPA receptor subunits type 1-4

GluN1-3 glutamate NMDA receptor subunits type 1-3

GPCR G-protein coupled receptor

HCN hyperpolarization-activated cyclic nucleotide-gated channel

HFS high frequency stimulation

iLTD long term depression of inhibitory transmission

IPSC inhibitory postsynaptic current

K^+ potassium ion

LDT laterodorsal tegmentum

LFS low frequency stimulation

LH lateral hypothalamus

LHb lateral habenula

LHbLB basal nucleus of the lateral lateral habenula

LHbLMc magnocellular nucleus of the lateral lateral habenula

LHbLMg marginal nucleus of the lateral lateral habenula

LHbLO oval nucleus of the lateral lateral habenula

LHbLPc parvocellular nucleus of the lateral lateral habenula

LHbMA anterior nucleus of the medial lateral habenula

LHbMC central nucleus of the medial lateral habenula

LHbMMg marginal nucleus of the medial lateral habenula

LHbMPc parvocellular nucleus of the medial lateral habenula

LHbMS superior nucleus of the medial lateral habenula

LPO lateral preoptic area

LS lateral septum

LTD long term depression

LTP long term potentiation

mAChR muscarinic acetylcholine receptor

MCH melanin concentrating hormone

MDD major depression disorder

mEPSC miniature excitatory postsynaptic current

mGluR metabotropic glutamate receptor

MHb medial habenula

mIPSC miniature inhibitory postsynaptic current

mPFC medial prefrontal cortex

mTOR mechanistic target of rapamycin

Na^+ sodium ion

NAc nucleus accumbens

NMDA N-methyl-D-aspartic acid

NpHR halorhodopsin from *Natronomonas*

PFC prefrontal cortex

PICK1 protein interacting with C kinase type 1

PKA protein kinase A

PKC protein kinase C

PLC phospholipase type C

PP2A protein phosphatase type 2

PSP postsynaptic potential

RMTg rostromedial tegmental nucleus

SK small conductance calcium-activated potassium channel

SNc substantia nigra pars compacta

TH tyrosine hydroxylase

TST tail suspension test

TTX tetrodotoxin

Vgat vesicular GABA transporter

Vglut2 vesicular glutamate transporter type 2

Vmat2 vesicular monoamine transporter type 2

VP ventral pallidum

VTA ventral tegmental area

Introduction

The central nervous system (CNS) is designed to promote at best the survival of the species. Indeed the brain is able to encode the valence of environmental stimuli, which allow the individual to pursue rewards essential for survival or to avoid potential threats. Single neurons within complex brain circuits represent such environmental information through changes in their spiking activity. During my PhD training I developed a strong interest in understanding how neurons encode and process valenced information at different space and time scales – from the single cell to the integrated circuit and from the millisecond duration of an action potential to the long-lasting synaptic remodeling. My particular interest is to understand how reward and aversion-related experience modifies the synaptic properties of neurons and how experience-induced synaptic plasticity controls neuronal activity to drive motivational states crucial for survival.

In the course of evolution, highly organized circuits have emerged to promote survival through reward-seeking and threat-avoiding behaviors. The meso-cortico-limbic circuit has gained a central role in the processing of rewarding and aversive environmental information and in orchestrating adaptive behavioral responses. It also refers as a 'reward' circuit since a large body of evidence collected over the years has revealed its critical role in appetitive and reinforcing behaviors (Berridge and Robinson, 1998; Robbins and Everitt, 1996; Schultz, 2007a; Wise and Rompre, 1989). It comprises a meso-limbic part represented by the ventral tegmental area (VTA) dopamine neurons projections to the nucleus accumbens (NAc) of the ventral striatum and a meso-cortical part represented by the VTA projection to the prefrontal cortex (PFC). However this system is highly interconnected and is tightly controlled by a much wider network of brain structures, including the lateral hypothalamus (LH), the amygdala and the lateral habenula (LHb) among others (Fig 1), which altogether operate to encode valenced stimuli and to transform them into behavioral output (Ikemoto, 2007; Ikemoto et al., 2015; LeDoux, 2000; Matsumoto and Hikosaka, 2007; Nieh et al., 2013; Stuber and Wise, 2016; Wise, 2005).

A key feature of the meso-cortico-limbic circuit is the attribution of motivational value to otherwise neutral stimuli. Indeed, a stimulus can acquire positive or negative valence through innate or learned mechanisms. Stimuli assigned with a positive value (rewards) are generally beneficial for survival and elicit approach behaviors. On the contrary, life-threatening or harmful stimuli are ascribed with a negative value (aversion) and the corresponding behavioral reaction is to avoid or escape them. When animals are repetitively exposed to valenced stimuli in a particular environmental context (i.e. in presence of visual or auditory cues), cue-stimulus associations are formed allowing to predict the timing of occurrence and magnitude of the stimulus, a process necessary to orchestrate an appropriate behavioral response. Indeed, the ability to predict the outcome of a stimulus is at the base of conditioned behaviors, such as conditioned place preference and avoidance, paradigms widely used to assess motivational states (Hollerman and Schultz, 1998; Schultz, 1998; Schultz et al., 1997; Tzschentke, 2007). In physiological conditions behaviors leading to obtaining a reward or escaping a danger can be reinforced, positively, when an animal actively works to obtain a reward or negatively, when the animal works to stop an aversive stimulus (Valenstein & Valenstein 1964; Ferster 1957). These behaviors are compromised in pathologies associated with deficits in reward and aversion processing such as depression or addiction (Lüscher, 2016; Russo and Nestler, 2013).

Over the last decades a great deal of attention has focused on the synaptic and cellular substrates of reward encoding, learning and behaviors within the meso-cortico-limbic system. However, it remains less known how this system processes aversion and which particular structures provide it with aversion informative signals. The lateral habenula is now emerging as a key structure capable to provide aversive information to the meso-cortico-limbic system likewise contributing to avoidance behaviors.

In this thesis I will first briefly summarize key functional features of the reward system to provide a general context of positive and negative motivational processing. Next, I will introduce how the lateral habenula interacts with this system in the context of aversion. Finally I will show how modulation of synaptic transmission in the lateral habenula can

tune neuronal output potentially driving opposing motivational states and how drug-experience changes lateral habenula function to promote negative emotional states.

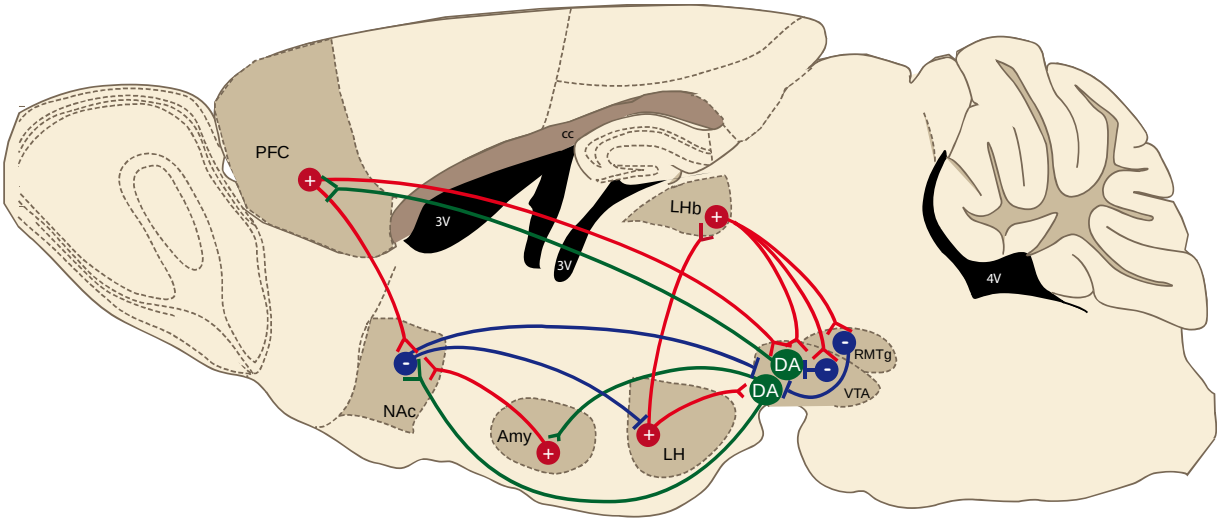

Figure 1 Simplified schematic of the meso-cortico-limbic and associated circuits in the rodent brain

The meso-cortico-limbic system comprises dopaminergic VTA-to-NAc and VTA-to-PFC projections, which release dopamine upon rewarding or aversive stimuli (Abercrombie et al., 1989; Hernandez and Hoebel, 1988; Kalivas and Duffy, 1995). The VTA also contains GABAergic interneurons which inhibit dopamine neurons. Apart from the input to the NAc and PFC, dopamine neurons also project to the amygdala (Amy), which in turn sends glutamatergic input to the NAc. VTA dopamine neurons receive GABAergic inhibitory inputs from local interneurons or from other structures including the rostromedial tegmental nucleus (RMTg) and the NAc. Excitatory glutamatergic afferents to the VTA arise from the LHb. LH and PFC. The VTA receives also both GABAergic and glutamatergic connections from the BNST (see Fig2).The LHb also projects to local GABA neurons in the VTA and RMTg, likewise exerting inhibitory control over dopamine neurons. The LH sends efferents to the LHb and VTA among others (not shown). The NAc receives glutamatergic innervation from the medial prefrontal cortex (mPFC) and amygdala (Amy) and projects to the LH and VTA. These various glutamatergic and GABAergic inputs to the VTA control aspects of reward and aversion-related behaviors (adapted from Russo and Nestler, 2013).

The circuits of motivation - is it all about dopamine?

In an attempt to understand the molecular bases of motivation, early studies in the 1970s and 1980s have proposed that the neuromodulator dopamine has a central role in controlling reward-related behaviors (Gerber et al., 1981; Ungerstedt, 1971; Wise et al., 1978). Dopamine is a monoamine produced mainly by neurons within the VTA and substantia nigra pars compacta (SNc) which innervate the cerebral cortex and limbic forebrain regions (Björklund and Dunnett, 2007). Initial studies using microdialysis measurements have suggested that dopamine release within the NAc (meso-limbic projection) is associated to self-stimulation reward (Fiorino et al., 1993), while stress specifically activates the meso-cortical projection (Thierry et al., 1976). Indeed, the function of dopamine in reward and aversive behaviors largely depend on the circuit connectivity of individual dopamine neurons (Bromberg-Martin et al., 2010; Lammel et al., 2011). Furthermore, depending on their specific identity, dopamine neurons undergo different experience-driven synaptic modifications which are instrumental for behavioral adaptations underlying opposing motivational states (Pignatelli and Bonci, 2015; Volman et al., 2013).

It is now largely established that dopaminergic neurons undergo phasic changes of activity in response to unexpected salient stimuli. Seminal studies in behaving monkeys using single-unit recordings have demonstrated that dopamine neurons firing increases in phasic and burst-like manner when an unexpected reward is presented (Schultz et al., 1997). Conversely, noxious foot pinch or foot shocks predominantly inhibit dopamine neurons burst activity (Ungless et al., 2004), although some neurons also show phasic excitation (Brischoux et al., 2009). After several conditioning sessions where animals are trained to associate a cue with the delivery of a reward, the firing of dopamine neurons and the subsequent release of dopamine in the NAc no longer occur at the time of reward delivery, but shift to the cue that predicts it (Schultz et al., 1997; Stuber et al., 2008). Moreover, the magnitude and direction of dopamine responses correlate with the predicted probability of the reward. Indeed, if an expected reward fails to occur or is smaller than expected, the activity of dopamine neurons is phasically inhibited, while if the reward is larger than expected dopamine neurons will fire at the time of reward

delivery (Fiorillo et al., 2003; Schultz, 1998; Schultz et al., 1997; Tobler et al., 2003). These experiments led to the idea that dopamine neurons signal a reward prediction error, defined as the difference between the outcome of an expected and actual reward (Schultz 1998; Keiflin & Janak 2015). Likewise, dopamine neurons serve as 'sensors' for any deviation from the expectancies, representing a teaching signal for future cue-reward associations and reward-seeking behaviors. The short bursts of dopamine neurons trigger phasic release events in the NAc, where motivational signals are considered to be translated into a motor output leading to reward seeking behaviors (Day et al., 2007; McClure et al., 2003; Mogenson et al., 1980).

More recently, a causal relationship between dopamine neurons activity and conditioned learning have been provided by temporally precise and pattern-specific optogenetic modulation of VTA dopamine neurons activity. Indeed, physiologically relevant phasic activation of dopamine neurons expressing the light-activated cation channel rhodopsin 2 (ChR2) induces conditioned place preference behaviors while their inhibition via the hyperpolarizing and light-activated chloride ion pump Halorhodopsin (NpHR) produces conditioned place avoidance (Tan et al., 2012; Tsai et al., 2009). Moreover, these learning mechanisms and reward-oriented behaviors involve transient synaptic potentiation of excitatory transmission onto dopamine neurons (Stuber et al., 2008). Similar synaptic plasticity occurs following single drug or stressful experience (Saal et al., 2003; Ungless et al., 2001). However, in the case of prolonged drug administration synaptic changes in VTA dopamine neurons and the NAc become persistent contributing to cue-induced reinstatement of drug-seeking behaviors after drug withdrawal (Chen et al., 2008; Mameli et al., 2009).

Taken together these data demonstrate an important role of dopamine neurons particularly in reward but also in aversion encoding and suggest that synaptic and circuit modifications within the meso-cortico-limbic system are instrumental for motivated behaviors. However, the dopamine system is far more complex in that it receives multiple inputs both from local GABAergic interneurons and from more distal structures, many of which also participate in motivational encoding (Fig1). Moreover, dopamine neurons present heterogeneity in terms of their physiological properties, input-output

connectivity and their responses to valenced stimuli (Lammel et al., 2014, 2011; Volman et al., 2013). These aspects need to be taken into account when considering dopamine neurons function in reward or aversion.

Although motivational states can be driven by rewarding and aversive conditions, during my thesis I focused mainly on the cellular substrates devoted to aversion processing.

Neurobiological substrates of aversion

Aversion is a common term to designate the behavioral reaction of avoidance or escape in response to negative, unpleasant, painful, stressful or fearful events or stimuli. Acute and chronic exposure to such aversive stimuli produces short or long-lasting synaptic, structural and circuit modifications that can often lead to neuropsychiatric disorders including depression, anxiety, post-traumatic stress disorder and addiction (Lüscher and Malenka, 2011; Nestler and Carlezon, 2006; Russo and Nestler, 2013). Many studies have implicated the VTA dopamine system in such modifications (Berton et al., 2006; Cao et al., 2010; Chaudhury et al., 2013; Krishnan et al., 2007; Lammel et al., 2011). However, it is now known that other structures directly or indirectly innervating the VTA, and often reciprocally connected, also contribute to different aspects of aversion (Fig1). The picture is even more complex given the large heterogeneity of different cell types forming local microcircuits within the VTA and challenging our understanding of the contribution of distinct pathways to aversion encoding and avoidance behaviors. With the advances of new technologies such as the generation of specific mouse lines, viral-based circuit- and cell type-specific mapping as well as optogenetics it is now possible to interrogate the implication of distinct neuronal circuits and neuronal subtypes for different aspects of aversion.

As a matter of example, specific cell type projections from the ventral bed nucleus of the stria terminalis (BNST) to GABAergic interneurons in the medial VTA have been involved in distinct motivational states. Indeed, glutamatergic BNST neurons, activating predominantly GABA neurons in the VTA, are excited by aversive conditions such as series of foot shocks or foot shock-associated cues. Moreover, ChR2-driven optogenetic

activation of this pathway produces real time avoidance and elevated anxiety states(Fig2A) (Jennings et al., 2013). This is consistent with evidence that activation of GABAergic VTA neurons inhibits dopamine neurons activity leading to conditioned place avoidance behaviors (Tan et al., 2012). In contrast, GABA neurons of the BNST predominantly inhibit GABA neurons of the VTA and are preferentially silenced by foot shock exposure and foot shock-cues. Optogenetic activation of this pathway leads to real time preference and reward seeking behaviors (Fig2A) (Jennings et al., 2013). Consistently, VTA GABA neurons inhibition drives preference, reinforces behavior and reduces anxiety states associated with previous aversive experience (Jennings et al., 2013). Similarly to this, activation of dopamine neurons of the VTA also promotes reward-related behaviors (Adamantidis et al., 2011; Tsai et al., 2009), suggesting that GABA neurons in the VTA may serve to break locally the activity of dopamine neurons and therefore control the expression of motivational states (Fig2B). These data raise the question whether other inputs onto dopamine neurons or onto GABA neurons of the midbrain can control different aspects of aversive behaviors. Indeed, a major challenge in the field is to identify the precise input-output and functional organization of the circuits of aversion.

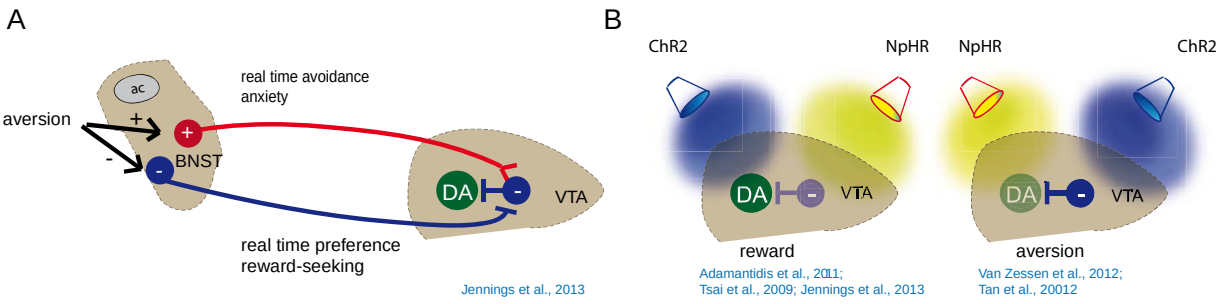

Figure 2 Cell-type specific modulation in the VTA for distinct motivational states

(A). BNST glutamate neurons activated by aversive stimuli or cues project to VTA GABA neurons. Their activation drives real time avoidance behavior and anxiety. BNST GABA neurons inhibited by aversive stimuli or cues also project to GABA neurons in the VTA. Their activation drives real time preference and reward-seeking (Jennings et al., 2013). (B). Direct optogenetic activation of VTA dopamine neurons (Tsai et al., 2009; Adamantidis et al., 2011) or inhibition of GABA neurons (Jennings et al., 2013) promote reward, while activation of GABA neurons (Tan et al., 2012; van Zessen et al., 2012) and inhibition of dopamine neurons (Tan et al., 2012) is aversive.

The lateral habenula: a control station of aversion

The lateral habenula (LHb) has gained considerable attention in the last decade because of its control on midbrain monoaminergic systems as well as for its crucial implication in aversion encoding and mood disorders (Hikosaka, 2010). My PhD work has focused on unraveling some of the circuit and synaptic functions of the LHb in the context of aversion and drug experience.

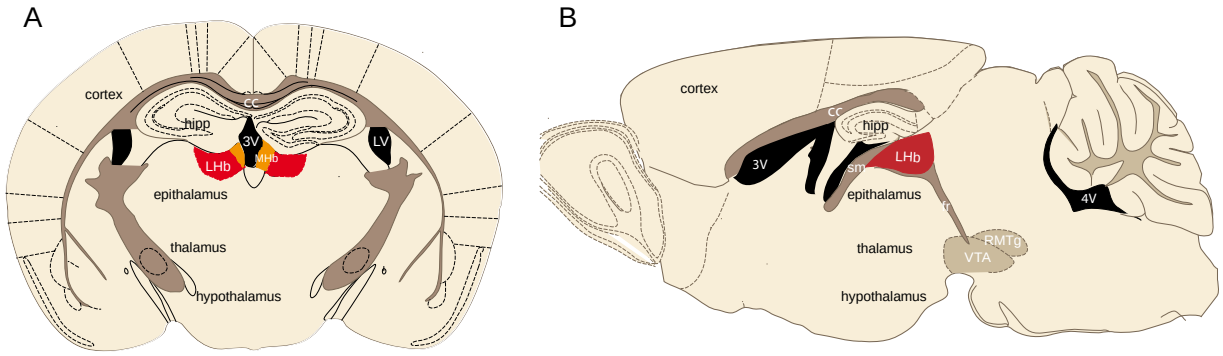

Figure 3 Anatomical localization of the habenular complex

The habenular complex is part of the epithalamus and is located at its medio-dorsal end close to the third ventricle (3V) and beneath the hippocampus (hipp). It comprises a lateral (LHb shown in red) and a medial portion (MHb shown in orange). (A).Coronal section representing the LHb. (B). Sagittal section representing the LHb, the *stria medullaris* (sm) containing LHb afferents and the *fasciculus retroflexus* (fr) containing LHb efferent axons projecting to midbrain targets, including the VTA and RMTg (cc corpus callosum; 4V 4th ventricle).

Phylogeny and anatomy of the LHb

The LHb is part of the habenular complex, which is located at the posterior-dorsal end of the epithalamus close to the midline and at the border of the third ventricle (Fig3). It comprises a lateral (LHb) and medial division (MHb) which are anatomically, morphologically and functionally distinct (Aizawa et al., 2011; Andres et al., 1999; Bianco and Wilson, 2009; Kim and Chang, 2005; Sutherland, 1982). The habenula is phylogenetically conserved among vertebrates (Aizawa et al., 2011; Bianco and Wilson,

2009). In birds, reptiles and mammals the MHb and the LHb are homologous to the dorsal and ventral habenulae respectively in fish and amphibians (Aizawa et al., 2011; Amo et al., 2010). The LHb and MHb relative proportion can vary across species. In mammals the size of the LHb is typically larger than the size of the MHb. Furthermore, a comparative analysis indicates that the proportional contribution of the LHb to the total surface of the habenular complex is considerably larger in humans compared to rats (Fig4A), supporting an increasing level of anatomical and functional specialization of the LHb throughout evolution (Díaz et al., 2011). The LHb can be divided into lateral and medial portions that receive inputs in a segregated manner (Fig5B). Each of these main divisions of the LHb can be further subdivided into smaller subnuclei based on distinct and topographic cell morphology and cytoarchitecture. Indeed, a total of ten subnuclei, five within the medial and five within the lateral LHb, have been described in rats based on morphological criteria and differential immunoreactivity for cellular markers (Andres et al., 1999; Geisler et al., 2003). The medial LHb comprises an anteriour subnucleus (LHbMA), located at the most rostral portion of the LHb, a superior (LHbMS), parvocellular (LHbMPc), central (LHbMC) and marginal subnuclei (LHbMMg). The lateral LHb contains a parvocellular (LHbLPc), magnocellular (LHbLMc), oval (LHbLO), marginal (LHbLMg) and basal subnuclei (LHbLB) (Fig4B). This subnuclear organization of the LHb seems to be well preserved in rodents since it is also present in the mouse (Wagner et al., 2014). In the human LHb five subnuclei have also been described although some discrepancies exist at the level of their relative position, size, morphology and cell organization compared to rodents (Díaz et al., 2011). Despite this detailed subnuclear organization and evidence indicating certain level of input-output-specific connectivity within some of the nuclei (Fig5B and Fig6B), LHb neurons seem to be relatively homogeneous in their basic cell properties (Weiss and Veh, 2011). A genetic profiling of LHb neurons would be required in order to identify potential discrimination criteria for different LHb subnuclei and would provide a tool to assess cell type-specific functions of LHb subpopulations in distinct aspects of motivated behaviors (Lecca et al., 2014; Proulx et al., 2014).

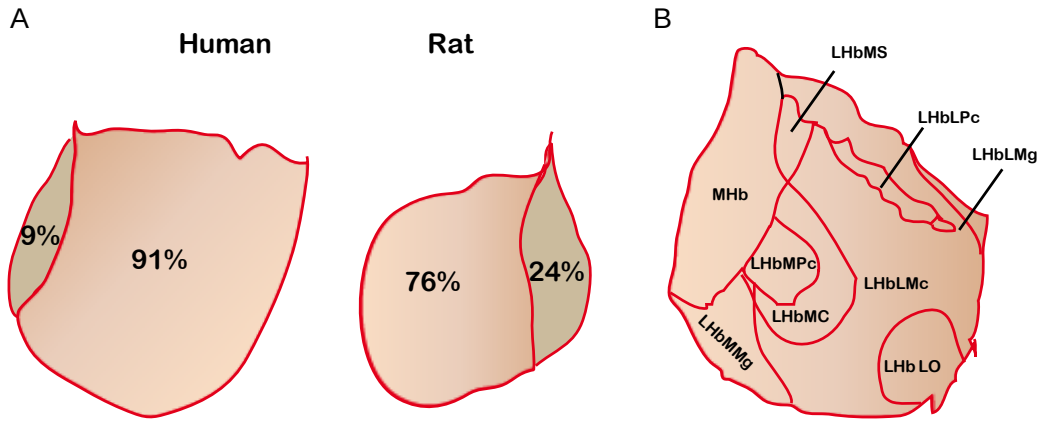

Figure 4 Comparative analysis of human and rat LHb and LHb subnuclear organization

(A). The habenular complex surface is increased in humans compared to rats as well as the relative contribution of the LHb to the total habenular size. In humans the LHb represents ~91% of the total habenular surface vs 9% MHb, while in the rat the LHb to MHb ratio is ~ 76% vs 24% respectively (adapted from Díaz et al., 2011). (B). Subnuclear organization of the LHb. The medial LHb comprises the anterior (LHbMA, not shown), superior (LHbMS), parvocellular (LHbMPc), central (LHbMC) and marginal (LHbMMg) subnuclei. The lateral LHb comprises the parvocellular (LHbLPc), magnocellular (LHbMc), oval (LHbLO), marginal (LHbLMg) and basal (LHbLB, not shown) subnuclei. This distinction has been made based on different cell organization and distinct expression patterns of cellular markers such as the $GABA_B$ receptor, the Kir3.2 potassium channel and neurofilament. (adapted from Geisler et al., 2003).

Inputs to the LHb

The habenular complex is positioned at the highway of a major information stream in the brain, connecting the limbic forebrain and basal ganglia regions with midbrain neuromodulatory systems. It receives most of its inputs through a fiber bundle called the *stria medullaris* and sends its projections to monoaminergic centers through the *fasciculus retroflexus* (Fig3B), which altogether form the diencephalic conduction system (Sutherland, 1982). Although the MHb and LHb receive their inputs and send their outputs using the same fiber tracts, they are differently innervated and target different brain nuclei. A potential connectivity between the MHb and LHb has been debated, but has never been anatomically or functionally proven.

The MHb receives inputs from septal and diagonal band of Broca (DBB) areas and sends in turn its axons to the interpeduncular nucleus of the midbrain (Herkenham and Nauta, 1979, 1977). In contrast, the LHb receives projections from the output structure

of the basal ganglia - the entopeduncular nucleus (EPN; homologue of the globus pallidus interna in primates and humans) and from limbic forebrain regions including the lateral hypothalamus (LH), lateral preoptic area (LPO), ventral pallidum (VP), BNST, DBB, lateral septum (LS) as well as feedback projections from the laterodorsal tegmentum (LDT), the VTA and the dorsal and median raphe nuclei (DRN and MRN) (Fig5A) (Herkenham & Nauta 1977; Nagy et al. 1978; Parent et al. 1981; Kowski et al. 2008; Li et al. 2011; Tripathi et al. 2013; Lammel et al. 2012; Swanson 1982; Aghajanian & Wang 1977). A projection from the PFC has also been described (Kim and Lee, 2012; Li et al., 2011; Warden et al., 2012). Some of the inputs to the LHb represent a topographical organization potentially important for LHb functions (Fig5B).

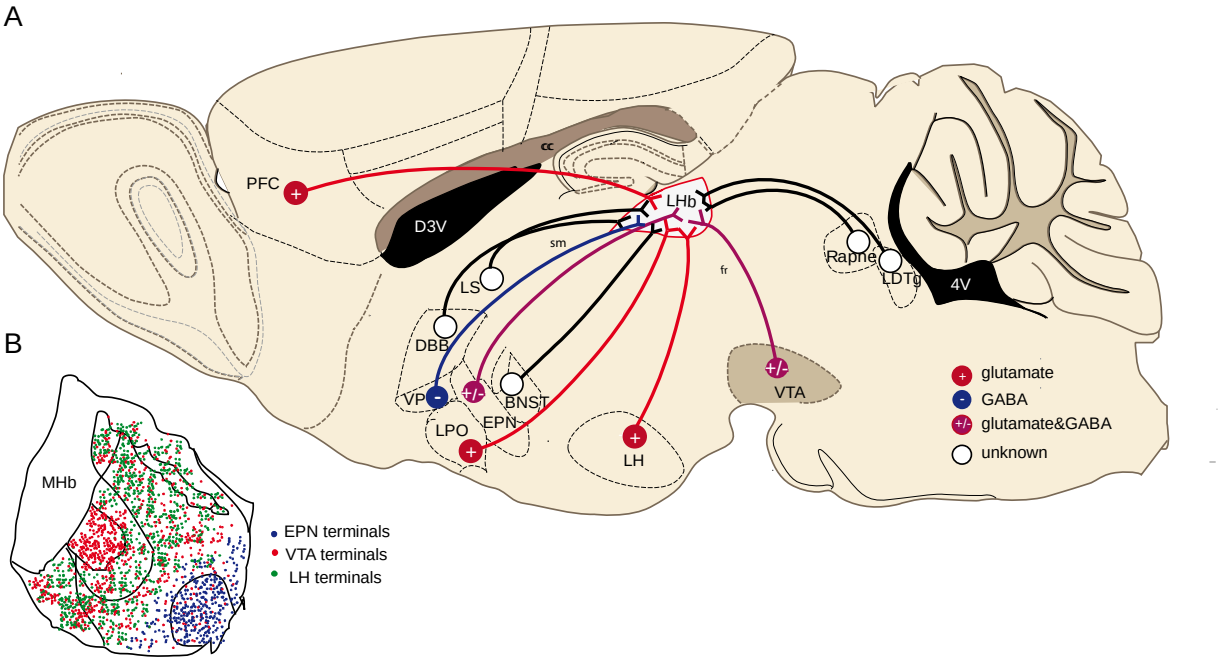

Figure 5 Afferents and their territorial distribution within the LHb

(A).The LHb receives glutamatergic (PFC, LPO, LH), GABAergic (VP) and mixed inputs (EPN, VTA and potentially LH). Other inputs and their neurotransmitters are not yet established (DBB, LS, BNST, LDT and raphe). (B). EPN terminals target the lateral LHb (LHbLO), while this subregion is devoid of LH and LPO inputs (Kowski et al., 2008; Poller et al., 2013; Shabel et al., 2012). LH axons are more concentrated in the medial aspect of the LHb (with the exception of the LHbMPc) (Poller et al., 2013). Other input terminals, such as the VTA ones are widely distributed throughout the LHb (Hnasko et al., 2012; Root et al., 2014b). sm: stria medullaris; fr: fasiculust retroflexus, cc: corpus callosum; D3V: dorsal 3th ventricle and 4V: 4th ventricle

Output connectivity of the LHb

LHb neurons are almost exclusively glutamatergic and long-range projecting (Kim and Chang, 2005; Li et al., 2011; Weiss and Veh, 2011). Although some studies have suggested the existence of local GABAergic neurons in the medial LHb, functional evidence about a potential LHb microcircuit is still lacking (Li et al., 2011; Zhang et al., 2016). Anatomical and physiological studies indicate that LHb neurons send their axons mainly to GABAergic neurons in the midbrain. Indeed, tracing experiments show that neurons located mainly within the lateral LHb project to the GABAergic rostro-medial tegmental nucleus (RMTg; (Balcita-Pedicino et al., 2011; Gonçalves et al., 2012; Jhou et al., 2009b; Meye et al., 2016; Sego et al., 2014), also called tail VTA (Kaufling et al., 2009; Perrotti et al., 2005). In contrast, LHb neurons originating from the medial aspect send their axons preferentially to monoaminergic nuclei (Gonçalves et al., 2012; Sego et al., 2014), where they form functional synapses with local GABAergic neurons (Lammel et al., 2012; Weissbourd et al., 2014) as well as with dopamine neurons of the VTA (Balcita-Pedicino et al., 2011; Lammel et al., 2012) or serotonin neurons in the caudal dorsal raphe (Dorocic et al., 2014; Sego et al., 2014) (Fig 6B). Further, it has been shown that individual neurons project either to VTA or to raphe nuclei without collateralizing, suggesting that single LHb neurons have distinct output targets (Bernard and Veh, 2012; Gonçalves et al., 2012; Li et al., 2011; Maroteaux and Mameli, 2012). In addition, the LHb has been recently shown to send axons to GABA neurons within the LDT and to orexin- and melanin concentrating hormone (MCH)-expressing neurons in the LH (González et al., 2016; Lammel et al., 2012; Yang et al., 2016). While the former has also been functionally proven, it remains to be confirmed whether LHb neurons establish functional synaptic connections in the LH (Fig6A).

Given that LHb neurons are of glutamatergic phenotype and that they project to a vast majority of GABA neurons in the midbrain it is plausible that they may disynaptically inhibit dopamine or serotonin neurons potentially providing aversive signals to the midbrain.

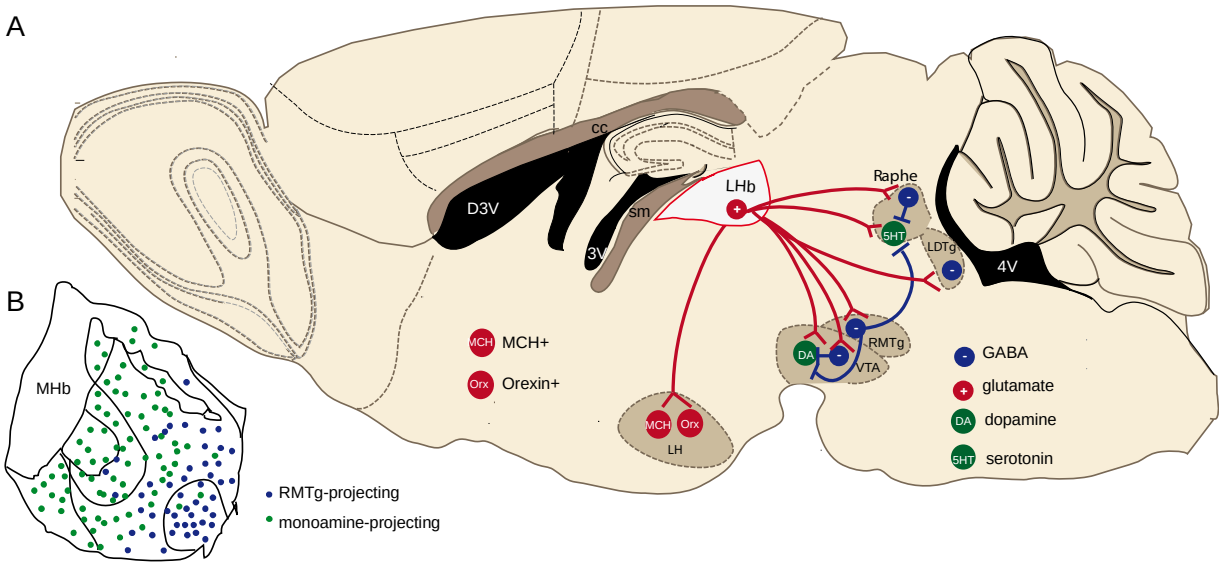

Figure 6 LHb efferents and territorial distribution of their cell bodies throughout the LHb

(A).The LHb sends glutamatergic projections mainly to GABA neurons of the midbrain (RMTg, VTA, Raphe and LDT), but also to dopamine and serotonin neurons in the VTA and dorsal raphe. The LHb also projects to MCH and Orexin-expressing neurons in the LH. (B). LHb neurons targeting the RMTg are mainly located in the lateral LHb (Kowski et al., 2008; Poller et al., 2013; Shabel et al., 2012), while those targeting the VTA and dorsal raphe are located in the medial LHb (Poller et al., 2013). sm: stria medullaris; fr: fasiculust retroflexus, cc: corpus callosum; 3V and 4V: 3th and 4th ventricle

Function of the LHb in reward and aversion encoding

Seminal studies in rhesus monkeys have suggested a role of the LHb in encoding aversive stimuli and in controlling dopaminergic neurons activity, crucially contributing to our understanding of motivational processing. When monkeys were exposed to unexpected aversive air puff, a cue predicting it (after conditioning sessions) or an omission of expected reward, the majority of LHb neurons increased phasically their firing activity. On the contrary, when an unexpected rewarding stimulus or reward-predictive cues were presented to the animals or alternatively an expected punishment was omitted, LHb neurons firing decreased or remained unchanged respectively (Fig7D) (Matsumoto and Hikosaka, 2009a, 2007). Moreover, there was a linear relationship between the objective value of the stimulus and the conditioned stimulus (cue) response for negative outcomes, but not for positive ones (Fig7A). This has led to the idea that

LHb neuronal activity discriminates the valence of stimuli and preferentially represents negative-valued events with respect to dopamine neurons, the activation of which preferentially represents reward (Matsumoto and Hikosaka, 2009b; Mirenowicz and Schultz, 1996). It is important to note that when a reward was fully predictable (100% reward predictive cue) LHb neurons did not respond to the unconditioned stimulus (reward delivery), whereas if the reward was not fully predictable (50% reward occurrence in previous sessions) LHb neurons were inhibited (Fig7B). The magnitude of the inhibitory response increased with the reward unpredictability. Similarly, in trials where an aversive stimulus was 100% predictable, LHb neurons responded with excitation to the unconditioned stimulus (air puff) and the response was reduced compared to trials where the aversive stimulus was not fully predictable (Fig7C). These data suggest that when an aversive or rewarding stimulus is predictable the response of LHb neurons during the stimulus presentation (excitation or inhibition) is decreased in magnitude or absent compared to when it occurs in an unpredictable manner (Matsumoto and Hikosaka, 2009a) (Fig7D). Altogether this evidence strongly indicates a role of LHb neurons in negative-reward prediction error. This behavior of LHb neurons appears opposite to the behavior of dopamine neurons in response to rewarding and aversive stimuli and their predictive cues (Fig7E). As discussed in the previous chapters, unpredicted rewarding stimuli or reward-predictive cues lead to rapid and brief bursts of activity in dopamine neurons. When the reward occurrence becomes predictable dopamine neurons no longer fire, whereas an omission of expected rewards inhibits them (Schultz et al., 1997). In contrast, aversive stimuli such as noxious foot pinch or foot shock mainly decrease dopamine neurons firing rates and bursting activity (Ungless et al., 2004), although few neurons respond with phasic excitation (Brischoux et al., 2009). This opposite processing of reward and aversion in the LHb and VTA led to the idea that LHb neurons provide a negative-reward predictive signal to dopamine neurons (Bromberg-Martin et al., 2010; Keiflin and Janak, 2015; Schultz, 2007b). Importantly, the activity of LHb neurons is not only opposed, but it also precedes the activity of SNc and VTA dopamine neurons in non-rewarded trials, indicating that LHb neurons exert inhibitory drive onto dopamine neurons (Matsumoto and Hikosaka, 2007). This is in line with an inhibitory effect of LHb electrical stimulation onto dopamine neurons activity

(Christoph et al., 1986; Ji and Shepard, 2007). Moreover, blocking excitatory transmission within the LHb leads to transient increase of dopamine release in the NAc, dorsal striatum and PFC, suggesting that LHb activity exerts a tonic inhibition on dopaminergic transmission (Lecourtier et al., 2008). However, in a recent study LHb lesions prevented a decrease in dopamine neurons activity only when a reward was omitted but not when an aversive stimulus was delivered, suggesting that LHb neurons are not the only source of negative reward prediction signal to dopamine neurons and that instead the LHb codes rather for disappointment (Tian and Uchida, 2015). A limitation, nonetheless, of this study is the use of electrolytic lesion of the LHb, where circuit adaptations might have occurred as a compensatory mechanism. In this regard, the use of optogenetic or chemogenetic silencing of the LHb activity could be more informative to determine its contribution to negative reward prediction error when controlling midbrain structures.

In humans, functional magnetic resonance imaging (fMRI) showed increased LHb activity when healthy volunteers received negative feedback after failing to perform a task or when they were exposed to aversive stimuli (Hennigan et al., 2015; Ullsperger and von Cramon, 2003). Furthermore, similarly to monkeys the LHb of humans responded preferentially to cues signaling negative outcomes (Lawson et al., 2014). Altogether data in human and non-human primates suggest an important role of the LHb in predicting negative outcomes necessary for motivated behaviors.

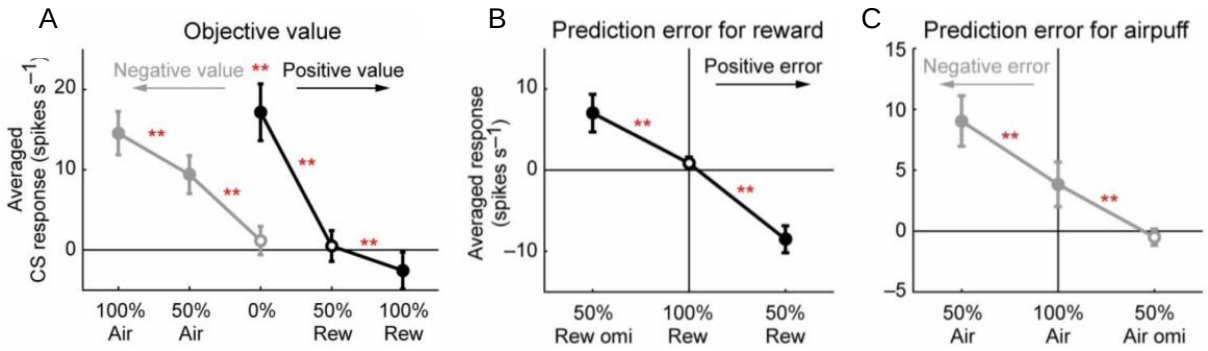

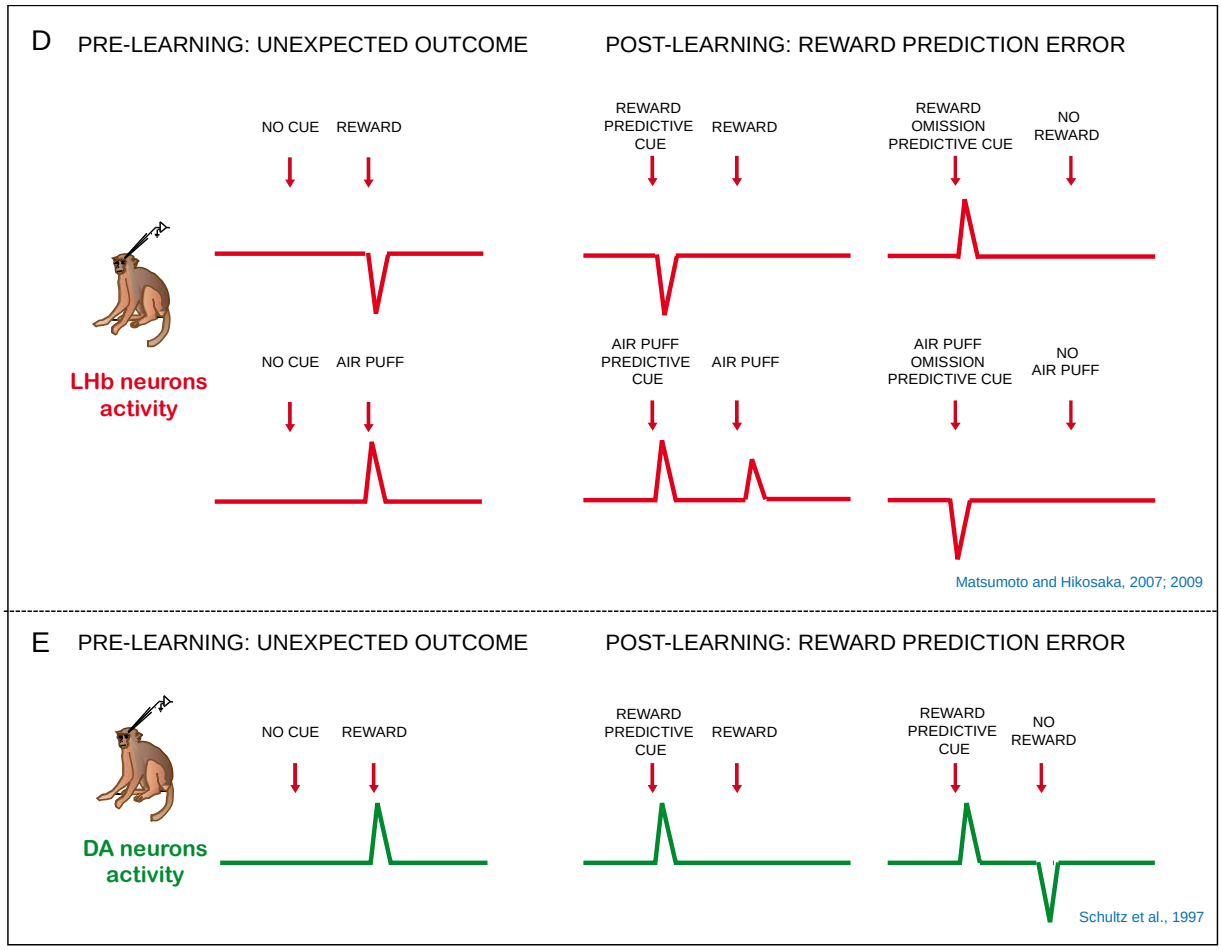

Figure 7 LHb function in aversion encoding and negative prediction error

(A). Linear relationship between averaged conditioned stimulus response (cue) and the objective value for negative outcomes and non-linear relationship for rewarding outcomes. (B). Relationship between the averaged LHb unconditioned stimulus (reward) response and the probability for reward or reward omission (positive prediction error). (C). Relationship between averaged LHb unconditioned stimulus (air puff) response and the probability for airpuff or airpuff omission (negative prediction error). (From Matsumoto and Hikosaka, 2009a). (D). LHb responses to unpredictable (non-learned) rewarding or aversive stimuli. After learning, LHb neurons responses shift to the cues predicting 100% reward or 100% punishment. However, LHb neurons respond also to the unconditioned stimulus when it is aversive but with smaller magnitude. When a cue predicts omission of reward LHb neurons increase firing and when a cue predicts omission of air puff LHb neurons decrease firing. (E). Dopamine neurons show opposite responses to unpredictable rewards and to cues predicting rewards (increased firing) compared to LHb neurons. When a cue predicts reward dopamine neurons fire, but if the reward is omitted dopamine neurons are phasically inhibited.

Role of LHb output for aversion processing

Following these studies an important question arose: given the excitatory nature of LHb neurons, how does their activity drive inhibition onto dopamine neurons? LHb neurons projections to GABA neurons of the midbrain might mediate LHb inhibitory control onto dopamine neurons. Indeed, an important link between the LHb and dopamine neurons function in reward/aversion encoding is the GABAergic RMTg. Anatomical and ultrastructural studies indicate that the LHb sends a major glutamatergic efferent to the RMTg. RMTg neurons in turn project to dopamine neurons within the VTA and SNc, although some synaptic contacts with non-dopaminergic cells have also been reported (Balcita-Pedicino et al., 2011; Brinschwitz et al., 2010; Jhou et al., 2009b; Kaufling et al., 2009). In line with this, retrogradely labeled RMTg neurons projecting to the VTA were found in close apposition to anterogradely labelled LHb axon terminals (Gonçalves et al., 2012). Importantly, RMTg neurons encode rewarding or aversive stimuli similarly to the LHb and opposite to dopamine neurons, by phasically decreasing (reward) or increasing (aversion) their firing (Fig8) (Jhou et al., 2009a; Matsumoto and Hikosaka, 2007). Functional data in anesthetized rats and in behaving monkeys indicate that RMTg neurons receiving LHb input increase phasically their firing in response to aversive stimuli and inhibit dopamine neurons, further supporting a role of RMTg in relaying LHb signals to dopamine neurons (Hong et al., 2011; Lecca et al., 2012; Matsui and Williams, 2011). In line with a role of LHb output to midbrain GABA neurons in driving negative teaching signals, light-activation of ChR2-expressing LHb terminals in the RMTg of mice produced real-time and conditioned-place avoidance behaviors (Stamatakis and Stuber, 2012). Moreover stimulation of this pathway produced negative reinforcement since animals nose-poked to terminate stimulation, while it disrupted positive reinforcement as animals nose-poked less to obtain a reward, suggesting that LHb-to-RMTg pathway activity provides a punishing signal (Fig8) (Stamatakis and Stuber, 2012).

Although LHb neurons strongly project to the RMTg, they also send, direct projections to GABA and dopamine neurons in the VTA. Moreover there is a topographic organization of this connectivity since the VTA projecting neurons are found mainly in the medial division of the LHb and send their axons to the ventral medio-posterior aspects of the

VTA (Gonçalves et al. 2012; Omelchenko et al. 2009; Swanson 1982; Phillipson & Pycock 1982; Skagerberg et al. 1984). Importantly, light activation of ChR2-expressing LHb terminals in the VTA of mice evoked responses in half of non-dopaminergic cells (putative GABA neurons), whereas only a very small percentage of dopamine neurons responded to the stimulation (Stamatakis and Stuber, 2012). Altogether these data indicate that the LHb preferentially connects to GABA neurons in the midbrain, likewise exerting an inhibitory control on dopamine neurons (Ji and Shepard, 2007; Matsumoto and Hikosaka, 2007). This is in line with the results obtained in monkeys showing that excitation of LHb neurons in response to aversive events is followed by inhibition of dopamine neurons (Matsumoto and Hikosaka, 2007). In agreement with this, light activation of ChR2-expressing GABA neurons in the VTA inhibits dopamine neurons firing, reduces reward-related behaviors (sucrose licking) and induces conditioned place avoidance (Fig2B), similarly to activation of the LHb-RMTg pathway (Fig8) (Stamatakis and Stuber, 2012; Tan et al., 2012; van Zessen et al., 2012). Moreover, inhibition of dopamine neurons expressing NpHR led to avoidance behaviors, further supporting that midbrain GABA-mediated inhibition of dopamine neurons is instrumental for the expression of aversive behaviors (Fig2B) (Tan et al., 2012).

The LHb also targets dopamine neurons in the ventromedial and posterior portion of the VTA, which preferentially send axons to the medial PFC and undergo aversive experience-dependent plasticity (Lammel et al., 2012, 2011). Furthermore, optogenetic activation of retrogradely labeled VTA-projecting LHb neurons produces conditioned place avoidance (Fig8) (Lammel et al., 2012).

In humans, together with an increased LHb activity a higher activation of the VTA, SNc and PFC regions were also detected after aversive stimuli and this was associated with increased functional connectivity between the habenula and VTA as well as VTA and PFC (Hennigan et al., 2015), suggesting that both in rodents and in humans the habenulo-meso-cortico-limbic circuit is involved in aversion processing.

Collectively, all these anatomical and functional data strongly suggest that LHb output conveys aversive signals via different anatomical connections and ultimately underlies aspects of aversive behaviors. The stimulation of each of these distinct LHb pathways to the midbrain is sufficient, but it remains still unclear whether it is necessary for aversive

behaviors. Other important questions arising following these studies are whether these pathways are simultaneously active or occur at different instances and which particular aspects of aversive behaviors do they encode.

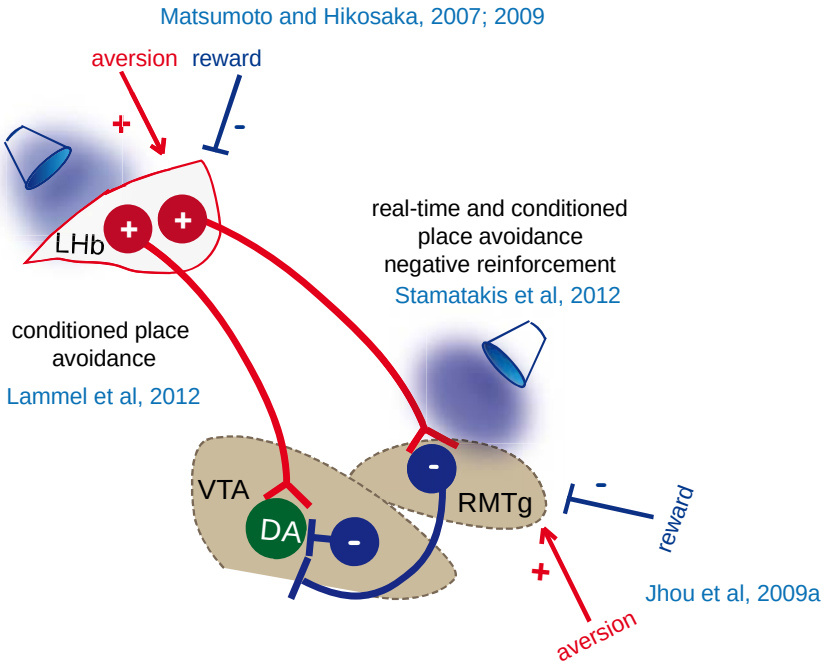

Figure 8 Contribution of LHb output to motivated behaviors

LHb neurons are glutamatergic and are connect predominantly to GABA neurons of the midbrain (Meye et al., 2016). ChR2-driven stimulation of LHb terminals within the RMTg induces real-time and conditioned place avoidance, negatively reinforces behavior and disrupts positive reinforcement. RMTg neurons inhibiting dopamine neurons are excited by aversive stimuli and are inhibited by rewards similarly to LHb neurons. Some VTA-projecting LHb neurons target predominantly dopamine neurons projecting to the PFC. Stimulation of LHb neurons projecting to the VTA induces conditioned place avoidance.

Role of inputs to the LHb for aversion processing

Data collected so far suggest that the LHb lacks local GABAergic control (Li et al., 2011). Instead its activity is largely shaped by multiple long-range synaptic inputs (Root et al., 2014b; Shabel et al., 2014, 2012; Stamatakis et al., 2016). Indeed, many forebrain and midbrain nuclei send glutamatergic and GABAergic terminals directly to the LHb contributing to its function in reward and aversion. Recent studies have proposed that some inputs to the LHb, including the EPN, VTA and potentially the LH are capable to co-release GABA and glutamate from the same synaptic terminal and to form functional postsynaptic connections with LHb neurons (Root et al., 2014b; Shabel et al., 2014; Stamatakis et al., 2016). Activating ChR2 specifically in glutamatergic neurons in a Vglut2-Cre-dependent manner (Vglut2: vesicular glutamate transporter 2) in any of these three inputs led to both AMPA receptor- and $GABA_A$ receptor-mediated postsynaptic currents. Similarly, a Vgat-Cre- or GAD67-Cre-dependent activation of ChR2 (Vgat: vesicular GABA transporter and GAD67: glutamate decarboxylase, the enzyme synthetizing GABA from glutamate) in GABAergic neurons of the VTA or EPN respectively triggered both excitatory and inhibitory postsynaptic currents (EPSCs and IPSCs respectively) in the LHb. A fine ultrastructural analysis in mouse and rat has shown that the majority of VTA-to-LHb neurons co-release glutamate and GABA from the same synaptic terminal forming functional asymmetrical and symmetrical synapses (Root et al., 2014b). Activation of the EPN and LH inputs drives LHb neurons to fire, while the predominant effect of VTA-to-LHb pathway stimulation *in vivo* was inhibitory (Fig9) (Root et al., 2014b; Shabel et al., 2014; Stamatakis et al., 2016). Interestingly, VTA-to-LHb optostimulation resulted in inhibition followed by rebound excitation in some LHb neurons, raising the possibility that the co-release of glutamate and GABA from the same synapse may have a role to temporally control LHb neuronal firing (Root et al., 2014b). This hypothesis is supported by previous evidence showing that phasic electrical stimulation of the midbrain decreases the firing rate of a subset of LHb neurons, whereas a tetanic stimulation tends to increase it (Shen et al., 2012).

Importantly, optogenetic activation of specific inputs to the LHb can drive distinct motivational states. Indeed, stimulation of the EPN-to-LHb synapses, which has an

overall excitatory effect on LHb firing, drives real-time place avoidance behavior (Fig9), consistent with the idea that an increased LHb activity is required for the expression of negative states (Shabel et al., 2012). EPN inputs impinge onto neurons of the lateral division of the LHb, which project mainly to GABA neurons of the midbrain, further supporting the role of this pathway in aversion encoding and avoidance behaviors (Fig5B and Fig6B) (Gonçalves et al., 2012; Lecca et al., 2014; Proulx et al., 2014; Shabel et al., 2012, Meye 2016). Interestingly, although the EPN participates mainly in the control of body movements (DeLong, 1971), some EPN neurons encode negative-reward prediction error similarly to the LHb, by phasic excitation upon unexpected aversive stimuli or reward omissions and phasic inhibition by unexpected rewards. The response of these negative-reward encoding neurons in the EPN precedes that of LHb neurons, suggesting that they may excite LHb neurons during aversive stimuli or reward omission (Fig9) (Hong and Hikosaka, 2008).

Optostimulation of the VTA-to-LHb pathway also produced avoidance of the light-associated chamber after conditioning, suggesting that this input may be involved in avoidance learning (Fig9) (Root et al., 2014a). Nevertheless, this effect seems puzzling considering that the VTA-to-LHb input inhibits the majority of LHb neurons, which would presumably lead to disinhibition of downstream dopamine neurons and would drive rewarding states. A possible explanation to this issue may reside in that in this study a continuous light activation has been employed when the animal was in the light-associated chamber, which may result in progressive increase of LHb neuronal activity and therefore to increased inhibitory drive onto downstream dopamine targets (Shen et al., 2012). Whether the balance of excitation and inhibition at co-releasing synapses is frequency or time-dependent remains however an open question. Alternatively, VTA inputs may target LHb neurons projecting directly onto dopamine neurons, therefore inhibiting them and contributing to avoidance behaviors.

Another important question arising is whether VTA neurons projecting to the LHb release dopamine and what the functional consequences would be on LHb neuronal activity. Indeed, early anatomical and tracing studies have described afferent projection from the ventromedial portion of the VTA to the medial aspect of the LHb (Swanson 1982; Phillipson & Pycock 1982; Skagerberg et al. 1984), where thyrosin hydroxylase

positive fibers (TH, the rate limiting enzyme for dopamine synthesis) are found (Aizawa et al., 2012; Geisler et al., 2003; Gruber et al., 2007). Some more recent studies instead report that VTA fibers are widely distributed across the LHb and are predominantly TH negative and Vglut2 positive (Hnasko et al., 2012; Root et al., 2014b). Despite this evidence, characterization of the expression profile of LHb-projecting VTA neurons showed that a non-negligible population expresses TH in addition to glutamate and GABA markers (Root et al., 2014b), suggesting that these neurons are potentially capable to release dopamine. Cre-dependent ChR2 expression in the VTA of TH-Cre mice led to detection of $ChR2^{+}$ terminals in the LHb, but a weak expression of TH. Optostimulation of these $VTA^{TH+/ChR2+}$ fibers in the LHb failed to release detectable dopamine levels as assessed by fast-scan voltametry. Moreover, these LHb-projecting $VTA^{TH+/CHR2+}$ neurons showed a reduced expression of Vmat2 (vesicular monoamine transporter 2), D2 dopamine receptor (D2R) and DAT (dopamine transporter) and exhibited different electrophysiological properties compared to classical dopamine releasing VTA-to-NAc neurons. Optogenetic activation of $VTA^{TH+/ChR2+}$ axons in the LHb evoked GABAergic postsynaptic responses and decreased firing activity of LHb and RMTg neurons, whereas the same stimulation increased VTA activity. Moreover, stimulation of this pathway led to conditioned place preference as well as to positive reinforcement (Fig9) (Stamatakis et al., 2013). This is in discrepancy with the aversive effect of VTA-to-LHb stimulation reported by Root et al., 2014a. This contradiction may arise from the different genetic approaches employed and the potential targeting of different LHb neuronal subpopulations which may in turn project to distinct downstream targets. Notably, it has also been shown recently that the TH-Cre line can present some ectopic expression in non-TH-expressing neurons, raising the issue of choosing appropriate Cre-driver lines to study complex circuits (Lammel et al., 2015; Stuber et al., 2015).

Other inputs to the LHb have also been implicated in different aversive behaviors. Anatomical studies indicate that predominantly glutamatergic LH inputs target mainly VTA-projecting LHb neurons in the medial division of the LHb (Fig5 and Fig6) (Gonçalves et al., 2012; Poller et al., 2013). Excitatory, Vglut2-expressing LH neurons projecting to the LHb (LH^{Vglut2}-to-LHb) bidirectionally modulate motivational states.

Indeed, optical stimulation of LH^{Vglut2}-to-LHb pathway increases LHb neurons activity and induces real-time place avoidance, whereas NpHR-driven inhibition of this pathway leads to real-time preference (Fig9) (Stamatakis et al., 2016). This is in line with the necessity of increased LHb output for the expression of aversive behaviors and a decreased LHb output for reward-related behaviors (Lammel et al., 2012; Stamatakis and Stuber, 2012).

Another glutamatergic projection described to date arises from the mPFC (Kim and Lee, 2012; Li et al., 2011; Warden et al., 2012). Indeed, a study in rats shows that activating glutamatergic mPFC inputs expressing ChR2 in the LHb leads to behavioral despair as shown by decreased mobility in the forced-swim test (FST), a paradigm widely use to screen for depressive-like behaviors (Fig9) (Warden et al., 2012). However, the authors did not further investigate the contribution of this input for LHb neurons activity, leaving it open for further investigation.

Altogether, these studies demonstrate that distinct excitatory or inhibitory pathways can drive LHb neuronal activity ultimately contributing to the encoding and expression of motivated behaviors. Importantly, excitatory inputs arising from the EPN, LH, VTA and mPFC are capable to drive avoidance behaviors, whereas inhibitory inputs such as the GABAergic VTA-to-LHb component can inhibit neuronal activity and produce preference behaviors (Fig9). A caveat however of these studies is the use of non-specific stimulation patterns to activate exogenously-expressed opsins, which may overcome other physiological mechanisms relevant for these behaviors. It is also interesting to address whether different frequency patterns lead to different glutamate/GABA release ratios from the co-releasing synapses. Another limitation of the so far described approaches is that in the majority of the cases, it has been shown sufficiency of a pathway in inducing specific behaviors, but not its necessity. Nevertheless these studies demonstrate the importance of investigating specific circuits within the LHb to the level of single cell-types for different aspects of motivated behaviors. Furthermore, it is of major interest to closely investigate whether and how synaptic plasticity occurs in the LHb following rewarding or aversive experience and what is its contribution on LHb neuronal output both in physiological and pathological conditions. This is particularly important in light of the role of LHb neurons activity in aversive behaviors (Lecca et al.,

2014; Proulx et al., 2014). A thorough examination of specific plasticity mechanisms could provide molecular targets to reverse maladaptations in disorders related to LHb dysfunction including addiction and depression.

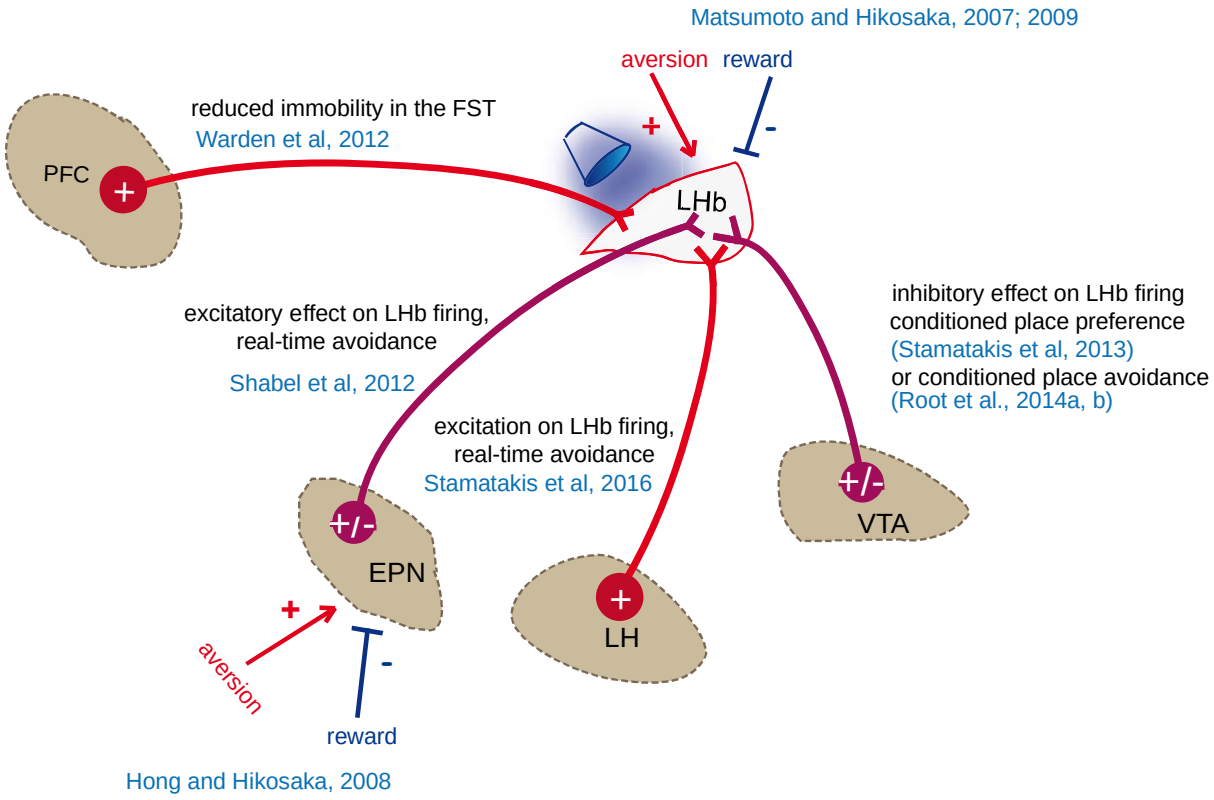

Figure 9 Contribution of inputs to the LHb to different motivational states

EPN neurons increase their firing in response to aversive stimuli and decrease their firing in response to rewards, similarly to LHb neurons. EPN-to-LHb and LH-to-LHb optogenetic stimulation increases LHb firing and drives real-time avoidance. Stimulation of the PFC-to-LHb input drives behavioral despair. Vglut2-expressing VTA terminals stimulation in the LHb predominantly inhibits LHb neurons firing and drive conditioned place avoidance, while TH-expressing VTA terminals stimulation drives conditioned place preference.

Dysfunction of the LHb: implications in depression and addiction

LHb in depression

Substantial evidence links LHb hyperactivity to the pathophysiology of mood disorders including depression and anxiety both in humans and rodent models (Lecca et al., 2014; Li et al., 2011, 2013; Proulx et al., 2014; Sartorius and Henn, 2007). In humans, positron emission tomography shows increased neural activity in the LHb and DRN with depletion of plasma levels of tryptophan (the precursor for serotonin), which also correlates with the degree of depressed mood (Morris et al., 1999). In line with this, the metabolic activity of the LHb of rodents correlates with the vulnerability to develop learned helpless behavior after uncontrollable, inescapable and unpredictable stress (Mirrione et al., 2014). Moreover, data from congenitally helpless rats susceptible to develop learned helplessness show a hypermetabolic activity in the habenular complex and a hypometabolic activity in the VTA-striatum pathway (Shumake and Gonzalez-Lima, 2003). The spontaneous firing activity within the LHb of such congenitally helpless rats is also increased (Li et al., 2011, 2013). Consistently, lesioning the LHb of depressed rats reduces depressive-like behaviors and increases the levels of serotonin in the DRN (Yang et al., 2008). Furthermore, pharmacological inactivation of the LHb with the $GABA_A$ receptor agonist muscimol has antidepressant effects in a rat model of treatment-resistant depression (Winter et al., 2011). Collectively, these data strongly suggest that an increased activity of LHb neurons can be responsible for behavioral despair both in humans and rodents.

In line with these data, the LHb activity of humans diagnosed with major depressive disorder shows abnormal responses to cues that predict punishment. As conditioned cues became more shock predictive the LHb activity of patients affected by major depressive disorders (MDD) decreased, while it increased in healthy volunteers. This also suggests that aberrant negative-reward prediction errors in the LHb can lead to impaired coping strategies with aversive situations characteristic of depressed patients (Lawson et al., 2016).

Deep brain stimulation (DBS), which has been extensively used to suppress neuronal hyperexcitability (Vitek, 2002), applied in the LHb of both humans and rodents had beneficial effects on depressed patients mood and animal performance in the forced swim test (Kiening and Sartorius, 2013; Li et al., 2011; Lim et al., 2015; Sartorius and Henn, 2007). Rats subjected to chronic mild stress, a paradigm that induces depressive-like states, had a significant improvement of their behavior following DBS in the LHb (Meng et al., 2011). Similarly, DBS in the *stria medullaris* led to substantial improvement of depressed mood in a patient with treatment-resistant depression (Sartorius et al., 2010). A potential way DBS exerts its beneficial effects in the LHb is by reducing excitatory drive (Li et al., 2011), however the exact mechanisms remain to be established.

LHb in addiction

Addiction is defined as chronic and relapsing condition characterized by compulsive drug use despite the negative consequences. It is considered to be a disease of learning and memory, where addicted individuals overlearn drug-associated cues and contexts and narrow their behavior to seeking and using the drug, while ignoring their health and social status (Hyman, 2005). One of the major problems of addiction is that individuals present a high risk of relapse even after long drug-free periods, which is often triggered by stress and negative emotional states (Self and Nestler; Sinha, 2008). One theory of addiction posits that drug-seeking and drug-relapse result from opponent processes represented by both the positive and negative reinforcing properties of the abused drugs. Indeed, the positive reinforcement after psychostimulant intake is produced by an initial euphoric ‘high’, whereas the negative reinforcement results from a following ‘down’ phase characterized by increased anxiety and drug craving. The desire to alleviate these aversive effects would further motivate the addicted subject to continue using the drug (Koob and Le Moal, 2008; Koob, 2013). Addictive psychostimulants have the common feature to target the DAT, likewise increasing dopamine levels in the NAc and other target regions of the dopamine system therefore acting as reinforcers. The reinforcing properties of abused drugs characterize the initial stages of addiction (Di Chiara and

Imperato, 1988; Vaughan and Foster, 2013). However, after persistent drug-taking, withdrawal and negative affective symptoms arise, involving a circuit reorganization and recruitment of anti-reward and stress systems (Ettenberg, 2009; George et al., 2014; Knackstedt et al., 2002; Koob, 2013).

The LHb has been proposed to participate in the pathophysiology of drug addiction because of its role in encoding rewarding and aversive stimuli as well as of its functional connection to the dopamine system. Indeed, the LHb is innervated by dopaminergic fibers, expresses dopamine receptors and the dopamine transporter, making it a potential target for drug-driven synaptic and behavioral adaptations (Freed et al., 1995; Good et al., 2013; Jhou et al., 2013; Kowski et al., 2009; Root et al., 2014b; Zuo et al., 2013). The LHb has been implicated in different aspects of drug-related behaviors. LHb metabolic activity negatively correlates with locomotor activity after cocaine administration (Fig10) (Porrino et al., 1988), while its pharmacological inactivation or lesion increases locomotor responses to psychostimulants (Gifuni et al., 2012; Gill et al., 2013), suggesting that LHb activity is decreased during the rewarding effects of drugs (i.e. locomotor sensitization). This is consistent with the idea that LHb activity needs to be decreased to relieve the inhibitory tone onto dopamine neurons allowing them to encode reward-related signals. In contrast, an increased expression of c-fos (c-fos is an immediate early gene, a marker for neuronal activity) in LHb neurons projecting to the VTA occurs in the withdrawal phase after extinction of cocaine-seeking behavior or in response to conditioned stimuli predicting absence of cocaine reward (Mahler and Aston-Jones, 2012). In line with this, rats that had unilateral lesions of the LHb failed to extinguish cocaine-seeking behavior, consistent with reduced inhibitory drive onto dopamine neurons. Interestingly, low-frequency stimulation of the LHb (10Hz) led to increased cocaine self-administration, while a mixed pattern of stimulation alternating low and high-frequencies (10 and 100Hz respectively) reduced this behavior (Friedman et al., 2010).

The LHb has also been associated to the susceptibility of drug relapse. Studies in mice have shown that some animals present higher vulnerability to cocaine relapse and that

this correlates with increased c-fos activity in the LHb (Brown et al., 2010; James et al., 2011). While the LHb seems to be a target for psychostimulants, relapse from opiates has also been linked to increased LHb activity, suggesting that the LHb is a common target for different classes of drugs (Madsen et al., 2012; Zhang et al., 2005). In contrast, LHb pharmacological inactivation does not affect cue-induced reinstatement of cocaine seeking, but reduces stress-induced reinstatement, in line with a role of the LHb in encoding stressful events (Gill et al., 2013). Recently, a study in our laboratory has demonstrated that the input from the EPN to the LHb contributes to withdrawal symptoms and relapse behaviors after chronic cocaine treatment (Meye et al., 2016).

Accumulating evidence suggests that the LHb plays a role in the aversive component of drug-taking associated to the withdrawal phase after acute drug experience. Indeed, a single cocaine injection in rats produces real-time place preference immediately after the injection and this behavior occurs along with reduction of LHb firing rate. Around 15 minutes later, when drug rewarding effects start to wear off, the animals exhibit a mild place avoidance which is paralleled with a rebound excitation of LHb neurons (Fig10). 30 minutes post-injection, when the effects of the drug should be almost completely dissipated no preference or avoidance occurs and LHb neurons activity returns to baseline levels (Ettenberg et al., 1999; Jhou et al., 2013). This supports a scenario where negative symptoms emerge during the down phase of acute cocaine exposure when the rewarding effects of the drug start to wear off. Importantly, acute cocaine administration also increases c-fos levels in the LHb and RMTg (Fig10) (Jhou et al., 2013, 2009b; Zahm et al., 2010). Indeed, a considerable proportion of c-fos positive LHb neurons are RMTg-projecting. In contrast, the majority of VTA-projecting LHb neurons do not express c-fos. In line with this, LHb and *fasciculus retroflexus* lesions reduce in half the number of c-fos expressing neurons in the RMTg after cocaine, suggesting that the cocaine-activated LHb neurons also activate downstream RMTg neurons (Jhou et al., 2013, 2009b). In the light of these data it has been proposed that LHb-to-RMTg neurons might encode an early rewarding phase (reflected by an inhibition of LHb neurons activity) and a later aversive phase (reflected by the rebound excitation after the acute cocaine effects have faded away). The runway operant paradigm has been used

to assess such conflicting rewarding and aversive conditioning. In this paradigm animals have to traverse a runway to self-administer cocaine. Progressively they show longer latencies to reach the goal compartment as well as increased frequency of approach and retreat, reflecting opponent processes and hesitating-like behavior after cocaine administration (Ettenberg & Geist 1993; Geist & Ettenberg 1997). Rats showed substantial decrease in this progressive hesitation-like behavior when lesioning the RMTg or the *fasciculus retroflexus*. Similarly, optogenetically silencing RMTg neurons 15-25 minutes after cocaine injection also reduced hesitation behavior in the runway task, further supporting that a delayed activity of the LHb-to-RMTg pathway may be involved in the aversive effects of cocaine (Jhou et al., 2013). This is also in line with data showing aversive conditioning after LHb-to-RMTg pathway stimulation (Stamatakis and Stuber, 2012). Altogether these data support a role of the LHb-to-RMTg pathway activity in aversive behaviors related to the acute and potentially long-lasting effects of drug withdrawal.

Taken together all these data support that aspects of addiction and depression share similar neurobiological substrates leading to increased activity in the LHb. The exact molecular, synaptic and circuit mechanisms leading to such modifications are underway investigation and new insights are emerging regarding potential targets within the LHb to reverse pathological neuroadaptations. During my thesis I addressed some of the molecular mechanisms leading to increased LHb output to the midbrain after cocaine withdrawal.

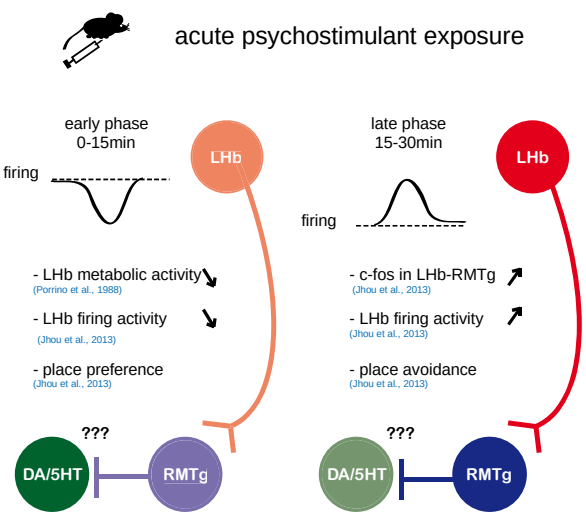

Figure 10 Acute effects of psychostimulants in the LHb

In the initial phase following acute drug administration LHb metabolic and firing activity is decreased and animals show place preference behaviors. During these initial stages monoaminergic activity is greatly increased but it is unknown to what extend the decreased LHb activity contributes to a higher dopamine neurons activity. 15-30 min following acute cocaine injection LHb firing activity increases as well as c-fos expression in LHb-to-RMTg pathway and animals display place avoidance behaviors. The activity and the subsequent release from dopamine neurons during this later stage after acute drug exposure are unknown.

Properties of lateral habenula neurons

Cell morphology and electrophysiology

The LHb is characterized by loosely dispersed cells with spherical, fusiform or polymorphic shape and rather small size. They have few very long dendrites stemming from the soma that can extend distally in the dorso-ventral and horizontal axis covering a large surface of the LHb. The dendritic arborization is not very branched as primary dendrites can give rise to few secondary ones (Weiss and Veh, 2011). The majority of LHb cells have spines along their dendrites (Fig12B) (Kim and Chang, 2005; Li et al., 2011; Maroteaux and Mameli, 2012) although aspiny neurons have also been described (Weiss and Veh, 2011). LHb neurons are almost exclusively glutamatergic and long-range projecting. The axons branch directly from the soma or from primary dendrites and run ventro-laterally to reach the root of the *fasiculus retroflexus*. Axonal reconstructions show the presence of varicosities along the axons, suggesting that they may form en passant synaptic connections and despite the lack of local collaterals they may interact in within the LHb (Kim and Chang, 2005). A recent study has proposed that single neurons with dense dendritic arbors can have their axonal terminals within the LHb, presumably forming a local microcircuit. These cells were mainly located within the medial division of the LHb and expressed GABAergic markers (Li et al., 2011; Zhang et al., 2016; Zhu et al., 2016). However, whether they can release GABA and inhibit locally other LHb neurons remains still unknown. Despite the different morphologies of LHb neurons, no clear correlation between their electrophysiological properties and a given morphological type has been observed.

LHb neurons present three major activity patterns: silent, tonically active and bursting. Most of LHb neurons have spontaneous tonic activity and a regular spiking pattern, although irregularly firing neurons also exist. The resting membrane potential of these neurons is around -55mV and they have a rather high input resistance ~ 450MΩ in mice (Meye et al., 2015) and ~ 1.16 GΩ in rats (Weiss and Veh, 2011), which contributes to the spontaneous activity of these neurons. The mean spontaneous firing frequency is ~ 4-5Hz *in vitro* (Weiss and Veh, 2011) and ~10-12Hz *in vivo* (Jhou et al., 2013; Kowski et

al., 2009). Virtually all LHb neurons have the capacity to generate a rebound burst discharge of action potentials in response to membrane hyperpolarization, which requires low-threshold Ca^{2+} channels activation (Chang and Kim, 2004; Huguenard et al., 1993; Wilcox et al., 1988). LHb neurons also express hyperpolarization activated cyclic nucleotide-gated cation (HCN) channels, responsible for the generation of pacemaker activity and potentially underlying the tonic inhibitory effect that LHb neurons exert on dopamine neurons (Lecourtier et al., 2008; Poller et al., 2011). Importantly, LHb neurons discharge properties strongly depend on the voltage. Cells that are more depolarized at rest show tonic regular firing and can shift their spiking pattern to burst firing if membrane hyperpolarization occurs. Inversely, more hyperpolarized cells present bursting activity that can turn into regular firing if the membrane is depolarized (Chang and Kim, 2004; Weiss and Veh, 2011). In line with these observations, brief high frequency stimulation of the *stria medullaris*, the fiber bundle conveying the majority of inputs to the LHb, induces brief hyperpolarization followed by rebound excitation and this phenomenon was mainly observed in the medial portion of the LHb (Chang and Kim, 2004). The membrane characteristics of LHb neurons including membrane resting potential, action potential duration and after-hyperpolarization potential (AHP) amplitude are similar (Weiss and Veh, 2011).

Taken together, these data suggests that LHb neurons cannot be distinguished on the bases of their morphology or electrophysiological properties alone. Their functional differences may rather arise from the integration of distinct inputs on their long dendritic arborization or alternatively from distinct expression of synaptic and cellular proteins important for their activity. Indeed, LHb neurons receive their inputs in a segregated manner, but also express differentially neuronal markers involved in synaptic transmission and neuronal activity (Geisler et al., 2003; Zhang et al., 2016). A genetic profiling as well as the generation of transgenic Cre-driver mouse lines can be of help to identify and target specific cell types within the LHb. It remains also to be established how synaptic inputs are organized along LHb dendrites as well as what type of dendritic integration these neurons perform to orchestrate their neuronal output.

Fast excitatory transmission via ionotropic glutamate receptors

Apart from voltage-gated ion channels, synaptic inputs onto the LHb also largely contribute to control neuronal activity. As described previously, the LHb receives several glutamatergic afferent inputs from forebrain and basal ganglia regions, whose activation can generate action potential firing (Root et al., 2014b; Shabel et al., 2012; Stamatakis et al., 2016). Glutamate release in the LHb leads to activation of both AMPA-type and NMDA-type of receptors.

AMPA receptors are cation channels responsible for the majority of the fast excitatory transmission in the brain. They are composed of a combination of the four subunits GluA1 to GluA4 forming homo- or hetrotetramere (Henley and Wilkinson, 2016; Malinow and Malenka, 2002; Nicoll et al., 2006). The C-terminal domain of each subunit harbors different interaction sites with kinases, phosphatases or other auxiliary proteins necessary for receptor trafficking and function during synaptic plasticity (Swope et al., 1999; Wang et al., 2005). Likewise, the C-terminal domain of the GluA1 subunit contains PKA and CaMKII phosphorylation sites controlling surface insertion of the receptor (Fig11A) (Ehlers, 2000; Esteban et al., 2003; Lee et al., 2000) as well as its channel properties (Banke et al., 2000; Barria et al., 1997; Derkach et al., 1999). GluA1-containing and GluA2-lacking AMPA receptors have particular biophysical properties such as Ca^{2+} permeability, high single channel conductance and inward rectification due to polyamine obstruction of the channel at positive potentials (Fig11B) (Burnashev et al., 1992; Donevan and Rogawski, 1995; Liu and Zukin, 2007). In contrast, GluA2-containing receptors are impermeable to Ca^{2+}, have smaller single channel conductance and are insensitive to polyamine block, therefore yielding linear current-voltage relationship (Fig11B). These different properties of GluA2-lacking and GluA2-containg AMPA receptors result from postnatal mRNA editing which leads to a replacement of a single amino acid, from glutamine to arginine, in the pore-lining domain of the GluA2 subunit (Barbon and Barlati, 2011; Lomeli et al., 1994; Swanson et al., 1997). The arginine residue present in the GluA2-containing receptors does not allow the flow of big ions such as Ca^{2+} and contributes to its lower single channel conductivity (Burnashev et al., 1992; Mameli et al., 2007).

AMPA receptors undergo experience-dependent modifications including trafficking and interactions with other synaptic proteins (Bellone and Lüscher, 2006; Clem and Barth, 2006; Rumpel et al., 2005) leading to augmentation or reduction of the efficacy of excitatory transmission. These phenomena known as long-term depression (LTD) and long-term potentiation (LTP) comprise multiple expression mechanisms depending on the structure and developmental stage: from changes in surface expression levels of functional receptors, to changes of their biophysical properties or their interactions with scaffolding proteins. Such synaptic remodeling is thought to be the corollary of learning and memory (Huganir and Nicoll, 2013; Malenka and Bear, 2004; Malinow and Malenka, 2002).

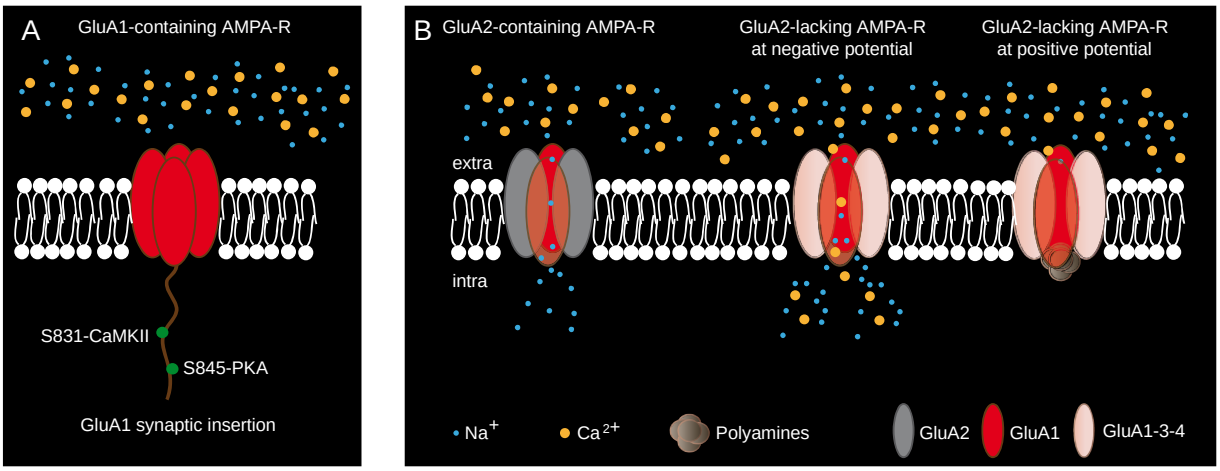

Figure 11 AMPA receptors trafficking and channel properties

(A). GluA1-containing AMPA receptors can undergo activity- or experience-dependent phosphorylation by CaMKII at serine 831 site or by PKA at serine 845 leading to receptor insertion at the membrane (Mammen et al., 1997; Roche et al., 1996). (B). GluA2-containig AMPA receptors are edited at the pore-lining domain, where a glutamine residue is replaced by arginine rendering the channel impermeable to Ca^{2+} ions and conferring smaller single channel conductance compared to GluA2-lacking AMPA receptors which are instead permeable to Ca^{2+}. GluA2-lacking AMPA receptors are blocked by intracellular polyamines at positive potentials and display inward rectification yielding non-linear current-voltage relationship.

The LHb expresses GluA2-lacking AMPA receptors as shown by inwardly rectifying current-voltage relationships (Fig12A,C) (Li et al., 2011; Maroteaux and Mameli, 2012). These receptors are of particular interest in the context of synaptic plasticity. Notably,

GluA2-lacking AMPA receptors are known to underlie anti-Hebbian type of plasticity, which requires paired afferent stimulation together with postsynaptic hyperpolarization for its induction as opposed to the Hebbian plasticity which instead relies on paired pre- and post-synaptic activity (Lamsa et al., 2007; Le Roux et al., 2013). These receptors are also involved in experience-dependent plasticity including reward- and drug-driven experience. Indeed, GluA2-lacking AMPA receptors are recruited at glutamatergic synapses onto VTA dopamine neurons after a single cocaine injection and are responsible for the increased strength of these synapses (Bellone and Lüscher, 2006). Moreover, they are permissive for further potentiation of the synapse since they allow the induction of an anti-Hebbian LTP in cocaine treated mice (Mameli et al., 2011). Similar experience-driven changes have been also reported in the NAc, where GluA2-lacking AMPA receptors accumulate following prolonged withdrawal from cocaine self-administration (McCutcheon et al., 2011a) or in the amygdala during acquisition of fear memories (Clem and Huganir, 2010). This information is also relevant for LHb function. Indeed in the LHb anti-Hebbian type of protocol (somatic hyperpolarization + 10Hz afferent stimulation) induces LTD of excitatory synaptic currents both in VTA-projecting and RMTg-projecting LHb neurons (Maroteaux and Mameli, 2012). Importantly, brief stimulation of the *stria medullaris* hyperpolarizes LHb neurons likewise providing gating conditions for anti-Hebbian plasticity (Chang and Kim, 2004).

The NMDA receptors are also ion channels and are typically di-heterotetrameres ot tri-heterotetramears. There are generally three subfamilies of NMDA receptors comprising in total seven distinct subunits: the GluN1, four GluN2 (GluN2A, GluN2B, GluN2C and GluN2D) and two GluN3 (GluN3A and GluN3B). The relative composition of the receptor is regulated throughout development and brain regions and confers distinct biophysical properties and synaptic plasticity mechanisms to each receptor subtype (Paoletti et al., 2013). NMDA receptors are one of the best studied triggers of long-term synaptic plasticity, the underlying expression mechanisms of which vary across synapses, developmental stages and structures (Malenka and Bear, 2004). NMDA receptors are expressed in the LHb (Fig12A). However, their relative contribution to excitatory transmission is relatively low (Fig12C) (Li et al., 2011; Maroteaux and Mameli, 2012).

The subunit composition and function of NMDA receptors in the LHb is poorly investigated and their potential role in synaptic plasticity remains to be addressed.

Fast inhibitory synaptic transmission via ionotropic $GABA_A$ receptors

The LHb is as well densely innervated by GABAergic axons (Araki et al., 1984; Smith et al., 1987). These inputs originate from the EPN, the LH and the VTA as optogenetic stimulation of these afferents evokes $GABA_A$ receptor–mediated currents (Root et al., 2014b; Shabel et al., 2014; Stamatakis et al., 2016). Other potential inhibitory projections may arise from LPO,VP, DBB and NAc, although their functional relevance remains to be tested (Hong and Hikosaka, 2013; Meye et al., 2013). Electrophysiological evidence suggests that fast inhibitory transmission in the LHb is mediated by $GABA_A$ receptors.

$GABA_A$ receptors are homo or hetero-pentameric ligand-gated ion channels permeable to chloride (Cl^-).They are composed of a combination of the 19 existing subunits (α1-α6; β1-β3; γ1-γ3; ρ1-ρ3;δ; ε; π; θ), which determine their channel and pharmacological properties, scaffolding, subcellular localization and trafficking (Birnir and Korpi, 2007; Luscher et al., 2011; Olsen and Sieghart, 2009). $GABA_A$ receptors are phasically activated upon GABA release. However, when GABA spills out of the synaptic cleft it activates extrasynaptic receptors ($GABA_A$ and $GABA_B$) which may underlie tonic inhibition. Most of synaptically expressed $GABA_A$ receptors contain a combination of α1-3, β and γ subunits, while extrasynaptic ones often contain α4-6 and a δ subunit instead of γ (Farrant and Nusser, 2005). $GABA_A$ receptors are highly regulated by phosphorylation-dephosphorylation processes, which play a major role in receptors trafficking and function (Comenencia-Ortiz et al., 2014; Kittler and Moss, 2003). Indeed, the β1-3 and γ2 subunits can be phosphorylated by cAMP-dependent protein kinase (PKA) and protein kinase C (PKC). Phosphorylation events can modify receptors conductance, but also can facilitate the interaction of specific subunits with membrane proteins controlling their insertion or removal from the synapse (Herring et al., 2005;

Luscher et al., 2011). This functional modulation of $GABA_A$ receptors by kinases, typically triggered by metabotropic receptors signaling, may represent important mechanisms of synaptic plasticity controlling the efficacy of inhibitory transmission.

In situ hybridization data suggests that LHb neurons express the α1-3, β1 and γ1-3 subunits in the mouse, with the strongest expression of α1 (Hörtnagl et al., 2013). Another study in the rat reports the highest expression of α1 and β2 and γ2 subunits in the LHb, suggesting a synaptic rather than extrasynaptic localization (Fig12A) (Pirker et al., 2000). Whether other subunits are also expressed in the LHb remains to be established.

LHb neurons activity is shaped by a balance of excitation and inhibition especially represented by the capacity of several inputs to co-release glutamate and GABA. Inhibition has a particularly important role in maintaining this fine balance to ensure the correct functioning of LHb neurons. Indeed, a decrease in inhibitory control over excitation at EPN synapses drives negative states in depression and drug withdrawal (Meye et al., 2016; Shabel et al., 2014). Therefore an important question which still needs to be addressed is how inhibitory transmission is modulated and what plasticity mechanisms govern GABAergic function in the LHb.

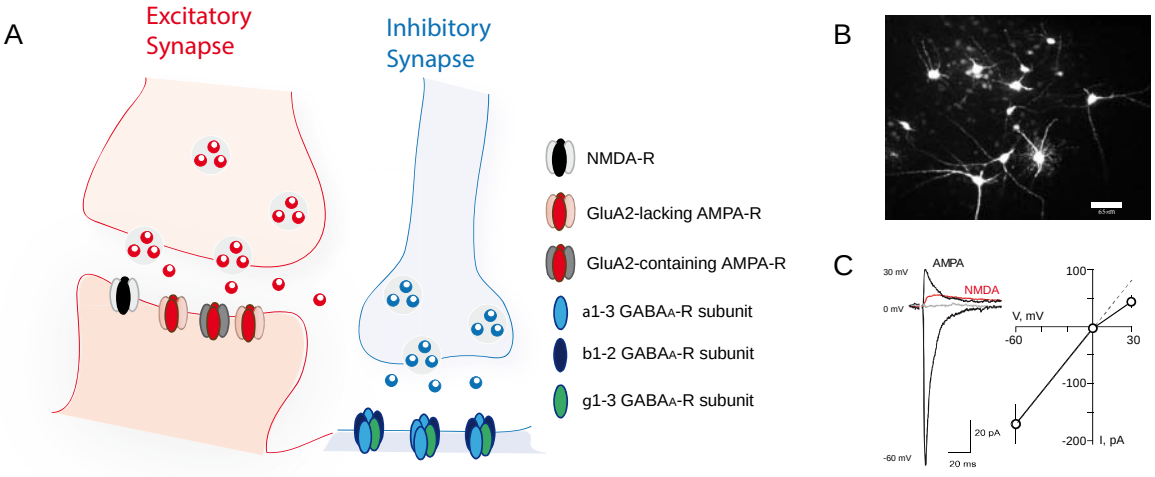

Figure 12 Excitatory and inhibitory synapses in the LHb

(A). Schematic of excitatory synapse in the LHb expressing high levels of GluA2-lacking, few GluA2-containg AMPA receptors and low levels of NMDA receptors. Inhibitory synapses express $GABA_A$ receptors composed of a combination of the α1-3, β1-2 and γ1-3 subunits. (B). Confocal image of LHb neurons filled with Alexa Fluor Red-594 (from Maroteaux and Mameli, 2012). (C). Sample trace showing AMPA receptors rectification at positive potentials and low NMDA component.

Modulation of fast excitatory and inhibitory transmission: role of mGluRs

Metabotropic glutamate receptors (mGluRs) are widely expressed throughout the CNS. They have been implicated in controlling excitatory and inhibitory transmission across synapses as well as neuronal excitability (Anwyl, 1999; Lüscher and Huber, 2010). The group I mGluRs are typically expressed postsynaptically and at the extra-or peri-synaptic membrane (Lujan et al., 1996). These receptors have seven transmembrane domains and are coupled to the Gq proteins triggering the PLC signaling cascade. This signaling leads to PKC activation and Ca^{2+} release from intracellular membrane compartments such as the endoplasmic reticulum (Fig13A) (Kim et al., 2008; Lüscher and Huber, 2010). The group I mGluR comprises the mGluR1 and mGluR5 subtypes which share the same signaling and can be expressed together or separately at synapses. mGluRs control excitatory and inhibitory synaptic transmission and most commonly they act to reduce their efficacy via different pre- and postsynaptic mechanisms (Bellone et al., 2008; Lüscher and Huber, 2010).

A very well studied form of mGluR-dependent long term depression (mGluR-LTD) occurs through a reduction of presynaptic transmitter release. Indeed, mGluRs trigger postsynaptically the generation of retrograde messengers such as endocannabinoids which subsequently diffuse through the lipid membrane and bind to their receptor, the cannabinoid type 1 receptor (CB1). CB1 receptors are typically expressed at presynaptic boutons and their activation inhibits Ca^{2+} channels thereby reducing the probability of both glutamate and GABA release throughout the brain (Fig13A) (Chevaleyre and Castillo, 2004; Kreitzer and Malenka, 2005; Maejima et al., 2001).

Postsynaptically, mGluRs strongly modulate synapses that express GluA2-lacking AMPA receptors. In many brain structures their activation induces rapid internalization of GluA2-lacking and insertion of GluA2-containing AMPA receptors ultimately leading to reduced efficacy of excitatory transmission (Fig13B) (Bellone and Lüscher, 2006; Clem and Huganir, 2010; Kelly et al., 2009; McCutcheon et al., 2011b). In the VTA this plasticity requires the mTOR signaling for rapid *de novo* synthesis of GluA2 subunits and their insertion to the membrane via the protein interacting with C kinase 1 (PICK1). This exchange of subunits leads to reduced single channel conductance of AMPA receptors (Bellone and Lüscher, 2006; Mameli et al., 2007). In the NAc, similar mechanisms require PKC signaling, likely through its interaction with PICK1 (McCutcheon et al., 2011b). In the cerebellum, the switch of subunits requires both mGluR and GluA2-lacking AMPA receptors activation leading to Ca^{2+} elevation and protein synthesis (Kelly et al., 2009).

Collectively, these data illustrate the variety of mechanisms that can be employed at different synapses for mGluR-dependent plasticity. Whether mGluRs are functionally expressed and whether they control the efficacy of excitatory and inhibitory synaptic transmission in the LHb remains so far unexplored. If mGluRs are expressed in the LHb and based on the fact that LHb neurons express GluA2-lacking AMPA receptors it is plausible that their activation may lead to LTD of excitatory transmission via a switch of AMPA receptors subunits. Alternatively, mGluRs may modulate synaptic transmission via changes in release probability of both glutamate and GABA. However, it is still unexplored whether functional endocannabinoid signaling exists in the LHb to trigger such presynaptic changes. During my thesis I addressed the possibility that mGluRs are expressed in the LHb and assessed their function in modulating excitatory and inhibitory synaptic transmission. I further extended my interest in understanding whether or not synaptic plasticity driven by mGluR is crucial for neuronal activity.

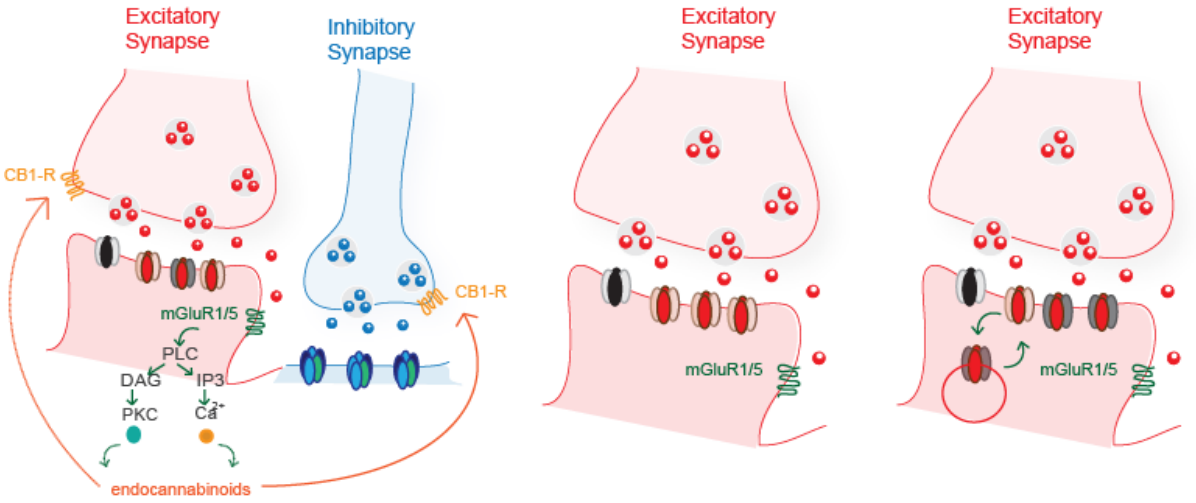

Figure 13 mGluR1/5 signaling and mechanisms of long term depression

(A). Group I mGluRs are Gq coupled proteins and trigger the PLC intracellular pathway. They can induce endocannabinoid synthesis, which subsequently diffuse through the membrane and activate presynaptically located CB1 receptors, which can be expressed both at excitatory and inhibitory synaptic terminals and whose activation leads to decreased neurotransmitter release. (B). mGluR activation at synapses expressing GluA2-lacking AMPA receptors trigger their internalization and insertion of GluA2-containig AMPA receptors. PLC (phospholipase C); DAG (diacylglycerol); IP3 (inositol triphosphate).

Synaptic plasticity in the LHb: a cellular substrate for motivated states in disease

Increasing evidence points to a crucial role of aberrant synaptic and cellular plasticity within the LHb in the pathophysiology of disorders of motivation. Changes in the balance of excitation and inhibition can drive LHb hyperactivity. Excessive activity of LHb neurons has been linked to the emergence of negative emotional states in depression and following withdrawal from drugs of abuse (Li et al., 2011, 2013; Meye et al., 2016; Neumann et al., 2015). This suggests that converging mechanisms can underlie the pathophysiology of these two highly comorbid disease states (Russo and Nestler, 2013).

Cellular mechanisms in the LHb in depression

Recent studies have begun to elucidate the cellular underpinnings of LHb dysfunction during depression. In rodent models of learned helplessness the excitatory drive onto LHb-to-VTA neurons is substantially increased and correlates with the extent of depressive-like behaviors. These adaptations occur along with increased spontaneous activity of LHb-to-VTA neurons (Li et al., 2011). In the same depressive model, the β form of the calcium/calmoduline-dependent kinase type II (βCaMKII) has higher expression levels in the LHb and occurs together with increased GluA1 membrane expression leading to increased spontaneous firing of LHb neurons (Li et al., 2013). In parallel, the balance of excitation/inhibition at the EPN-to-LHb synapse is shifted towards more excitation in congenitally learned helpless rats (Shabel et al., 2014). These studies suggest that different synaptic modifications potentially at different synapses or in different LHb output pathways converge to increase the overall activity of LHb neurons. Future studies are needed to address the exact induction mechanisms of these synaptic and cellular adaptations as well as their circuit relevance.

Recently, $GABA_B$ receptors plasticity in the LHb has also been implicated in depressive-like behaviors after acute aversive experience as well as in depression mouse models. Animals submitted to unescapable and randomly delivered foot-shocks led to a reduction of $GABA_B$ receptors and their inwardly rectifying potassium channels (GIRKs)

effectors function, whose activation normally leads to hyperpolarization and acts as a break for excessive excitability (Lecca et al., 2016; Lüscher and Slesinger, 2010). These changes led to increased spontaneous firing and excitability of LHb neurons as soon as one hour after the procedure and persisted up to two weeks. Electron microscopy data showed that both the $GABA_B$ receptor and the GIRK are internalized following acute foot shock exposure (Lecca et al., 2016). Importantly, the protein phosphatase 2A (PP2A), which has a role in regulating $GABA_B$-GIRK complex surface expression (Hearing et al., 2013; Padgett et al., 2012; Terunuma et al., 2010), had an increased activity in these animals and was required for the increased LHb excitability and depressive phenotype. These results raise the interesting hypothesis that $GABA_B$-GIRK complexes in the LHb serve as a general substrate to control excitability of these neurons and that their function is affected in pathologies characterized with depressive symptoms. It is interesting to understand whether this is a general phenomenon occurring after traumatic life events permissive for further pathological adaptations to take place or whether there are other vulnerability traits necessary for abnormal plasticity in the LHb in depression.

Cellular mechanisms in the LHb in addiction

Dysfunction of the LHb leads to negative emotional states also in addictive disorders particularly following drug withdrawal. Some of the molecular mechanisms underlying pathological plasticity in the LHb after acute or prolonged exposure to psychostimulants are now beginning to be elucidated. Bath application of cocaine directly depolarizes LHb neurons and induced reversible acceleration of firing. This effect is largely reduced in presence of blockers for excitatory synaptic transmission. Moreover, acute cocaine transiently increases the frequency of spontaneous and electrically evoked EPSCs and increases the paired pulse ratio, which are all measurements assessing presynaptic release probability. These results confirm that the increase in LHb firing is partly due to increased presynaptic glutamate release. However, cocaine also depolarizes reversibly LHb neurons independently of synaptic inputs since it induces inward currents in presence of blockers for glutamatergic and GABAergic synaptic transmission as well as

in presence of the voltage-gated sodium channel blocker tetradotoxin (TTX) which prevents action potential-driven neurotransmitter release. The cocaine-induced facilitation of spontaneous firing and glutamatergic transmission is blocked either by D1 or D2 receptor antagonists, although a combination of both does not further decrease firing or mini EPSCs frequency (Zuo et al., 2013). As already mentioned, some LHb neurons show bidirectional spontaneous firing responses to cocaine (initial inhibition followed by excitation) both *in vivo* and *in vitro* (Jhou et al., 2013). Another subset of neurons, which are phasically excited by tail pinch were also excited by cocaine and glucocorticoids, while those that were inhibited by tail pinch were also inhibited by cocaine and did not respond to glucocorticoids, suggesting that cocaine may share common pathways with stress-related factors in the LHb (Zhang et al., 2013). Altogether, these data suggest that LHb neurons respond in a non-homogeneous way to acute cocaine, raising the possibility that different subsets of LHb neurons, potentially dependent on their output targets, display different physiological responses to cocaine.

Chronic psychostimulant exposure produces long-lasting circuit and synaptic adaptations (Kasanetz et al., 2010; Mameli et al., 2009). Indeed, cocaine administration for two consecutive days leads to increased number of activated postsynaptic AMPA receptors specifically onto RMTg-projecting LHb neurons and 24 hours after the last injection. Moreover, the same protocol changes the rules for synaptic plasticity in these same RMTg-projecting neurons. Indeed, in saline treated mice pairing afferent stimulation (10Hz) with postsynaptic hyperpolarization induced long-term depression, while this protocol switched the direction of the plasticity to an LTP in cocaine treated ones (Maroteaux and Mameli, 2012). This suggests that cocaine induces long term adaptations of excitatory synaptic transmission in a target-specific fashion.
Synaptic long-lasting modifications of inhibitory synaptic transmission in the LHb after chronic psychostimulant intake have been recently reported. Five consecutive cocaine injections followed by two or fourteen days of withdrawal produced a reduction of $GABA_A$/AMPA and $GABA_A$/NMDA ratios at EPN-to-LHb synapses without significantly changing its glutamatergic component. This occurred along with decreased Vgat labeling specifically at EPN terminals, suggesting a decreased GABA filling into synaptic

vesicles and the subsequent reduction of the amount of GABA released at this synapse. These modifications led to reduced GABAergic modulation of evoked EPN-to-LHb neurons firing, shifting the balance of excitation/inhibition towards more excitation. This cocaine-evoked and synapse-specific plasticity was instrumental for withdrawal depressive-like symptoms and stress-induced relapse since rescuing the synaptic modifications by overexpressing Vgat specifically at EPN-to-LHb terminals ameliorated the behavioral phenotype (Meye et al., 2016).

Altogether these studies suggest that LHb synapses undergo long-lasting modifications after cocaine withdrawal which generally increases excitatory synaptic transmission and decreases inhibitory transmission, overall promoting an increase in LHb neuronal activity. This is supported also by evidence indicating that LHb neurons are hyperexcitable following withdrawal from cocaine self-administration (Neumann et al., 2015).

In conclusion, LHb neurons are not only a direct target of psychostimulants but also undergo long-term synaptic and cellular adaptations potentially leading to different aspects of drug-driven behaviors. Although recent insights have shed light onto some specific cellular mechanisms underlying drug-evoked behaviors, it remains to be established which specific habenular circuits and which precise cellular mechansims drive distinct negative emotional aspects of drug-taking. Given the circuit and functional specialization of the LHb different classes of drugs can act onto distinct LHb subpopulations and at different time points to produce persistent cellular adaptations. In depth studies addressing these questions are still needed. Some of the work to which I have contributed during my thesis identified specific molecular and cellular mechanisms in the LHb-to-RMTg pathway following cocaine withdrawal ultimately leading to depressive-like states. This work will be described in detail in the results section.

Context and objectives for the studies

I. mGluR-LTD at excitatory and inhibitory synapses controls lateral habenula output

The so far presented literature illustrates that the lateral habenula has a key position to control downstream monoaminergic systems therefore participating in motivational processing. A large effort has been focused in the recent years to elucidate the functional connectivity of the LHb as it receives dense innervation from and projects to multiple structures implicated in reward and aversion processing. With the advances of optogenetics and circuit mapping tools it has been possible to probe the contribution of specific inputs and output targets of the LHb in motivated behaviors. This is how it became clear that excitatory inputs activation increases LHb neuronal output likewise contributing to aversive behaviors, whereas inhibitory inputs tend to decrease LHb firing therefore promoting preference behaviors (Root et al., 2014b; Stamatakis et al., 2013; Stamatakis et al., 2016; Warden et al., 2012). However, in physiological conditions LHb neuronal activity is shaped by the simultaneous activity of all inputs and depends on the synaptic and integration properties of each neuron. Indeed, many of the so far described studies lack information regarding the precise synaptic mechanisms engaged following specific input stimulation and whether long-term synaptic plasticity at these inputs is required for the establishment of the observed behaviors.

We aimed to understand how synaptic transmission in the LHb can be modulated under different activity conditions and how synaptic plasticity impacts neuronal output. We focused on the group I mGluR receptors because they are capable to induce long-term synaptic changes throughout the CNS as well as to modify intrinsic neuronal properties (Anwyl, 1999; Bellone et al., 2008). The group I mGluRs mostly reduce the efficacy of excitatory, but also inhibitory synaptic transmission and have been implicated in several pathological conditions also linked to LHb dysfunction, such as addiction (Lüscher and Huber, 2010). Whether mGluRs are functionally expressed and whether they underlie long-term synaptic modifications in the LHb remains so far elusive. We hypothesized that if mGluRs are present in the LHb they may trigger long lasting decrease in the

efficacy of excitatory and/or inhibitory neurotransmission. Given that LHb neurons express predominantly GluA2-lacking AMPA receptors, a potential mGluR modulation could occur postsynaptically via a switch of AMPA receptors subunits (from rectifying, larger conductance GluA2-lacking to non-rectifying, smaller conductance GluA2-containing AMPA receptors) (Bellone and Lüscher, 2006; Kelly et al., 2009; McCutcheon et al., 2011b). Alternatively they could induce retrograde messengers capable to modify presynaptic release probability at excitatory and inhibitory synapses (Chevaleyre et al., 2006; Heifets and Castillo, 2009). Here we probed the mechanisms of mGluR-dependent modulation of synaptic transmission and its impact on LHb neuronal activity. Our results provide insights on so far unexplored cellular mechanisms, through which mGluRs control excitatory and inhibitory synaptic strength and highlight the functional repercussions of mGluR-plasticity for LHb neuronal output.

Report

Cell Reports

mGluR-LTD at Excitatory and Inhibitory Synapses in the Lateral Habenula Tunes Neuronal Output

Graphical Abstract

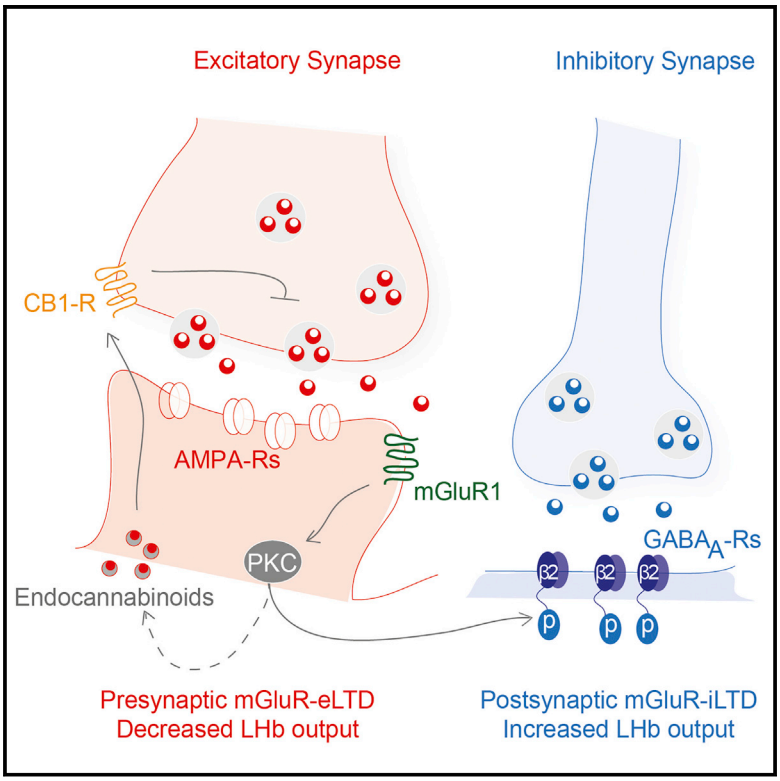

Authors

Kristina Valentinova, Manuel Mameli

Correspondence

manuel.mameli@inserm.fr

In Brief

Valentinova and Mameli show that mGluR1s in the lateral habenula (LHb) triggers PKC-dependent depression of excitatory and inhibitory transmission, allowing for bidirectional tuning of neuronal output via distinct presynaptic and postsynaptic mechanisms.

Highlights

- mGluR1 induces LTD of excitatory and inhibitory transmission in the LHb
- PKC mediates the induction of mGluR-LTD in the LHb
- Divergent expression mechanisms underlie mGluR-eLTD and -iLTD
- mGluR-eLTD and -iLTD decide the direction of LHb neuronal output

Valentinova & Mameli, 2016, Cell Reports *16*, 2298–2307
August 30, 2016
http://dx.doi.org/10.1016/j.celrep.2016.07.064

OPEN ACCESS
CellPress

Cell Reports
Report

mGluR-LTD at Excitatory and Inhibitory Synapses in the Lateral Habenula Tunes Neuronal Output

Kristina Valentinova[1,2,3] and Manuel Mameli[1,2,3,4,*]
[1]Institut du Fer à Moulin, 75005 Paris, France
[2]Inserm, UMR-S 839, 75005 Paris, France
[3]Université Pierre et Marie Curie, 75005 Paris, France
[4]Lead Contact
*Correspondence: manuel.mameli@inserm.fr
http://dx.doi.org/10.1016/j.celrep.2016.07.064

SUMMARY

Excitatory and inhibitory transmission onto lateral habenula (LHb) neurons is instrumental for the expression of positive and negative motivational states. However, insights into the molecular mechanisms modulating synaptic transmission and the repercussions for neuronal activity within the LHb remain elusive. Here, we report that, in mice, activation of group I metabotropic glutamate receptors triggers long-term depression at excitatory (eLTD) and inhibitory (iLTD) synapses in the LHb. mGluR-eLTD and iLTD rely on mGluR1 and PKC signaling. However, mGluR-dependent adaptations of excitatory and inhibitory synaptic transmission differ in their expression mechanisms. mGluR-eLTD occurs via an endocannabinoid receptor-dependent decrease in glutamate release. Conversely, mGluR-iLTD occurs postsynaptically through PKC-dependent reduction of β2-containing $GABA_A$-R function. Finally, mGluR-dependent plasticity of excitation or inhibition decides the direction of neuronal firing, providing a synaptic mechanism to bidirectionally control LHb output. We propose mGluR-LTD as a cellular substrate that underlies LHb-dependent encoding of opposing motivational states.

INTRODUCTION

Excitatory and inhibitory projections onto the lateral habenula (LHb) control the direction of neuronal output, contributing to the encoding of rewarding and aversive stimuli (Shabel et al., 2012, 2014; Stamatakis et al., 2013). Moreover, in rodent models of addiction and depression, glutamatergic and GABAergic synaptic plasticity modulates LHb neuronal firing, which is in turn instrumental for depression-like phenotypes (Lecca et al., 2016; Maroteaux and Mameli, 2012; Meye et al., 2015; Shabel et al., 2014). This highlights the behavioral relevance of synaptic adaptations in the LHb, heightening the need of understanding its underlying cellular processes.

Group I metabotropic glutamate receptor (mGluR) signaling and expression undergo modifications in disorders such as addiction and depression, disease states also characterized by aberrant LHb neuronal firing (Bellone and Mameli, 2012; Hovelsø et al., 2012; Lecca et al., 2014). Group 1 mGluRs consist of mGluR1 and mGluR5 subtypes (Lüscher and Huber, 2010). Their activation modulates the strength of excitatory and inhibitory synapses through G_q/G_{11}-mediated calcium mobilization and activation of downstream effectors, including protein kinase C (PKC) (Lüscher and Huber, 2010; Page et al., 2001). Pre- and postsynaptic mechanisms underlie mGluR-dependent long-term plasticity, but its relevance for controlling neuronal activity remains poorly understood (Galante and Diana, 2004; Kammermeier et al., 2000; Mameli et al., 2007).

We combine electrophysiology in LHb-containing acute slices with pharmacology and find that activation of mGluR1 receptors, but not of mGluR5, triggers long-term depression of excitatory and inhibitory synaptic transmission (mGluR-eLTD and mGluR-iLTD, respectively). mGluR-eLTD and -iLTD induction requires postsynaptic PKC signaling, but their maintenance relies on divergent expression mechanisms. mGluR-eLTD occurs via a presynaptic cannabinoid 1 receptor (CB1-R)-dependent decrease in glutamate release. In contrast, mGluR-iLTD is independent of presynaptic changes. Instead, mGluR-iLTD is postsynaptically expressed and requires PKC targeting onto $GABA_A$-R β2-subunits and a reduction in $GABA_A$-R single-channel conductance. The functional relevance of mGluR activation in the LHb is represented by opposing effects on neuronal output. Indeed, in the LHb, the mGluR-driven modulation of synaptic responses and output firing correlate positively. These data unravel the distinct molecular mechanisms underlying mGluR control of synaptic strength and the subsequent regulation of LHb neuronal activity.

RESULTS

mGluRs Drive Long-Term Synaptic Depression in the LHb

To examine the presence of group I mGluRs, we microdissected the LHb of mice and employed RT-PCR, which revealed mGluR1 and mGluR5 expression (Figure 1A). Accordingly, bath application (3–5 min) of the mGluR1/5 agonist

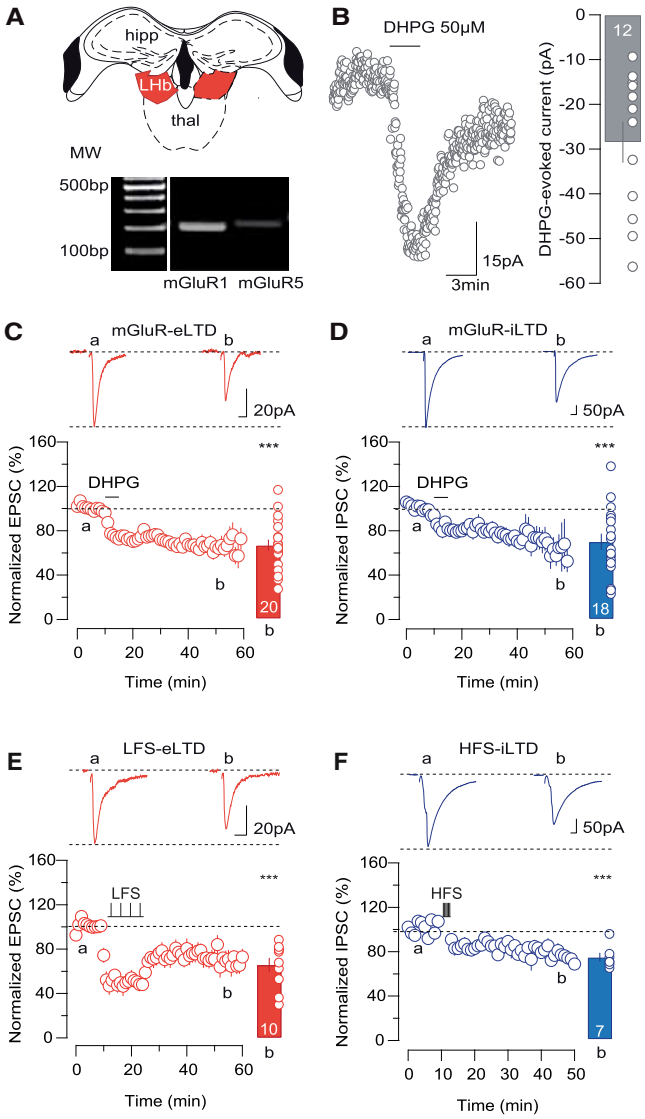

Figure 1. mGluR-eLTD and -iLTD in the LHb

(A) Schematic depicting the LHb microdissection (hipp, hippocampus; thal, thalamus) and mGluR1 and mGluR5 expression in the LHb. MW, molecular weight; bp: base pairs.

(B) Sample trace, bar graph, and scatterplot representing DHPG-evoked current (−28.5 ± 4.6 pA, 12 of 22 responding neurons).

(C) Sample traces representing EPSCs at baseline (a) and 20 min following DHPG (b). The timeline represents the DHPG effect (50 μM) on EPSCs. The bar graph and scatterplot show normalized averaged EPSCs ~40 min after DHPG (66.3 ± 5%, t_{19} = 6.306, ***p < 0.0001).

(D) The same as (C) but for IPSCs (69.9 ± 7.3%, t_{17} = 4.235, ***p < 0.0001).

(E) LFS-driven (1 Hz, 15 min) eLTD. The bar graph and scatterplot show normalized averaged EPSCs ~40 min after the protocol (65.8 ± 6.4%, t_9 = 5.3, ***p < 0.0001).

(F) HFS-driven (100 Hz, 1 s, at 0 mV) iLTD (top). The bar graph and scatterplot show normalized averaged IPSCs ~40 min after the protocol (74.2 ± 3.9%, t_6 = 7.086, ***p < 0.0001).

When not indicated, the timescale represents 5 ms. Error bars represent SEM. n indicates number of recorded neurons.

3,5-dihydroxyphenylglycine (DHPG, 50 μM) led to a transient inward current (Figure 1B; Gee et al., 2003). These data indicate the presence of functional postsynaptic group I mGluRs in LHb neurons.

To investigate whether mGluR activation modulates neurotransmission in the LHb, we tested the effect of DHPG application (5 min) on pharmacologically isolated AMPA receptor (AMPA-R)-mediated excitatory and $GABA_A$-R-mediated inhibitory postsynaptic currents (excitatory postsynaptic currents [EPSCs] and inhibitory postsynaptic currents [IPSCs], respectively). DHPG produced long-term depression of EPSCs and IPSCs (Figures 1C and 1D), termed eLTD and iLTD, respectively. mGluRs are activated by wide ranges of presynaptic activity (Lüscher and Huber 2010; Chevaleyre et al., 2006). Accordingly, we found that low-frequency stimulation (LFS) of presynaptic fibers (1 Hz) led to eLTD (Figure 1E). Instead, at inhibitory synapses, high-frequency stimulation (HFS) of presynaptic afferents (100 Hz at 0 mV) triggered iLTD (Figure 1F). Thus, mGluR activation and a distinct pattern of presynaptic activity in the LHb efficiently reduce excitatory and inhibitory synaptic transmission.

mGluR-eLTD and -iLTD Require mGluR1 and PKC Signaling

Group I mGluRs comprise mGluR1 and mGluR5 subtypes. To assess the induction requirement for mGluR- eLTD and -iLTD, we first exposed slices to either mGluR1 or mGluR5 antagonists (LY367385 or 3-2-methyl-4-thiazolyl-ethynyl-pyridine [MTEP], respectively). The mGluR1 antagonist LY367385 prevented DHPG eLTD/iLTD as well as LFS eLTD and HFS iLTD (Figures 2A and 2B; Figures S1A and S1B). Although the LFS protocol also reduced IPSCs, LY367385 failed to block this form of plasticity, indicating a different mechanism of induction (Figure S1C). Importantly, DHPG eLTD and iLTD remained intact in presence of the mGluR5 antagonist MTEP (Figures 2C and 2D).

Downstream of mGluRs, the G_q-coupled cascade leads to PKC activation, which targets a wide spectrum of synaptic proteins crucial for synaptic adaptations (Lüscher and Huber, 2010). To test PKC implication for mGluR-eLTD and -iLTD, we dialyzed neurons through a patch pipette with a pseudosubstrate peptide inhibitor of PKC, PKC[19-36] (Oliet et al., 1997). mGluR-eLTD and -iLTD were abolished in the presence of PKC[19-36] (Figures 2E and 2F). If PKC underlies mGluR-eLTD and -iLTD, we reasoned that its activation would occlude mGluR-driven synaptic plasticity. To test this, we bath-applied the PKC activator phorbol-12-myristate-13-acetate (PMA). When PMA successfully decreased EPSCs and IPSCs (seven of ten and five of six cells, respectively; Figures 2G and 2H), subsequent DHPG application failed to further reduce excitatory and inhibitory synaptic responses (Figures 2G and 2H). These data indicate that mGluR activation decreases excitatory and inhibitory synaptic transmission via a common mechanism requiring mGluR1-driven PKC signaling.

Presynaptic Expression Mechanism of eLTD in the LHb

Excitatory synapses in the LHb contain GluA2-lacking AMPA-Rs, as indicated by inwardly rectifying EPSCs (Maroteaux and Mameli, 2012). In brain structures such as the ventral tegmental

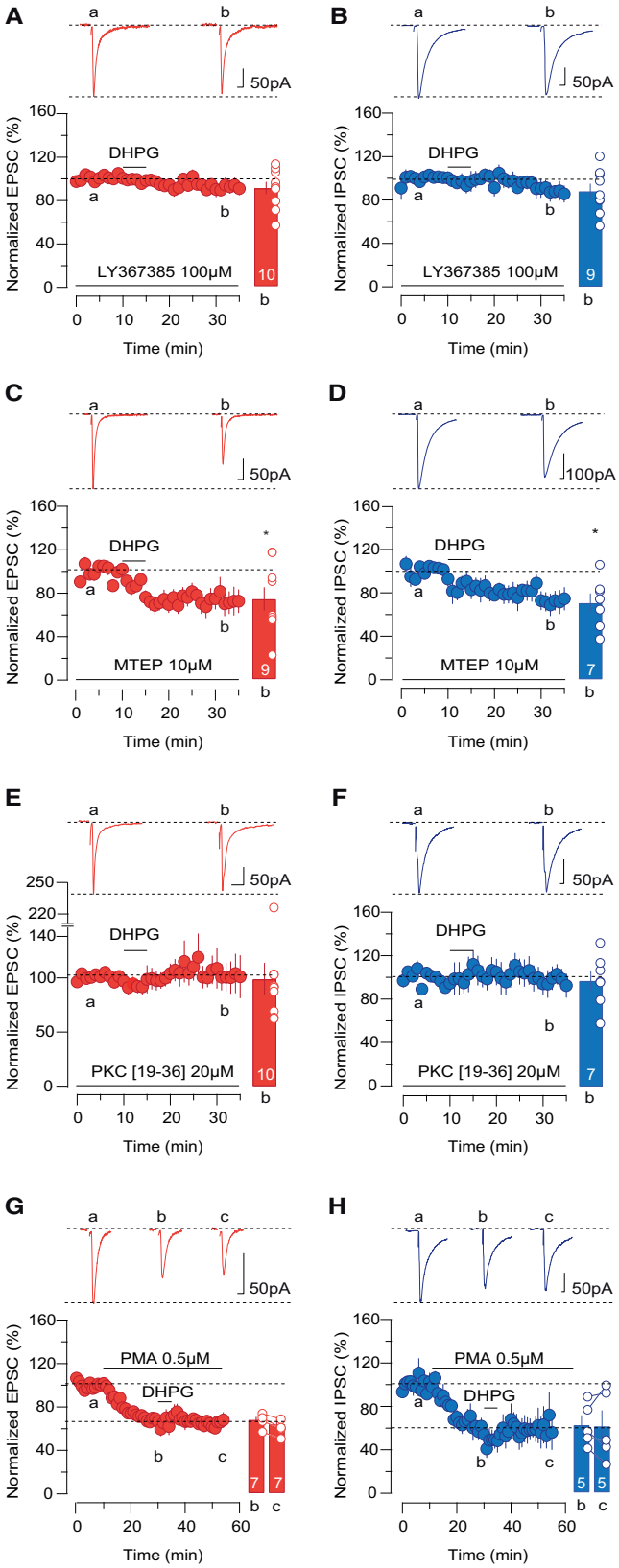

Figure 2. mGluR1 and PKC-Dependent Induction for eLTD and iLTD

(A) DHPG effect on EPSCs in the presence of the mGluR1 antagonist LY367385 (91.1 ± 5.6%, t_9 = 2.063, p > 0.05).

(B) The same as (A) but for IPSCs (88.7 ± 6.7%, t_8 = 1.680, p > 0.05).

(C) DHPG effect on EPSCs in the presence of the mGluR5 antagonist MTEP (74.5 ± 10.8%, t_8 = 2.377, *p < 0.05).

(D) The same as (C) but for IPSCs (71 ± 8.7%, t_6 = 3.425, *p < 0.05).

(E) DHPG effect on EPSCs during intracellular dialysis of PKC[19-36] (99.2 ± 14.8%, t_9 = 0.066, p > 0.5).

(F) The same as (E) but for IPSCs (98.1 ± 9.1%, t_6 = 0.088, p > 0.05).

(G) Effect of PMA on EPSCs (b, baseline versus PMA, 68.2 ± 2.4%, t_6 = 13.39, ***p < 0.0001) and subsequent occlusion of DHPG eLTD (c, PMA versus post-DHPG, 64.2 ± 5%, t_6 = 1.260, p > 0.05).

(H) The same as (G) but for IPSCs (b, baseline versus PMA, 62.7 ± 8.7%, t_4 = 4.285, *p < 0.05; c, PMA versus post-DHPG, 61.7 ± 14.4%, t_4 = 0.155, p > 0.05).

Error bars represent SEM. n indicates number of recorded neurons.

area, nucleus accumbens, and cerebellum, the presence of GluA2-lacking AMPA-Rs is a requirement for mGluRs to trigger postsynaptic LTD. This form of plasticity occurs via a switch from GluA2-lacking high-conductive to GluA2-containing low-conductive AMPA-Rs (Bellone and Lüscher, 2005; Kelly et al., 2009; McCutcheon et al., 2011). To test whether this scenario also applies to the LHb, we evoked EPSCs at different holding potentials (–60, 0, and +40 mV) before and after mGluR-eLTD (Figure 3A). EPSCs at baseline were inwardly rectifying, yielding a rectification index of >1, indicative of GluA2-lacking AMPA-R expression. DHPG reduced EPSC amplitude at negative and positive potentials, leaving the rectification index unaltered (Figure 3A). Thus, mGluR-eLTD in the LHb does not require postsynaptic modifications of AMPA-R subunit composition.

Aside from postsynaptic modifications, mGluRs can also trigger presynaptic long-term adaptations. To examine whether a decrease in presynaptic glutamate release underlies mGluR-eLTD, we monitored the paired-pulse ratio (PPR) of EPSCs before and after DHPG and LFS. Along with the reduced EPSC amplitude, DHPG application as well as the LFS produced a long-lasting increase in the PPR, indicating reduced glutamate release (Figure 3B; Figures S2A–S2C). In line with the mGluR1 and PKC requirements for mGluR-eLTD, the PPR remained unaltered after DHPG in the presence of the mGluR1 antagonist and PKC inhibitor but not in the presence of the mGluR5 blocker (Figure 3B). Interestingly, PMA-driven reduction in EPSCs occurred along with an increased PPR, which remained unaffected after subsequent DHPG application (Figure 3B). The different pharmacological agents did not alter the baseline PPR, suggesting the absence of drug-induced modifications in the probability of glutamate release (Figure 3B; black columns for all conditions). To corroborate our findings on the presynaptic mechanism underlying mGluR-eLTD, we examined quantal release by recording miniature EPSCs (mEPSCs). In the presence of tetrodotoxin, DHPG application led to a decrease in mEPSC frequency without significant changes in mEPSC amplitude (Figure 3C). This supports a scenario for a presynaptic expression of mGluR-eLTD. mGluR activation can trigger the release of endocannabinoids from postsynaptic neurons in several brain structures, including the striatum, hippocampus, and ventral tegmental area. mGluR-driven endocannabinoid mobilization acts retrogradely on presynaptic CB1-Rs,

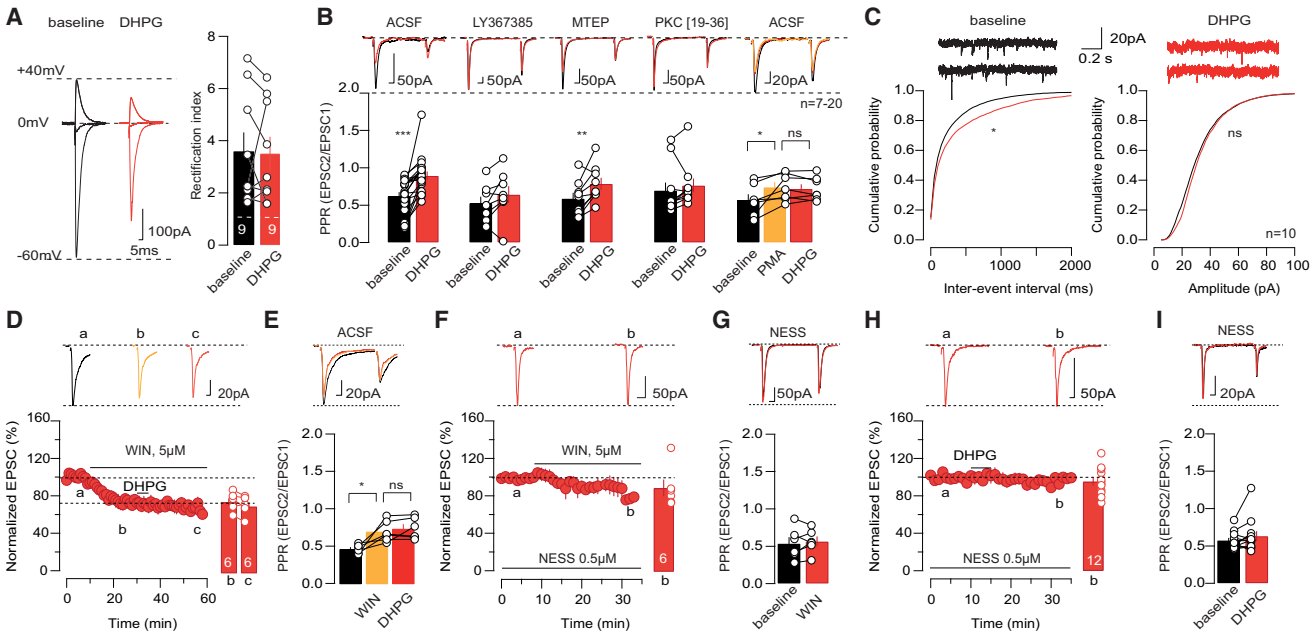

Figure 3. mGluR-eLTD Expression via CB1-R Activation

(A) Sample traces of AMPA-EPSCs at –60, 0, and +40 mV at baseline and after DHPG and average rectification index (baseline 3.6 ± 0.7 versus post-DHPG 3.5 ± 0.6, $t_8 = 0.192$, $p > 0.05$).

(B) PPR of EPSCs in artificial cerebrospinal fluid (ASCF; baseline 0.62 ± 0.05 versus post-DHPG 0.9 ± 0.05, $t_{19} = 4.963$, ***$p < 0.0001$); in the presence of LY367385 (baseline 0.53 ± 0.08 versus post-DHPG 0.64 ± 0.11, $t_7 = 1.860$, $p > 0.05$); of MTEP (baseline 0.59 ± 0.08 versus post-DHPG 0.79 ± 0.08, $t_8 = 3.432$, **$p < 0.01$); of PKC[19-36] in the recording pipette (baseline 0.7 ± 0.1 versus post-DHPG 0.76 ± 0.1, $t_9 = 1.214$, $p > 0.05$); after PMA and PMA + DHPG (baseline 0.57 ± 0.08 versus PMA 0.74 ± 0.07, $t_6 = 2.799$,*$p < 0.05$; PMA baseline versus PMA post-DHPG, $t_6 = 0.829$, $p > 0.05$). Shown are neurons represented in Figures 1 and 2. One-way ANOVA among all baseline PPR conditions: $F_{(9, 83)} = 0.485$, $p > 0.05$.

(C) Top: sample traces for mEPSCs. Cumulative probability plots show amplitudes and inter-event intervals for mEPSCs at baseline (black) and after DHPG (red). (mEPSC amplitude: baseline 30 ± 3.8 pA versus post-DHPG 32.1 ± 4.1 pA, KS test, $p > 0.05$; mEPSC frequency: baseline 3.8 ± 1.6 Hz versus post-DHPG 2.5 ± 1.1 Hz, KS test, *$p < 0.05$).

(D) Effect of WIN-55,212-2 on EPSCs (72.7 ± 3.8%, $t_5 = 7.246$, ***$p < 0.001$) and subsequent occlusion after DHPG application (68.5 ± 3.9%, $t_5 = 5.559$, $p > 0.05$).

(E) PPR of EPSCs after WIN application and subsequent DHPG application (baseline 0.45 ± 0.02, post-WIN 0.67 ± 0.05, post-DHPG 0.71 ± 0.06; baseline versus post-WIN, $t_5 = 3.411$, *$p < 0.05$; post-WIN versus post-DHPG, $t_5 = 1.004$, $p > 0.05$).

(F) The same as (D) but in the presence of NESS-0327 (90.79 ± 9.02%, $t_5 = 1.001$, $p > 0.05$).

(G) The same as (E) but in the presence of NESS-0327 (baseline 0.54 ± 0.09 versus post-WIN 0.57 ± 0.06, $t_5 = 0.672$ $p > 0.05$).

(H) Effect of DHPG on EPSCs in the presence of NESS-0327 (95.9 ± 4.3%, $t_{11} = 0.766$, $p > 0.05$).

(I) PPR after DHPG in the presence of NESS-0327 (baseline 0.58 ± 0.03 versus post-DHPG 0.63 ± 0.06, $t_{11} = 1.404$, $p > 0.05$).

Error bars represent SEM. n indicates number of recorded neurons.

negatively modulating neurotransmitter release (Heifets and Castillo, 2009). However, whether mGluRs trigger endocannabinoid signaling within the LHb is unknown. We first tested whether CB1-Rs are functionally expressed in the LHb. The CB1-R agonist WIN-55,212-2 reduced EPSC amplitude and increased the PPR (Figures 3D and 3E). This intervention occluded DHPG eLTD, suggesting that mGluR-eLTD expresses through CB1-R activation (Figures 3D and 3E). We pharmacologically confirmed that CB1-Rs are required for WIN-55,212-2-driven EPSC reduction because this was prevented by bath application of the CB1-R neutral antagonist NESS-0327 (Meye et al., 2013; Figures 3F and 3G). Consistent with the idea that CB1-Rs underlie the presynaptic expression of mGluR-eLTD, NESS-0327 also prevented mGluR-dependent plasticity and the concomitant increase in PPR (Figures 3H and 3I). This suggests that mGluR-eLTD requires a PKC-dependent and CB1-Rs-mediated reduction in presynaptic glutamate release.

Postsynaptic Mechanisms for mGluR-iLTD in the LHb

Because mGluR-driven endocannabinoid mobilization can also modulate GABA transmission (Chevaleyre et al., 2006), we questioned whether mGluR-iLTD requires a reduction in GABA release. We first examined the PPR of IPSCs before and after DHPG or HFS. mGluR-iLTD and HFS-iLTD occurred without PPR modifications, independent of the pharmacological intervention, suggesting the absence of presynaptic adaptations at inhibitory synapses (Figure 4A; Figures S2B and S2D). In line with this finding, mIPSC frequency remained unchanged, whereas mIPSCs amplitude decreased after DHPG application (Figure 4B). Moreover, NESS-0327 did not prevent the mGluR-dependent reduction in GABAergic transmission (Figure 4C). Together, these findings support that mGluR-iLTD is independent of endocannabinoid-driven presynaptic modifications. These data suggest instead a postsynaptic expression mechanism for mGluR-iLTD in contrast to the presynaptically expressed mGluR-eLTD.

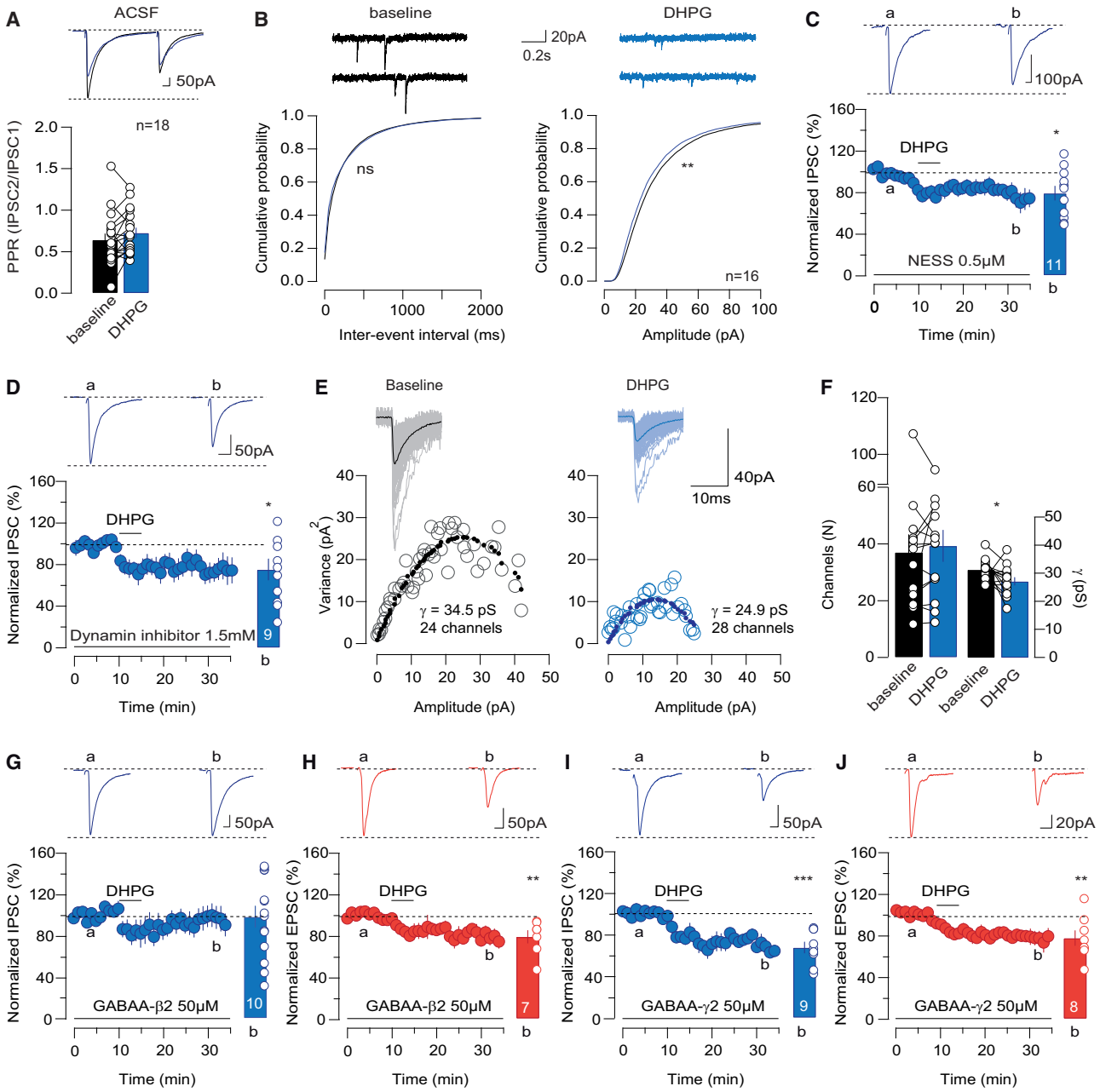

Figure 4. PKC Action on the $GABA_A$-Rs-β2 Subunit Underlies mGluR-iLTD

(A) PPR of IPSCs after DHPG (baseline 0.64 ± 0.07 versus post-DHPG 0.73 ± 0.06, t_{17} = 1.739, p > 0.05).

(B) Top: sample traces of mIPSCs. Cumulative probability plots show inter-event intervals and amplitudes for IPSCs at baseline (black) and after DHPG (blue) (mIPSC amplitude: baseline 41.3 ± 5.9 pA versus post-DHPG 39.2 ± 4.83 pA, KS test, **p < 0.01; mIPSC frequency: baseline 3.6 ± 1.09 Hz versus post-DHPG 3.45 ± 1.13 Hz, KS test, p > 0.05).

(C) Effect of DHPG on IPSCs in the presence of NESS-0327 (79.1 ± 7.06%, t_{10} = 2.621, *p < 0.05).

(D) DHPG effect on IPSCs in the presence of intracellular dynamin inhibitor (75.2 ± 10.2%, t_8 = 2.378, *p < 0.05).

(E) Example of peak-scaled NSFA of mIPSCs at baseline (black) and after DHPG (blue). Insets, overlay and average of analyzed traces.

(F) Pooled data for N and γ after NSFA (N: baseline 37 ± 6.3 versus post-DHPG 39.3 ± 5.6; t_{13} = 0.8, p > 0.05; γ: baseline 31.4 ± 1 versus post-DHPG 27.2 ± 1.4; t_{13} = 2.4, *p < 0.05).

(G) The same as (D) but in the presence of intracellular $GABA_A$-β2 peptide (97.7 ± 10.4%, t_{13} = 0.225, p > 0.05).

(H) The same as (G) but for EPSCs (78.8 ± 6.3%, t_6 = 3.488, *p < 0.05).

(I) The same as (G) but in the presence of intracellular $GABA_A$-γ2 peptide (67.7 ± 5.5%, t_8 = 6.141, ***p < 0.001).

(J) The same as (I) but for EPSCs (77.7 ± 7.4%, t_7 = 3.014, *p < 0.05).

Error bars represent SEM. n indicates number of recorded neurons.

Whether and how mGluR-PKC signaling modulates postsynaptic $GABA_A$-R function remains unknown. PKC can directly target $GABA_A$-Rs as well as auxiliary proteins modifying receptors' membrane expression and function (Kittler and Moss, 2003). For instance, PKC activation can increase $GABA_A$-R internalization via a dynamin-dependent mechanism (Herring et al., 2005). To examine whether mGluR-iLTD in the LHb requires $GABA_A$-R internalization, we dialyzed neurons with a membrane-impermeable dynamin inhibitor to prevent endocytosis. This intervention left mGluR-iLTD intact (Figure 4D), suggesting that $GABA_A$-R internalization is not required. To corroborate the absence of changes in the number of postsynaptic $GABA_A$-Rs during mGluR-iLTD, we employed peak-scaled non-stationary fluctuation analysis (NSFA) of mIPSCs (Maroteaux and Mameli, 2012; Nusser et al., 2001). Based on the stochastic closing of ion channels, this statistical method allows us to estimate the number of receptors opened (N) by neurotransmitter release as well as their single-channel conductance (γ). Plotting the decay variance as a function of the mean current amplitude for all recorded neurons yielded $\gamma_{GABA\text{-}A\text{-}R}$ values comparable to previous studies (31.4 ± 1 pS; Figures 4E and 4F; Nusser et al., 2001). DHPG decreased estimated $\gamma_{GABA\text{-}A\text{-}Rs}$ without altering estimated $N_{GABA\text{-}A\text{-}Rs}$ (Figures 4E and 4F). Together, this supports the absence of mGluR-driven $GABA_A$-R internalization. Conversely, a reduction in $\gamma_{GABA\text{-}A\text{-}R}$ suggests a decrease in $GABA_A$-R function, a modulation that may result from subunit-specific PKC-mediated phosphorylation (Kittler and Moss, 2003). Consistently, PKC-driven phosphorylation of specific serine residues on the $GABA_A$-R β1-3 and γ2 subunits reduces receptor function without altering the total receptor pool (Brandon et al., 2002a; Feng et al., 2001; Kittler and Moss, 2003). Given the reported expression of $GABA_A$-R β2 and γ2 subunits within the LHb (Hörtnagl et al., 2013), we predicted that the described mGluR-iLTD results from the direct PKC modulation of specific $GABA_A$-R subunits. To test this, we dialyzed dominant-negative peptides corresponding to the PKC-targeted sequences of $GABA_A$-R β2 or γ2 subunits (Brandon et al., 2000; Feng et al., 2001). The presence of the β2 peptide ($GABA_A$-β2) prevented mGluR-iLTD. In contrast, mGluR-eLTD and the concomitant PPR increase remained intact, ruling out non-specific actions of $GABA_A$-β2 dialysis (Figures 4G and 4H; Figures S2C and S2D). Intracellular infusion of the γ2 peptide ($GABA_A$-γ2) did not affect the expression of mGluR-iLTD or mGluR-eLTD (Figures 4I and 4J; Figures S2C and S2D). These data suggest that mGluRs trigger a PKC-dependent reduction in $GABA_A$-R conductance, likely occurring via phosphorylation of the β2 but not γ2 receptor subunits.

mGluRs Decide the Direction of LHb Neuronal Output

Opposed motivational states (i.e., reward and aversion) require bidirectional modification of LHb neuronal output, which can result in part from glutamatergic and GABAergic synaptic adaptations (Shabel et al., 2012; Stamatakis et al., 2013; Meye et al., 2015). What would be the functional repercussions of mGluR-eLTD and iLTD for LHb activity? To test the consequences of mGluR-LTD on LHb neuronal output, we recorded synaptically evoked postsynaptic potentials (PSPs) in current clamp mode. In the absence of synaptic blockers, PSPs result from a mixture of glutamatergic and GABAergic components and are therefore susceptible to mGluR-eLTD and -iLTD. We delivered trains of ten stimuli (20 Hz) and set the stimulation intensity so that ~50% of evoked PSPs would produce action potentials (APs) (Figure 5A). Ten minutes after DHPG washout, a time point where mGluR-eLTD and -iLTD are fully expressed, AP numbers either increased or decreased (>20% change in APs) in ~64% of neurons. Because of this dual modulation, DHPG did not, on average, modify the extent of evoked APs (Figure 5A). However, the bidirectional mGluR-driven change in neuronal activity may result from the expression of either mGluR-eLTD or -iLTD. Therefore, we examined whether the direction of LHb neuronal output after DHPG application correlates with mGluR-mediated modulation of PSPs. The area under individual PSPs (not including APs) was computed and averaged before and after DHPG to assess the PSPs potentiation or inhibition after mGluR activation. We predicted that the mGluR-mediated increase in PSPs would facilitate firing as a consequence of mGluR-iLTD. Conversely, predominant mGluReLTD would reduce the PSP area, decreasing neuronal output. In line with this scenario, the mGluR-driven change in PSP area positively correlated with the DHPG-driven modulation of AP number (Figures 5A and 5B). To determine the causality between mGluR-eLTD/iLTD and the firing adaptations, we prevented the expression mechanisms underlying mGluR-LTD at excitatory and inhibitory synapses. Concomitantly blocking CB1-R and PKC action on $GABA_A$-β2 receptors led to DHPG-driven modulation of LHb neuronal firing (>20% change in APs) in only 12.5% of recorded neurons. Under this condition, no correlation occurred between PSP area and firing after mGluR activation (Figures 5C and 5D). In contrast, independently preventing either mGluR-eLTD or -iLTD expression mechanisms revealed a marked bidirectional DHPG-induced modulation of evoked firing (Figures S3A and S3B). Furthermore, input resistance and AP properties did not change or correlate with DHPG-mediated firing changes (Figures S3C–S3H).

If the occurrence of mGluR-dependent plasticity differs at excitatory or inhibitory synapses from specific inputs, this would partly explain the predominant influence of either mGluR-eLTD or -iLTD on neuronal output. LHb neurons receive axons from the entopeduncular nucleus (EPN, EPN^{LHb}) that co-release glutamate and GABA (Shabel et al., 2012). This allows us to examine whether mGluR-LTD occurs in a neurotransmission-specific fashion at a precise synaptic input. As a proof of concept, we virally expressed channelrhodopsin-2 (ChR2) in the EPN. This led to $ChR2^+$ terminals within the lateral aspect of the LHb (Shabel et al., 2012; Meye et al., 2016; Figure S4A). DHPG bath application triggered a LTD of light-evoked EPN^{LHb} IPSCs, whereas light-evoked EPN^{LHb} EPSCs remained unaffected (Figures S4B and S4C). Together, these findings suggest that mGluRs in the LHb can control the direction of neuronal activity, likely via input-specific eLTD or iLTD.

DISCUSSION

Here we demonstrate that group I mGluRs decrease excitatory and inhibitory synaptic transmission in the LHb in a

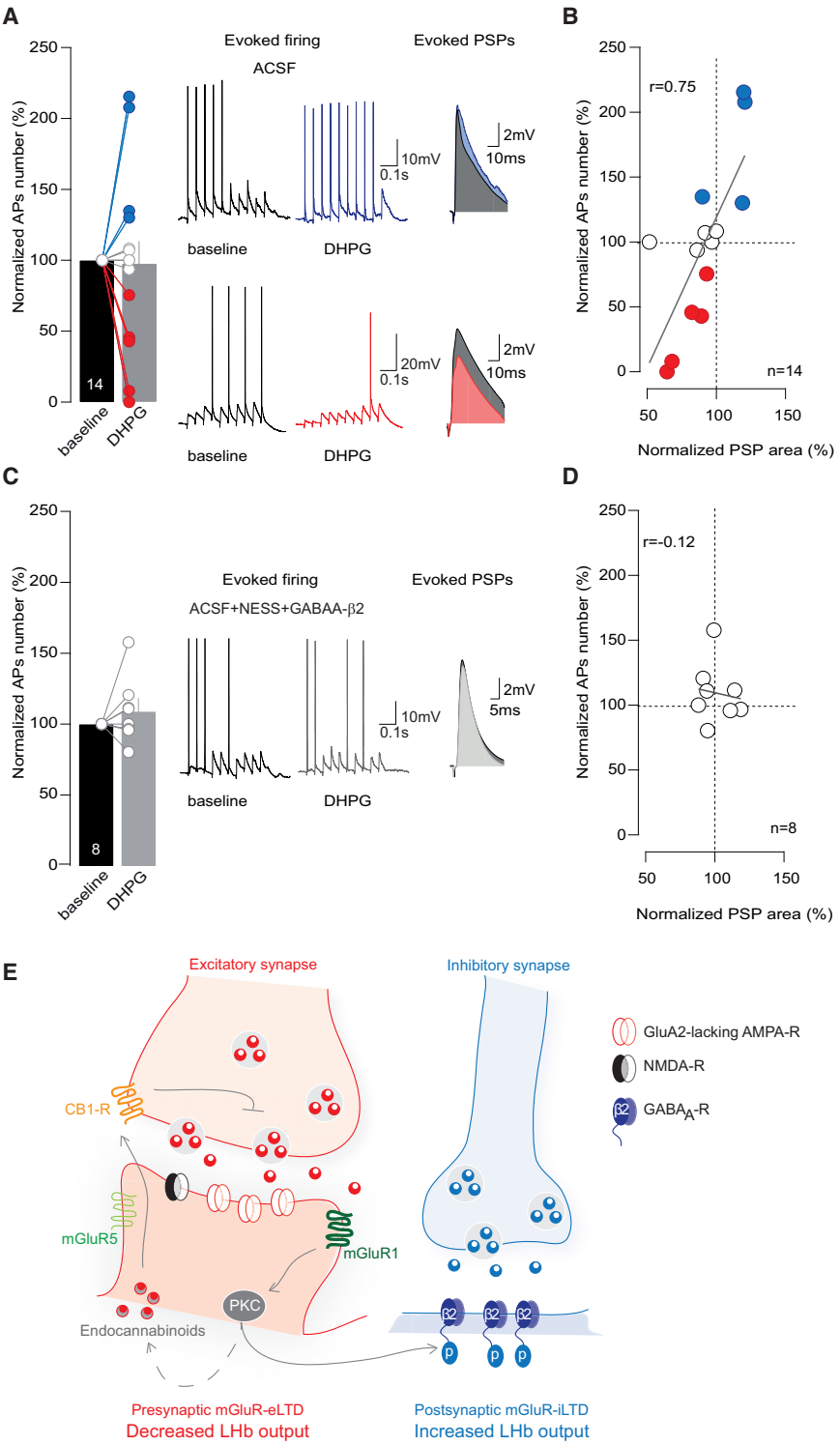

Figure 5. mGluR-Dependent Bidirectional Control of LHb Neuronal Output

(A) DHPG effect on synaptically evoked AP numbers in ACSF (97.7 ± 19.6; $t_{13} = 0.13$, $p > 0.05$). 4 of 14 recorded neurons increased in firing (blue), and 5 of 14 decreased in firing (red) following DHPG. Sample traces indicate the bidirectional nature (blue increased firing, red decreased firing) of mGluR activation. Shown are superimposed EPSPs at baseline (black) and after DHPG (blue, increased firing; red, decreased firing).

(B) Correlation between normalized mGluR-driven firing and normalized PSP area (Pearson correlation, $r = 0.75$, $^{**}p < 0.01$).

(C) The same as (A) but in the presence of NESS-0327 and $GABA_A$-β2 peptide in the internal solution (109.2 ± 8.2, $t_7 = 1.12$, $p > 0.05$). Black and gray traces represent before and after DHPG.

(D) The same as (B) but in the presence of NESS-0327 in the ACSF and $GABA_A$-β2 peptide in the internal solution (Pearson correlation, $r = -0.12$, $p > 0.05$). Fisher r-to-z transformation for (B) versus (D) correlations yielded a Z score of 2.03. $^{*}p < 0.05$.

(E) Schematic indicating the induction and expression mechanisms for mGluR-eLTD and -iLTD and their relative contribution to LHb neuronal output.

Error bars represent SEM. n indicates number of recorded neurons.

PKC-dependent manner. On one hand, mGluR1-driven PKC activation in LHb represents a common process at excitatory and inhibitory synapses. On the other hand, mGluR1 signaling diverges at the level of PKC, targeting distinct substrates but leading to decreased glutamatergic and GABAergic neurotransmission. mGluR-eLTD and -iLTD modulate PSPs to decide the direction of LHb neuronal output. Our data support a scenario in which mGluRs modulate glutamatergic and GABAergic synapses in the LHb, contributing to adaptations in their computational properties potentially relevant for motivational states.

Notably, excitatory synapses in the LHb contain rectifying GluA2-lacking AMPA-Rs (Maroteaux and Mameli, 2012). A recent hypothesis posits that GluA2-lacking AMPA-R expression represents a predictive factor for a postsynaptic mGluR1-LTD requiring a subunit composition switch (Loweth et al., 2013). However, mGluR1 activation in the LHb reduces excitatory synaptic transmission while leaving the GluA2-lacking AMPA-R current-voltage relationship unchanged. This unaffected AMPA-Rs rectification may result from LHb-specific interactions between receptors and scaffolding proteins or, alternatively, from unidentified AMPA-Rs subtypes that would need to be further investigated.

In contrast, mGluR1s in the LHb act through postsynaptic PKC signaling to reduce glutamate release via CB1-R activation. Together with evidence indicating that LHb contains the endocannabinoid-synthesizing enzyme diacylglicerol lipase (Suárez et al., 2011), our data support functional endocannabinoid

signaling within the LHb. mGluR-driven endocannabinoid LTD is also observed at inhibitory synapses (Chevaleyre et al., 2006); however, this does not hold true in the LHb. Indeed, mGluR-iLTD is independent of presynaptic modifications and remains intact in the presence of CB1-R blockers. Although mGluR-iLTD does not require CB1-Rs, other G_q protein-coupled receptors (GPCRs) may mobilize endocannabinoids to drive iLTD. Future studies need to address whether CB1-R activation modifies GABA transmission or whether other GPCRs mediate endocannabinoid-dependent iLTD in the LHb.

Although PKC mediates the presynaptic expression of mGluR-eLTD, it reduces GABA transmission through a postsynaptic mechanism. Importantly, postsynaptic PKC signaling controls the strength of inhibitory neurotransmission (Kittler and Moss, 2003). For instance, PKC can induce rapid internalization of $GABA_A$-Rs through its actions on specific serine residues (Chapell et al., 1998; Herring et al., 2005). However, mGluR-iLTD in the LHb is independent of dynamin-mediated endocytosis and does not involve a reduction in the number of activated receptors. Instead, mGluRs promote a reduction in $GABA_A$-R single-channel conductance. This modification in $GABA_A$-R function may result from alterations in subunit composition, scaffolding proteins, and phosphorylation events (Kittler and Moss, 2003). Indeed, PKC reduces $GABA_A$-R function, but not receptor expression, via phosphorylation of key residues on the $GABA_A$-R β and γ subunits (Brandon et al., 2000, 2002b; Feng et al., 2001). We report that PKC action on $GABA_A$-R β2-subunits, but not on γ2 subunits, is crucial for mGluR-iLTD in the LHb. Interestingly, different subtypes of G_q-PCRs other than group I mGluRs (i.e., muscarinic acetylcholine and serotonin receptors) also reduce $GABA_A$-R function by PKC targeting of $GABA_A$-R β1 and γ2 subunits (Feng et al., 2001; Brandon et al., 2002a). This evidence therefore raises the possibility that different classes of G_q-PCRs across the CNS may reduce synaptic inhibition via PKC phosphorylation of specific $GABA_A$-R subunits (i.e., β2, γ2, β1) (Brandon et al., 2002b; Feng et al., 2001; Kittler and Moss, 2003).

mGluR-eLTD and -iLTD are widespread across many synapses (Chevaleyre et al., 2006), but their functional repercussions on neuronal output remain elusive. mGluR1 can affect potassium and calcium conductances, crucial for neuronal activity (Anwyl, 1999). However, the reported absence of changes in input resistance and AP properties suggests that mGluR-driven modulation of neuronal activity likely arises from synaptic adaptations. The mGluR-dependent potentiation and inhibition of PSPs indeed predicts the direction of neuronal output after mGluR activation. Moreover, precluding mGluR-eLTD and -iLTD concomitantly or independently unravels the causality between synaptic plasticity and mGluR-dependent control of LHb neuronal firing. This result also suggests that mGluR-eLTD and -iLTD likely do not occur simultaneously at the same locus and with the same extent. Instead, one predominates over the other, to drive, in different neurons, opposite neuronal output changes. mGluR-eLTD and -iLTD may occur together with similar magnitude but on distinct postsynaptic sites or even distinct LHb neuronal populations. In both cases, mGluR plasticity would ultimately lead to a bidirectional modulation of LHb global activity. These scenarios may rely, to some degree, on circuit specificity. The observation that the EPN^{LHb} GABAergic but not glutamatergic component is affected by mGluRs strongly suggests that, in the LHb, mGluR1 modulation may occur in a neurotransmission- and input-specific fashion. This is in in line with our data indicating that different patterns of activity trigger either mGluR-eLTD or -iLTD, and it is further supported by findings describing that input/output-specific plasticity controls LHb output firing (Shabel et al., 2014; Meye et al., 2016). In conclusion, these findings identify how mGluR1 signaling in the LHb diverges at the level of PKC, leading to reduced presynaptic glutamate release and postsynaptic $GABA_A$-R function. Based on our results, we speculate that mGluR-LTD in the LHb can decide the direction of neuronal activity, potentially influencing opposing motivational states.

EXPERIMENTAL PROCEDURES

Animals

C57Bl/6J male mice (~30 days old) were used in accordance with the guidelines of the French Agriculture and Forestry Ministry for handling animals, and protocols were validated by the Darwin#5 ethical committee of the University Pierre et Marie Curie. Mice were anesthetized (i.p.) with ketamine (150 mg/kg)/xylazine (100 mg/kg) (Sigma-Aldrich) prior to brain slice preparation or viral injections (Supplemental Experimental Procedures).

In Vitro Electrophysiology

Sagittal slices (250 μm) containing the LHb were prepared, and recordings were performed as described previously (Maroteaux and Mameli, 2012). For voltage clamp experiments, the internal solution contained 130 mM CsCl, 4 mM NaCl, 2 mM $MgCl_2$, 1.1 mM EGTA, 5 mM HEPES, 2 mM Na_2ATP, 0.6 mM Na_3GTP, 5 mM Na^+ creatine phosphate, 2 mM QX-314, and 0.1 mM spermine ; (pH 7.3), osmolarity ~300 mOsm. The holding potential was –50 mV. Synaptic currents were evoked through a glass pipette placed in the stria medullaris (60 μs at 0.1 Hz). The PPR was monitored (2 pulses, 20 Hz) and calculated as follows: $EPSC_2/EPSC_1$. mGluRs were activated by DHPG (50 μM) in the presence of 2,3-dihydroxy-6-nitro-7-sulfamoyl-benzo[f]quinoxaline-2,3-dione (NBQX; 10 μM) and D-(2*R*)-amino-5-phosphonovaleric acid; (2*R*)-amino-5-phosphonopentanoate (D-APV; 50–100 μM) or picrotoxin (100 μM). An LFS protocol (1 Hz, 15 min) or an HFS protocol (100 Hz at 0 mV for 1 s, 5 times every 10 s) was used for synaptic activation of mGluRs. The rectification index of AMPA-EPSCs was calculated as follows: $((I_{EPSC(-60)}/I_{EPSC(+40)})/1.5)$. Experiments assessing the postsynaptic effects of DHPG (voltage clamp) and output firing (current clamp) were performed with internal solution containing 140 mM KGluconate, 5 mM KCl, 10 mM HEPES, 0.2 mM EGTA, 2 mM $MgCl_2$, 4 mM Na_2ATP, 0.3 mM Na_3GTP, and 10 mM creatine phosphate; (pH 7.3), osmolarity ~300 mOsm. The input resistance was calculated via a 50-ms hyperpolarizing current (I = 20 pA) step (Ri = resting membrane potential [RMP]/I).

Non-stationary Fluctuation Analysis

A peak-scaled non-stationary fluctuation analysis was made from mIPSCs (Synaptosoft; Supplemental Experimental Procedures).

Drugs and Peptides

Drugs were obtained from Abcam, Tocris, Hello Bio, or Latoxan and dissolved in water. Tetrodotoxin (TTX) was dissolved in citric acid (1%); picrotoxin, NESS-0327, WIN-55,212-2, and PMA in DMSO; and LY367385 in NaOH 10%. For PMA experiments, only cells responding to drug application were included in the analysis. Peptides used in the study were custom-made (GeneScript) or obtained from Tocris (Supplemental Experimental Procedures) and, when indicated, included in the internal solution.

Analysis

Analysis was performed using IGOR-6 (Wavemetrics) and MiniAnalysis (Synaptosoft). Kolmogorov-Smirnov (KS) test, Student's t test, or ANOVA were used throughout the study. n in the figures indicates number of recorded

neurons. All data are expressed as mean ± SEM. Significance was set at alpha = 0.05 using paired t test.

SUPPLEMENTAL INFORMATION

Supplemental Information includes Supplemental Experimental Procedures and four figures and can be found with this article online at http://dx.doi.org/10.1016/j.celrep.2016.07.064.

AUTHOR CONTRIBUTIONS

K.V. and M.M. designed and performed the experiments, analyzed the data, and wrote the paper.

ACKNOWLEDGMENTS

We thank M. Carta, V. Chevaleyre, C. Bellone, N. Gervasi, and the Poncer-Levi and M.M. laboratory for helpful discussions and comments. We thank I. Moutkine for help with PCR experiments. This work was supported by Inserm ATIP-AVENIR, the City of Paris, and the European Research Council (ERC) under the European Union's Seventh Framework Program (FP7/2007-2013)/ERC grant agreement number 335333 SalienSy (to M.M.). K.V. is supported by a Ph.D. fellowship from the doctoral school ED3C Paris.

Received: December 14, 2015
Revised: June 27, 2016
Accepted: July 25, 2016
Published: August 18, 2016

REFERENCES

Anwyl, R. (1999). Metabotropic glutamate receptors: electrophysiological properties and role in plasticity. Brain Res. Brain Res. Rev. *29*, 83–120.

Bellone, C., and Lüscher, C. (2005). mGluRs induce a long-term depression in the ventral tegmental area that involves a switch of the subunit composition of AMPA receptors. Eur. J. Neurosci. *21*, 1280–1288.

Bellone, C., and Mameli, M. (2012). mGluR-Dependent Synaptic Plasticity in Drug-Seeking. Front. Pharmacol. *3*, 159.

Brandon, N.J., Delmas, P., Kittler, J.T., McDonald, B.J., Sieghart, W., Brown, D.A., Smart, T.G., and Moss, S.J. (2000). GABAA receptor phosphorylation and functional modulation in cortical neurons by a protein kinase C-dependent pathway. J. Biol. Chem. *275*, 38856–38862.

Brandon, N., Jovanovic, J., and Moss, S. (2002a). Multiple roles of protein kinases in the modulation of gamma-aminobutyric acid(A) receptor function and cell surface expression. Pharmacol. Ther. *94*, 113–122.

Brandon, N.J., Jovanovic, J.N., Smart, T.G., and Moss, S.J. (2002b). Receptor for activated C kinase-1 facilitates protein kinase C-dependent phosphorylation and functional modulation of GABA(A) receptors with the activation of G-protein-coupled receptors. J. Neurosci. *22*, 6353–6361.

Chapell, R., Bueno, O.F., Alvarez-Hernandez, X., Robinson, L.C., and Leidenheimer, N.J. (1998). Activation of protein kinase C induces gamma-aminobutyric acid type A receptor internalization in Xenopus oocytes. J. Biol. Chem. *273*, 32595–32601.

Chevaleyre, V., Takahashi, K.A., and Castillo, P.E. (2006). Endocannabinoid-mediated synaptic plasticity in the CNS. Annu. Rev. Neurosci. *29*, 37–76.

Feng, J., Cai, X., Zhao, J., and Yan, Z. (2001). Serotonin receptors modulate GABA(A) receptor channels through activation of anchored protein kinase C in prefrontal cortical neurons. J. Neurosci. *21*, 6502–6511.

Galante, M., and Diana, M.A. (2004). Group I metabotropic glutamate receptors inhibit GABA release at interneuron-Purkinje cell synapses through endocannabinoid production. J. Neurosci. *24*, 4865–4874.

Gee, C.E., Benquet, P., and Gerber, U. (2003). Group I metabotropic glutamate receptors activate a calcium-sensitive transient receptor potential-like conductance in rat hippocampus. J. Physiol. *546*, 655–664.

Heifets, B.D., and Castillo, P.E. (2009). Endocannabinoid signaling and long-term synaptic plasticity. Annu. Rev. Physiol. *71*, 283–306.

Herring, D., Huang, R., Singh, M., Dillon, G.H., and Leidenheimer, N.J. (2005). PKC modulation of GABAA receptor endocytosis and function is inhibited by mutation of a dileucine motif within the receptor beta 2 subunit. Neuropharmacology *48*, 181–194.

Hörtnagl, H., Tasan, R.O., Wieselthaler, A., Kirchmair, E., Sieghart, W., and Sperk, G. (2013). Patterns of mRNA and protein expression for 12 GABAA receptor subunits in the mouse brain. Neuroscience *236*, 345–372.

Hovelsø, N., Sotty, F., Montezinho, L.P., Pinheiro, P.S., Herrik, K.F., and Mørk, A. (2012). Therapeutic potential of metabotropic glutamate receptor modulators. Curr. Neuropharmacol. *10*, 12–48.

Kammermeier, P.J., Xiao, B., Tu, J.C., Worley, P.F., and Ikeda, S.R. (2000). Homer proteins regulate coupling of group I metabotropic glutamate receptors to N-type calcium and M-type potassium channels. J. Neurosci. *20*, 7238–7245.

Kelly, L., Farrant, M., and Cull-Candy, S.G. (2009). Synaptic mGluR activation drives plasticity of calcium-permeable AMPA receptors. Nat. Neurosci. *12*, 593–601.

Kittler, J.T., and Moss, S.J. (2003). Modulation of GABAA receptor activity by phosphorylation and receptor trafficking: implications for the efficacy of synaptic inhibition. Curr. Opin. Neurobiol. *13*, 341–347.

Lecca, S., Meye, F.J., and Mameli, M. (2014). The lateral habenula in addiction and depression: an anatomical, synaptic and behavioral overview. Eur. J. Neurosci. *39*, 1170–1178.

Lecca, S., Pelosi, A., Tchenio, A., Moutkine, I., Lujan, R., Hervé, D., and Mameli, M. (2016). Rescue of GABAB and GIRK function in the lateral habenula by protein phosphatase 2A inhibition ameliorates depression-like phenotypes in mice. Nat. Med. *22*, 254–261.

Loweth, J.A., Tseng, K.Y., and Wolf, M.E. (2013). Using metabotropic glutamate receptors to modulate cocaine's synaptic and behavioral effects: mGluR1 finds a niche. Curr. Opin. Neurobiol. *23*, 500–506.

Lüscher, C., and Huber, K.M. (2010). Group 1 mGluR-dependent synaptic long-term depression: mechanisms and implications for circuitry and disease. Neuron *65*, 445–459.

Mameli, M., Balland, B., Luján, R., and Lüscher, C. (2007). Rapid synthesis and synaptic insertion of GluR2 for mGluR-LTD in the ventral tegmental area. Science *317*, 530–533.

Maroteaux, M., and Mameli, M. (2012). Cocaine evokes projection-specific synaptic plasticity of lateral habenula neurons. J. Neurosci. *32*, 12641–12646.

McCutcheon, J.E., Loweth, J.A., Ford, K.A., Marinelli, M., Wolf, M.E., and Tseng, K.Y. (2011). Group I mGluR activation reverses cocaine-induced accumulation of calcium-permeable AMPA receptors in nucleus accumbens synapses via a protein kinase C-dependent mechanism. J. Neurosci. *31*, 14536–14541.

Meye, F.J., Trezza, V., Vanderschuren, L.J., Ramakers, G.M., and Adan, R.A. (2013). Neutral antagonism at the cannabinoid 1 receptor: a safer treatment for obesity. Mol. Psychiatry *18*, 1294–1301.

Meye, F.J., Valentinova, K., Lecca, S., Marion-Poll, L., Maroteaux, M.J., Musardo, S., Moutkine, I., Gardoni, F., Huganir, R.L., Georges, F., and Mameli, M. (2015). Cocaine-evoked negative symptoms require AMPA receptor trafficking in the lateral habenula. Nat. Neurosci. *18*, 376–378.

Meye, F.J., Soiza-Reilly, M., Smit, T., Diana, M.A., Schwarz, M.K., and Mameli, M. (2016). Shifted pallidal co-release of GABA and glutamate in habenula drives cocaine withdrawal and relapse. Nat. Neurosci. *19*, 1019–1024.

Nusser, Z., Naylor, D., and Mody, I. (2001). Synapse-specific contribution of the variation of transmitter concentration to the decay of inhibitory postsynaptic currents. Biophys. J. *80*, 1251–1261.

Oliet, S.H., Malenka, R.C., and Nicoll, R.A. (1997). Two distinct forms of long-term depression coexist in CA1 hippocampal pyramidal cells. Neuron *18*, 969–982.

Page, G., Peeters, M., Najimi, M., Maloteaux, J.M., and Hermans, E. (2001). Modulation of the neuronal dopamine transporter activity by the metabotropic

glutamate receptor mGluR5 in rat striatal synaptosomes through phosphorylation mediated processes. J. Neurochem. *76*, 1282–1290.

Shabel, S.J., Proulx, C.D., Trias, A., Murphy, R.T., and Malinow, R. (2012). Input to the lateral habenula from the basal ganglia is excitatory, aversive, and suppressed by serotonin. Neuron *74*, 475–481.

Shabel, S.J., Proulx, C.D., Piriz, J., and Malinow, R. (2014). Mood regulation. GABA/glutamate co-release controls habenula output and is modified by antidepressant treatment. Science *345*, 1494–1498.

Stamatakis, A.M., Jennings, J.H., Ung, R.L., Blair, G.A., Weinberg, R.J., Neve, R.L., Boyce, F., Mattis, J., Ramakrishnan, C., Deisseroth, K., and Stuber, G.D. (2013). A unique population of ventral tegmental area neurons inhibits the lateral habenula to promote reward. Neuron *80*, 1039–1053.

Suárez, J., Ortíz, O., Puente, N., Bermúdez-Silva, F.J., Blanco, E., Fernández-Llebrez, P., Grandes, P., de Fonseca, F.R., and Moratalla, R. (2011). Distribution of diacylglycerol lipase alpha, an endocannabinoid synthesizing enzyme, in the rat forebrain. Neuroscience *192*, 112–131.

Cell Reports, Volume *16*

Supplemental Information

mGluR-LTD at Excitatory and Inhibitory Synapses in the Lateral Habenula Tunes Neuronal Output

Kristina Valentinova and Manuel Mameli

Supplemental information.

mGluR-LTD at excitatory and inhibitory synapses in the lateral habenula tune neuronal output

Kristina Valentinova[1,2,3], and Manuel Mameli[1,2,3]

[1] Institut du Fer à Moulin, 75005 Paris, France.

[2]Inserm, UMR-S 839, 75005 Paris, France.

[3]Université Pierre et Marie Curie 75005 Paris, France.

Correspondance to manuel.mameli@inserm.fr

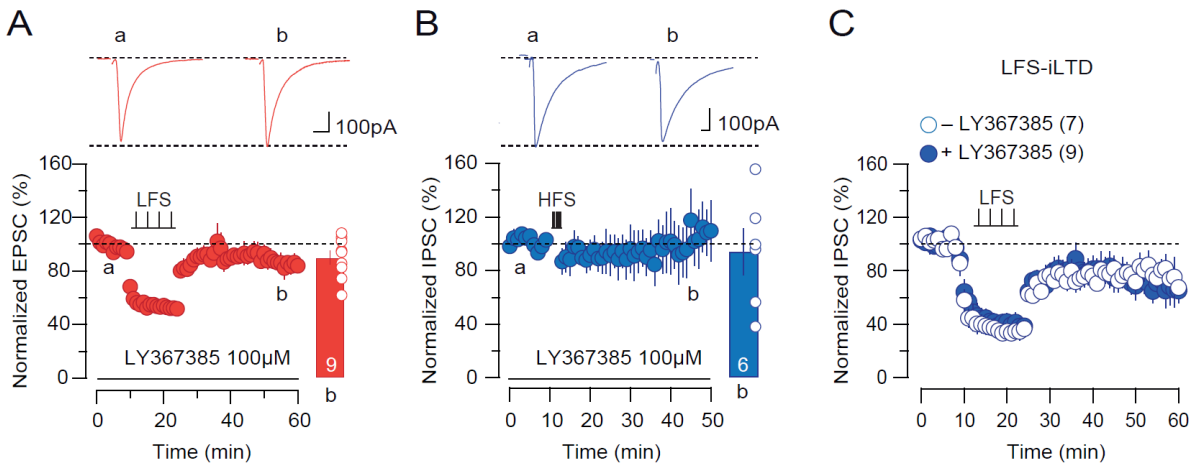

Figure S1. mGluR1-dependent LFS-eLTD and HFS-iLTD in the LHb. Related to Figure 1 and Figure 2.

(A). Low frequency stimulation (1 Hz, 15 min) eLTD is blocked by the mGluR1 antagonist LY367385. Bar graph and scatter plot show normalized averaged EPSCs ~40 min after the protocol (89.9±5%, t_8=1.941, p>0.05).

(B). Effect of the mGluR1 antagonist LY367385 on high frequency stimulation (100 Hz, 1 sec, at 0 mV)-driven iLTD (94.2±17.4%, t_5=0.394, p>0.05).

(C). Low frequency stimulation (1 Hz, 15 min) drives an iLTD (full circles) that remains not affected by the mGluR1 antagonist LY367385 (empty circles) (in ACSF, 77.4±8%, t_6=2.842, *p<0.05; in LY367385, 70.1.2±8.7%, t_8=3.415, **p<0.01). N in the figures indicates number of recorded neurons.

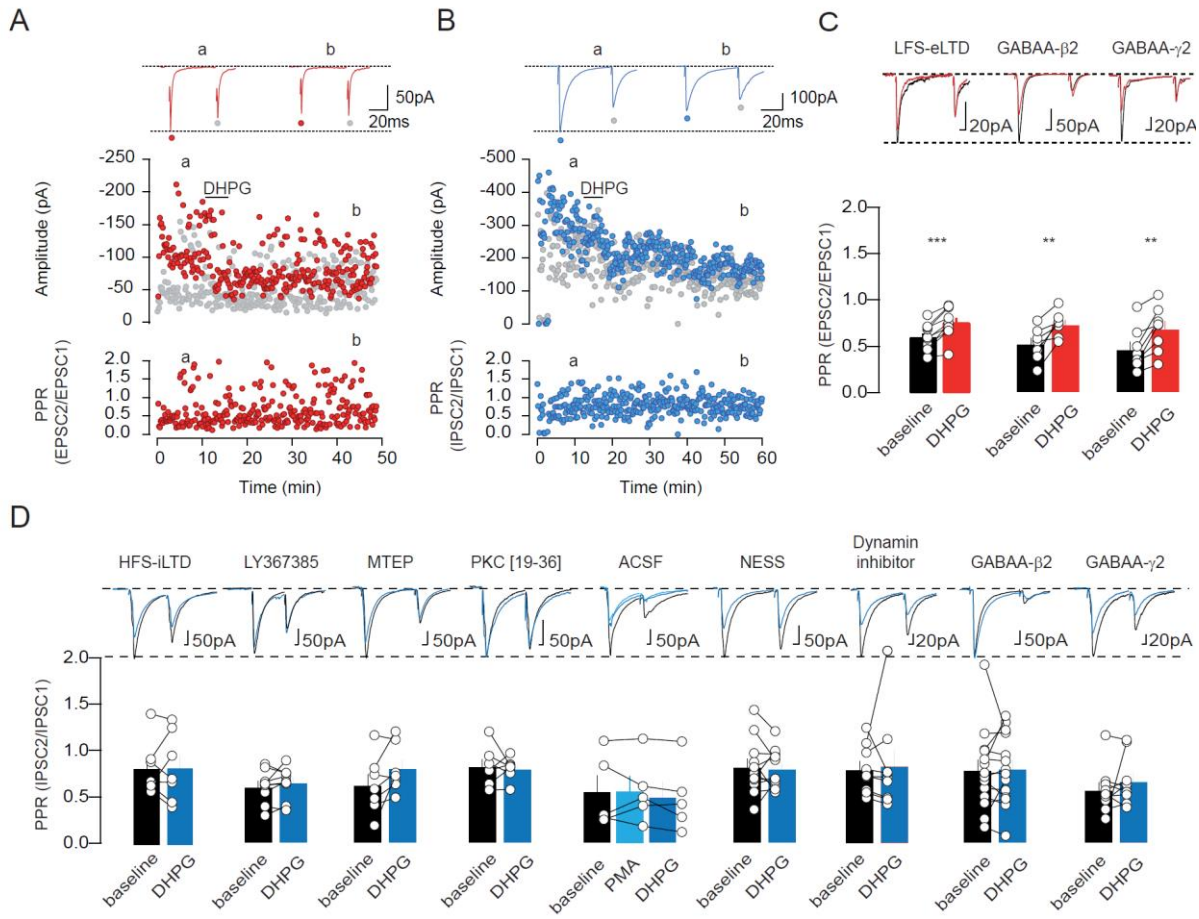

Figure S2. PPR analysis for EPSC and IPSC after mGluR activation. Related to Figure 1–4.

(A). Sample recordings indicating the parallel modulation of EPSCs and PPR after DHPG application.

(B). Same as A but for IPSCs.

(C). PPR of EPSCs after LFS (baseline 0.6±0.04 vs post-LFS 0.76±0.05, t_9=6.699, ***p<0.0001); PPR of EPSCs in the presence of intracellular $GABA_A$-β2 and γ2 peptide ($GABA_A$-β2, baseline 0.52±0.07 vs post-DHPG 0.73±0.05, t_6=4.127, **p<0.01; $GABA_A$-γ2, baseline 0.47±0.08 vs post-DHPG 0.68±0.09, t_7=4.303, **p<0.05). When not indicated time scale represents 5ms.

(D). PPR of IPSCs after HFS (baseline 0.79±0.1 vs post-HFS 0.79±0.1, t_6=0.1, p>0.05); PPR of IPSCs in presence of LY367385 (baseline 0.61±0.06 vs post-DHPG 0.65±0.06, t_8=1.166, p>0.05); of MTEP (baseline 0.63±0.12 vs post-DHPG 0.8±0.1, t_6=2.179, p>0.05); of PKC[19-36] in the recording pipette (baseline 0.83±0.08 vs post-DHPG 0.8±0.04, t_6=0.318, p>0.05); after PMA and DHPG (baseline 0.56±0.2 vs

PMA 0.56±0.16, t_4=0.107, p>0.05; baseline-PMA vs PMA-post-DHPG 0.5±0.2, t_4=0.794, p>0.05; PMA vs post-DHPG+PMA, t_4=1.812, p>0.05); in presence of NESS-0327 (baseline 0.82±0.09 vs post-DHPG 0.8±0.06, t_{10}=0.310, p>0.05); of dynamin inhibitor in the recording pipette (baseline 0.8±0.09 vs post-DHPG 0.83±0.2, t_8=0.280, p>0.05); of the GABA-β2 peptide in the recording pipette (baseline 0.79±0.12 vs post-DHPG 0.8±0.1, t_{13}=0.192, p>0.05); of the GABA-γ2 peptide in the recording pipette (baseline 0.57±0.08 vs post-DHPG 0.67±0.09, t_8=0.973, p>0.05). One way ANOVA among all baseline PPR conditions: $F_{(8, 80)}$=0.693, p>0.05. N in the figures indicates number of recorded neurons.

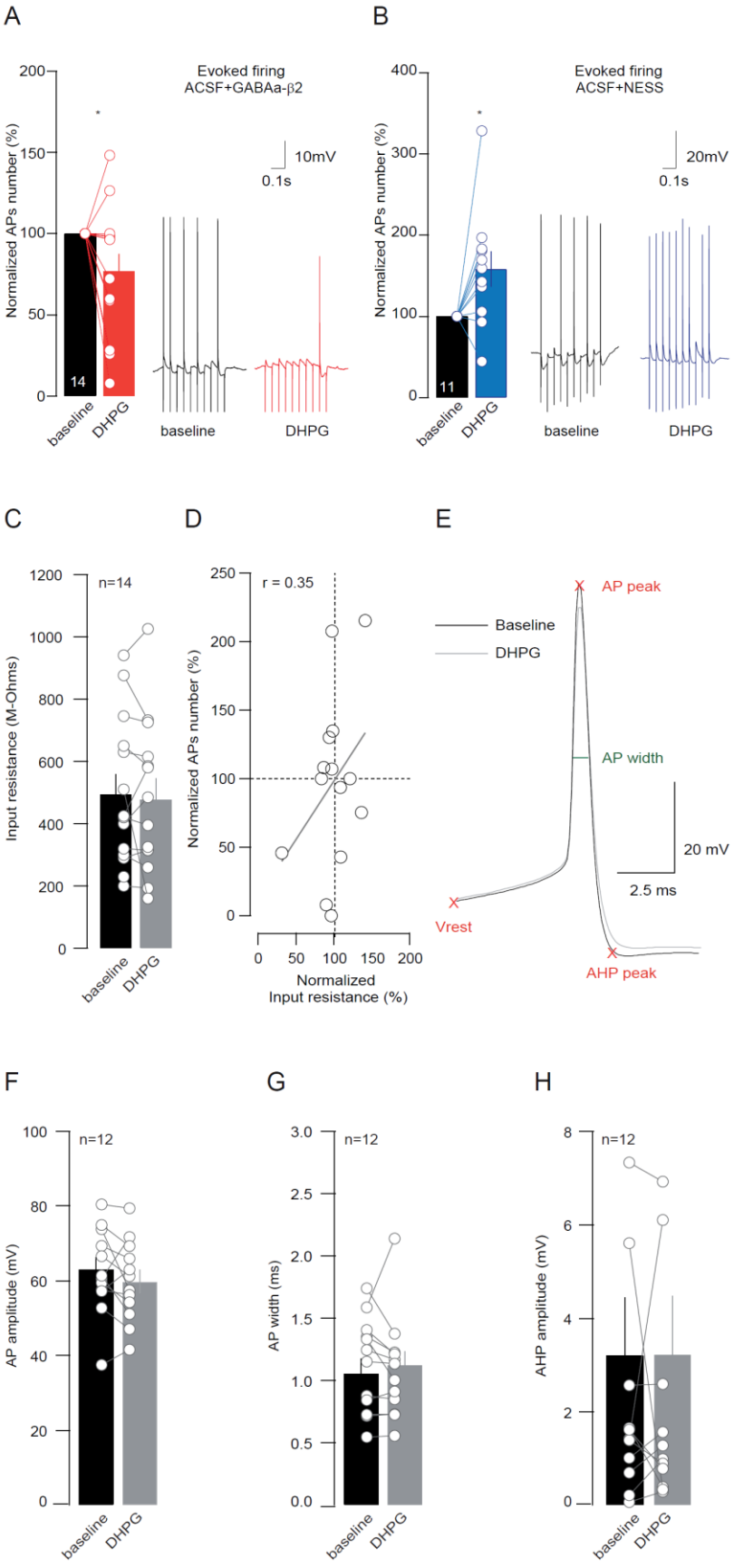
A
Evoked firing
ACSF+GABAa-β2
Normalized APs number (%)
200
150
100
50
0
14
baseline
DHPG
10mV
0.1s
baseline
DHPG
B
Evoked firing
ACSF+NESS
Normalized APs number (%)
400
300
200
100
0
11
baseline
DHPG
20mV
0.1s
baseline
DHPG
C
Input resistance (M-Ohms)
1200
1000
800
600
400
200
0
n=14
baseline
DHPG
D
Normalized APs number (%)
250
200
150
100
50
0
r = 0.35
0
50
100
150
200
Normalized
Input resistance (%)
E
AP peak
Baseline
DHPG
AP width
20 mV
2.5 ms
Vrest
AHP peak
F
AP amplitude (mV)
100
80
60
40
20
0
n=12
baseline
DHPG
G
AP width (ms)
3.0
2.5
2.0
1.5
1.0
0.5
0.0
n=12
baseline
DHPG
H
AHP amplitude (mV)
8
6
4
2
0
n=12
baseline
DHPG

Figure S3. Bidirectional control of firing by mGluR-LTD, unaltered input resistance and action potential properties after mGluR activation. Related to Figure 5.

(A). Normalized effect of DHPG on synaptically-evoked APs number in the presence of $GABA_A$-β2 peptide in the internal solution (76.9±10.6, t_{13}=2.183, *p<0.05).

(B). Normalized effect of DHPG on synaptically-evoked APs number in the presence of NESS-0327 (158.2±21.8; t_{10}=2.667, *p<0.05).

(C). Averaged input resistance and scatter plot for recordings obtained in current clamp (baseline 495.5±63.6 vs post-DHPG 479.4±65.4, t_{13}=0.49, p>0.05).

(D). No correlation between mGluR-driven change in firing vs input resistance (r=0.35, p>0.05).

(E). Averaged action potential traces indicating the parameters analyzed before and after mGluR activation.

(F). Pooled data and scatter plots for AP amplitude (baseline 63.2±3.1 vs post-DHPG 59.8±3.1, t_{11}=1.31, p>0.05)

(G). Same as D but for AP width (baseline 1.06±0.1 vs post-DHPG 1.12±0.1, t_{11}=0.60, p>0.05)

(H). Same as D and E but for AP afterhyperpolarization amplitude (AHP, baseline 3.21±1.2 vs post-DHPG 3.22±1.2). No correlation of firing vs AP amplitude (r=0.36, p>0.05); vs width (r=-0.11, p>0.05); vs AHP (r=0.039, p>0.05). N in the figures indicates number of recorded neurons.

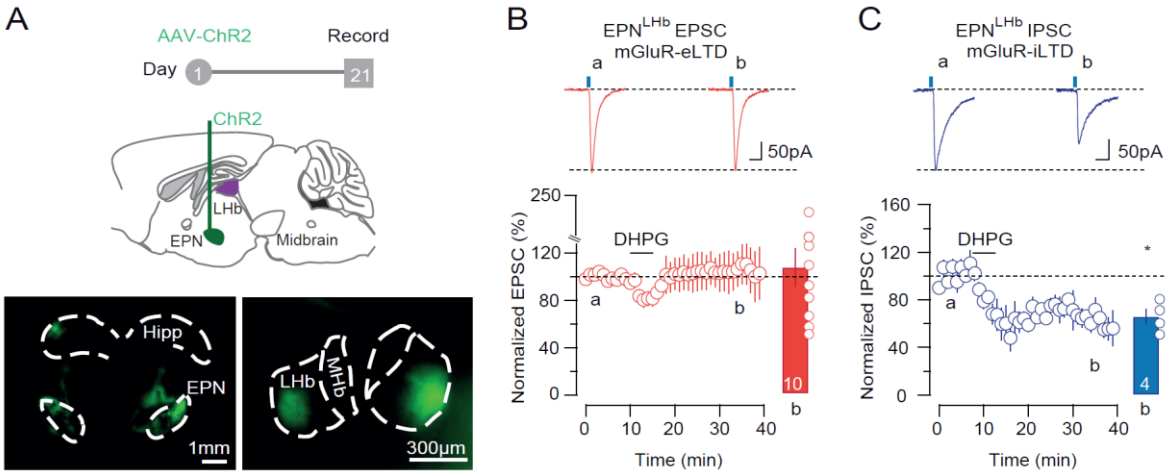

Figure S4. mGluR-dependent modulation of IPSCs, but not EPSCs, at EPN inputs onto the LHb. Related to Figure 1 and Figure 5.

(A). Experimental protocol and sample images representing stereotaxic injection of rAAV-ChR2 within the EPN, and EPN terminals within the LHb.

(B). DHPG effect on EPN^{LHb} EPSCs (109.4±6.5%, t_9=0.414, p>0.05).

(C). DHPG effect on EPN^{LHb} IPSCs (65.4±6.5%, t_3=5.27, *p<0.05). N in the figures indicates number of recorded neurons.

mGluR-LTD at excitatory and inhibitory synapses in the lateral habenula tunes neuronal output

Kristina Valentinova[1,2,3], and Manuel Mameli[1,2,3]
[1] Institut du Fer à Moulin, 75005 Paris, France.
[2]Inserm, UMR-S 839, 75005 Paris, France.
[3]Université Pierre et Marie Curie 75005 Paris, France.

Supplemental Experimental Procedures

Stereotactic injections of viral constructs

Bilateral injections (~300 nl per hemisphere) in anaesthetized mice were performed using a glass pipette on a stereotactic frame (Kopf, France). Viral constructs allowing the expression of Channelrhodopsin-2 or Cheta (rAAV2/1-CAG-hChR2(H134R)-mCherry; rAAV9-hSyn-Cheta-EYFP; titers: $1*10^{12}$–$1.3*10^{13}$ gc/ml; University of Pennsylvania, USA) were injected in the entopeduncular nucleus (EPN) (–1.25 mm AP, 1.80 mm ML, –4.65 mm DV). Animals were allowed to recover for a minimum of 3 weeks before recordings were made. Only mice showing fluorescence within the lateral portion of the LHb were used for recordings.

In vitro electrophysiology

Sagittal slices (250 µm) containing the LHb were prepared as previously described (Maroteaux and Mameli, 2012). Slices were used for recordings in artificial cerebro-spinal fluid (ACSF) equilibrated with 95% O_2 /5 % CO_2 and containing (in mM): NaCl 124; $NaHCO_3$ 26.2; glucose 11; KCl 2.5; $CaCl_2$ 2.5; $MgCl_2$ 1.3; NaH_2PO_4 1. The ACSF flow rate was 2 ml/min and the temperature was set at ~30°C. Currents were amplified, filtered at 2.5-5 kHz and digitized at 10 kHz. Access resistance was monitored by a 4 mV hyperpolarizing step, and experiments were discarded if access resistance increased >20%. For voltage-clamp experiments the internal solution contained (in mM): CsCl 130; NaCl 4; $MgCl_2$ 2; EGTA 1.1; HEPES 5; Na_2ATP 2; Na_3GTP 0.6; Na^+- creatine-phosphate 5, QX-314 2, and spermine 0.1, pH 7.3, osmolarity ~300 mOsm. The liquid junction potential was –3 mV and pipette resistance was 3-4 MΩ. Holding potential was –50 mV. Synaptic currents were evoked through a glass pipette placed in the stria medullaris (60 µs at 0.1 Hz). Paired pulse ratio (PPR) was monitored (2 pulses, 20 Hz) and calculated as follows:

$EPSC_2/EPSC_1$. mGluRs were activated by R,S-3,5-dihydroxyphenylglycine (DHPG, 50 µM) in presence of NBQX (10 µM) and D-APV (50-100 µM) or Picrotoxin, 100 µM. mGluRs were synaptically activated using a low frequency stimulation protocol (LFS, 1 Hz, 15 min) or a high frequency stimulation protocol (HFS, 100 Hz at 0 mV for 1 sec; 5 times every 10 sec). Experiments assessing postsynaptic effects of DHPG (voltage-clamp) and output firing (current-clamp) were performed with internal solution containing (in mM): KGluconate 140; KCl 5; HEPES 10; EGTA 0.2; $MgCl_2$ 2; Na_2ATP 4; Na_3GTP 0.3; Creatine Phosphate 10, pH 7.3, osmolarity ~300mOsm. QX-314 2mM was included when blocking action potentials. Liquid junction potential (12 mV) was not corrected. AMPA-EPSCs current-voltage relationships were performed at –60, 0 and +40 mV. The rectification index was calculated as follows: $((I_{EPSC(-60)}/I_{EPSC(+40)})/1.5)$. Miniature EPSCs (mEPSCs) or IPSCs (mIPSCs) were recorded at –60mV in presence of Tetrodotoxin (TTX, 1 µM) and frequency and amplitudes were computed during baseline and 20 minutes after DHPG. Current clamp recordings were performed in ACSF or in presence of the CB1-Rs neutral antagonist NESS-0327 (0.5 µM) and the $GABA_A$-β2 peptide (50 µM) in the patch pipette. Cells were kept around their resting membrane potential (RMP –55 mV) throughout the recording. EPSPs and action potentials were evoked by 10 electrical pulses 50 ms apart through a glass pipette. Stimulation intensity was set to evoke ~50% of spikes out of the 10 delivered pulses. 10-20 min following DHPG the number of spikes were counted for a period of 3 minute (19 sweeps) and compared to the same period at baseline. The changes in firing following DHPG were normalized to the baseline number of action potentials. Only regular firing neurons were included in the analysis. The area under individual EPSPs (Synaptosoft Inc, USA) during baseline and following DHPG was averaged and the normalized total area was correlated to the normalized firing after DHPG. The input resistance was calculated via a 50ms hyperpolarizing current (I=20pA) step (Ri=RMP/I). Action potential waveform analysis (Synaptosoft Inc, USA) of the amplitude, width and afterhyperpolarization amplitude for traces at baseline and after DHPG allowed to assess action potential properties changes.

Non-stationary fluctuation analysis

A peak-scaled non-stationary fluctuation analysis was made from mIPSCs (Synaptosoft Inc., USA). mIPSCs were selected by: fast rise time alignment; stable

baseline holding current; absence of spurious fluctuations during the mIPSC decay. Variance-amplitude relationship of mIPSC decay was plotted and fitted with the equation: $\sigma 2 = iI - I2/N + \sigma b2$, (*i:* mean single-channel GABA current; *I*: mean current; *N:* the number of channels activated at the peak, *N* = mean amplitude/*i*; σ_b^2: baseline variance). *i* was estimated as the slope of the linear fit of the first portion of the parabola. The goodness of the fit was assessed with a least-square algorithm. Unitary current was converted in conductance based on holding potential (–60mV). Conductance and average IPSC amplitude, mean rise time, mean decay time, access resistance or background noise variance had no correlation (*P* > 0.4) (Maroteaux and Mameli, 2012).

Reverse Transcription-PCR

Total RNA from LHb (4 mice) was extracted using Trizol (Invitrogen) and transcribed into cDNA using SuperScript II Reverse Transcriptase (Invitrogen). PCR were conducted with Taq DNA polymerase (Invitrogen) using the following primers: mGluR1: forward primer 5'-CAAATCGCCTATTCTGCCAC-3', reverse primer 5'-CCATTCCACTCTCGCCGTAATTC-3'; mGluR5: forward primer 5'-GAGGAGGGGCTCGTCTGGGG-3', reverse primer 5'-ACAGTCGCTGCCACAGGTGC -3'

Drugs and Peptides

Drugs were obtained from Abcam (Cambridge, UK), Tocris (Bristol, UK), Hello Bio (Bristol, UK) or Latoxan (France) and dissolved in water. TTX was dissolved in citric acid (1%), Picrotoxin, NESS-0327, WIN-55,212-2 and PMA in DMSO and LY367385 (in NaOH 10%). For PMA experiments, only cells responding to drug application were included in the analysis. When indicated peptides were included in the internal solution: PKC inhibitor PKC [19-36] (20 µM), dynamin inhibitor (QVPSRPNRAP; 1.5 mM), $GABA_AR$-β2 subunit peptide (KSRLRRRASQLKITI; 50 µM), $GABA_AR$- γ2 subunit peptide (SNRKPSKDKDKKKKNPAPT; 50 µM). Peptide sequences for β2 and γ2 were custom-synthesized (GeneScript, USA). When recording in presence of peptides, baseline was taken ~10 min after entering in whole-cell to allow intracellular dialysis.

Analysis

Analysis was performed using IGOR-6 (Wavemetrics, USA) and MiniAnalysis (Synaptosoft Inc,USA). Cumulative plots for mPSCs were obtained by compiling all recorded neurons at baseline and after DHPG conditions. Data were binned at 2.5 pA and 150 ms to normalize the sample size across recordings and significance was assessed by the Kolmogorov-Smirnov test (KS). A linear fit was used for correlations and significance was tested with Pearson Coefficient (r). N in the figures indicates number of recorded neurons. All data are expressed as mean ± s.e.m. Significance was set at alpha=0.05 using paired t-test.

II. Cocaine-evoked negative symptoms require AMPA receptor trafficking in the lateral habenula

One of the theories of addiction posits that addiction is a process engaging initial hedonic effects after drug intake, but with repetitive use soon after the drug effects dissipate a multitude of aversive states arises motivating further use and ending up in an uncontrollable intake (Koob and Le Moal, 2008; Koob, 2013). These aversive effects are characterized by increased anxiety and depressed mood. However, the neurobiological substrates of psychostimulant-induced aversive states are poorly understood.

As presented above, the lateral habenula has been proposed to participate in the pathophysiology of addictive disorders mainly because of its function in encoding aversive stimuli (Matsumoto and Hikosaka, 2009a), in establishing memories associated with negative events (Stamatakis and Stuber, 2012) and its ability to control the dopamine system (Hong et al., 2011; Ji and Shepard, 2007; Matsumoto and Hikosaka, 2007). Indeed, the LHb has an indirect inhibitory effect on dopamine neurons via its projections to GABA neurons of the midbrain (Jhou et al., 2009b; Meye et al., 2016). Moreover, single cocaine exposure directly modifies LHb neuronal function and induces aversive conditioning via LHb connection to the RMTg when drugs effects start to wear off (Jhou et al., 2013; Zuo et al., 2013).

Repeated cocaine exposure induces synaptic adaptations in the LHb leading to increased excitatory transmission specifically in LHb neurons projecting to the RMTg (Maroteaux and Mameli, 2012). However, the persistence of these modifications, their precise molecular mechanisms and impact on neuronal activity remain so far unknown. Given that synaptic potentiation onto LHb neurons can drive hyperexcitable states and depressive-like behaviors (Li et al., 2011), we tested the hypothesis that cocaine-induced synaptic plasticity may trigger persistent increase in neuronal output specifically to GABA neurons of the midbrain therefore contributing to the establishment of depressive-like symptoms. Our results provide causal relationship between synaptic and cellular drug-induced adaptations in the LHb and the emergence of negative emotional states potentially leading to subsequent compulsive drug use.

nature neuroscience

Cocaine-evoked negative symptoms require AMPA receptor trafficking in the lateral habenula

Frank J Meye[1–3,8], Kristina Valentinova[1–3,8], Salvatore Lecca[1–3,8], Lucile Marion-Poll[1–3], Matthieu J Maroteaux[1–3], Stefano Musardo[4], Imane Moutkine[1–3], Fabrizio Gardoni[4], Richard L Huganir[5], François Georges[6,7] & Manuel Mameli[1–3]

Addictive substances mediate positive and negative states promoting persistent drug use. However, substrates for aversive effects of drugs remain elusive. We found that, in mouse lateral habenula (LHb) neurons targeting the rostromedial tegmental nucleus, cocaine enhanced glutamatergic transmission, reduced K^+ currents and increased excitability. GluA1 trafficking in LHb was instrumental for these cocaine-evoked modifications and drug-driven aversive behaviors. Altogether, our results suggest that long-lasting adaptations in LHb shape negative symptoms after drug taking.

Withdrawal from addictive substances, including cocaine, produces negative symptoms such as a depressive-like phenotype that contributes to compulsive drug abuse[1,2]. The lateral habenula (LHb) inhibits monoaminergic systems via the GABAergic rostromedial tegmental nucleus (RMTg), encoding aversion-related stimuli[3,4]. Notably, functional modifications of the LHb are associated with neuropsychiatric disorders, including addiction and depression[5–7]. However, whether a drug-mediated depressive-like phenotype is a consequence of drug-evoked adaptations in the habenulo-mesencephalic pathway remains unknown.

We examined the effects of cocaine on glutamatergic synaptic transmission onto mouse retrogradely labeled RMTg-projecting LHb neurons ($LHb^{\rightarrow RMTg}$; **Fig. 1a** and **Supplementary Fig. 1a**,**b**). Miniature excitatory postsynaptic current (mEPSC) amplitudes, but not frequencies, were larger in $LHb^{\rightarrow RMTg}$ neurons 24 h after two consecutive cocaine injections (20 mg per kg of body weight, intraperitoneal; **Fig. 1b**,**c**)[6]. This cocaine-induced synaptic potentiation persisted 1 week after cocaine exposure, as well as 14 d after a chronic cocaine regimen (**Supplementary Fig. 1c**,**d**). This time course parallels the emergence of strong negative symptoms during drug-free periods[1]. Drug-evoked plasticity was detected only in $LHb^{\rightarrow RMTg}$, but not LHb neurons sending axons to the ventral tegmental area ($LHb^{\rightarrow VTA}$; **Supplementary Fig. 1e**). This suggests that cocaine promotes a projection-specific and enduring postsynaptic strengthening of excitatory transmission onto $LHb^{\rightarrow RMTg}$ neurons. However, whether cocaine alters LHb subpopulations other than RMTg/VTA-projecting neurons remains to be tested.

LHb synapses largely express GluA1-containing rectifying AMPARs[8]. Based on this subunit composition, we tested the necessity of GluA1 trafficking for cocaine-induced synaptic potentiation. We designed a viral vector encoding a dominant-negative form of the GluA1 C terminus (GluA1ct) to temporally prevent activity-dependent synaptic delivery of GluA1 (ref. 9) via doxycycline-driven recombination[10]. Doxycycline administration led to GluA1ct expression solely in the LHb (**Fig. 1d** and **Supplementary Fig. 1f**,**g**). We performed consecutive recordings from neighboring $LHb^{\rightarrow RMTg}$ neurons infected or uninfected with GluA1ct (**Fig. 1d** and Online Methods). GluA1ct overexpression left basal transmission unaltered (**Fig. 1e**,**f**)[9]. After cocaine administration, mEPSC amplitude was increased in GluA1ct-uninfected $LHb^{\rightarrow RMTg}$ neurons. Notably, in neighboring neurons expressing GluA1ct, the cocaine-evoked potentiation was prevented (**Fig. 1f**). Accordingly, cocaine increased evoked AMPAR-EPSCs (−70 mV) and AMPAR-NMDAR ratios (+50 mV; **Fig. 1g**,**h** and **Supplementary Fig. 1h**,**i**), which was precluded in $LHb^{\rightarrow RMTg}$ neurons expressing GluA1ct. We detected no substantial change in EPSC rectification index, suggesting that, despite the insertion of new AMPARs at the synapse, the overall AMPAR subunit composition remained similar after cocaine treatment (**Supplementary Fig. 1j**).

The phosphorylation of serine 845 (S845) and serine 831 (S831) on the GluA1 C terminus crucially controls AMPAR membrane delivery in various structures[11]. Immunoblots from microdissected LHbs revealed that phosphorylation of S845 was markedly increased following cocaine treatment. We observed no modifications of phospho-S831 or total GluA1 (**Supplementary Fig. 2a**,**b**). Accordingly, S845 phospho-mutant mice (S845A) showed no cocaine-induced mESPC amplitude enhancement, whereas this plasticity in S831 phospho-mutant mice (S831A) was left intact (**Supplementary Fig. 2c**–**f**). Thus, cocaine drives S845 phosphorylation–dependent GluA1 delivery onto $LHb^{\rightarrow RMTg}$ neurons.

We assessed the importance of cocaine exposure on the *in vivo* firing rate of $LHb^{\rightarrow RMTg}$ neurons in anesthetized mice (**Fig. 2a** and **Supplementary Fig. 2g**). $LHb^{\rightarrow RMTg}$ neuronal firing rate was higher in cocaine- than saline-treated mice (**Figs. 1c** and **2b**,**c**). Given that single-cell GluA1ct expression is difficult to assess *in vivo*, we evaluated the necessity of GluA1 trafficking for $LHb^{\rightarrow RMTg}$ neuronal hyperexcitability in acute brain slices. Cocaine increased the excitability of $LHb^{\rightarrow RMTg}$ neurons not expressing GluA1ct. However, excitability in GluA1ct-infected $LHb^{\rightarrow RMTg}$ neurons was comparable to that of saline controls (**Figs. 1f** and **2d**,**e**). Similar to the synaptic adaptations, hyperexcitability was still present 14 d after chronic cocaine exposure (**Fig. 2g**,**h** and **Supplementary Fig. 2h**). Notably, blockade of AMPARs by NBQX in slices did not affect cocaine-evoked hyperexcitability, suggesting a causal, but indirect, effect of GluA1

[1]Institut du Fer à Moulin, Paris, France. [2]Inserm, UMR-S 839, Paris, France. [3]Université Pierre et Marie Curie, Paris, France. [4]DiSFeB, Dipartimento di Scienze Farmacologiche e Biomolecolari, Università degli Studi di Milano, Milano, Italy. [5]Solomon H. Snyder Department of Neuroscience, The Johns Hopkins University School of Medicine, Baltimore, Maryland, USA. [6]Centre National de la Recherche Scientifique, Interdisciplinary Institute for Neuroscience, UMR 5297, Bordeaux, France. [7]Université de Bordeaux, Bordeaux, France. [8]These authors contributed equally to this work. Correspondence should be addressed to M.M. (manuel.mameli@inserm.fr).

Received 19 September 2014; accepted 15 December 2014; published online 2 February 2015; doi:10.1038/nn.3923

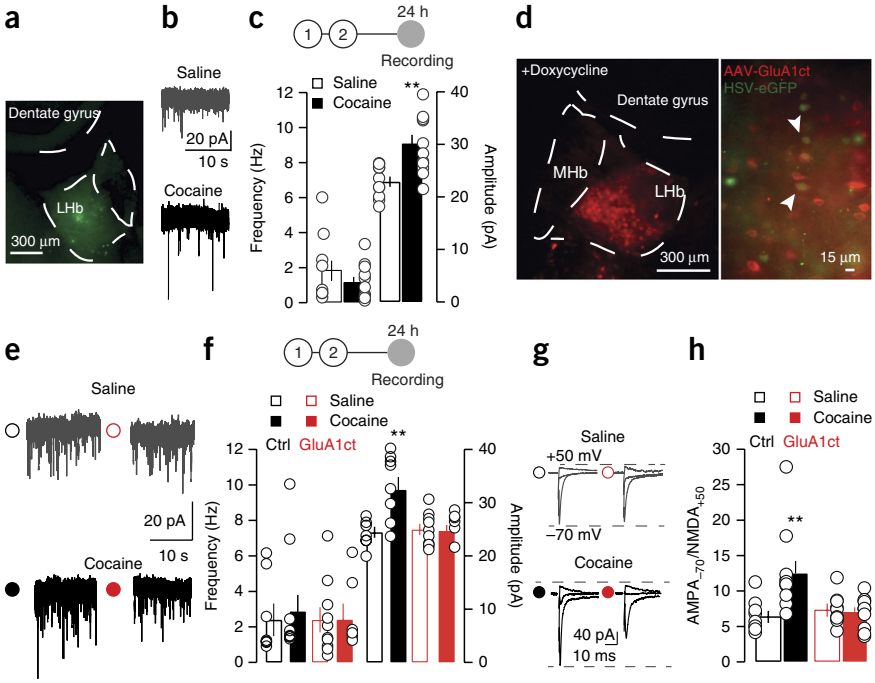

Figure 1 Cocaine-evoked synaptic potentiation onto LHb$^{\rightarrow RMTg}$ neurons requires GluA1 delivery. (**a**) Schematic and images indicating the retrograde labeling of LHb$^{\rightarrow RMTg}$ neurons. (**b**) Sample mEPSCs from LHb$^{\rightarrow RMTg}$ neurons. (**c**) Scatter plot and grouped data for mEPSC frequency and amplitude (n = 10–12 cells, 4 mice of 4–5 weeks; frequency, saline versus cocaine t_{20} = 1.1, P = 0.27; amplitude, saline versus cocaine t_{20} = 3.7, $^{**}P$ = 0.0013). (**d**) Images indicating the AAV-GluA1ct injection site, infected LHb neurons, and GluA1ct-mCherry expression and eGFP labeling in LHb$^{\rightarrow RMTg}$ neurons. (**e**) Sample mEPSCs obtained in AAV-GluA1ct–infected and uninfected LHb$^{\rightarrow RMTg}$ neurons. (**f**) Scatter plot and grouped data for mEPSC frequency and amplitude (n = 6–10, 3 mice of 7–9 weeks; frequency interaction factor $F_{1,\,36}$ = 0.4, P = 0.27, two-way ANOVA; amplitude interaction factor $F_{1,\,36}$ = 15.5, $^{**}P$ = 0.0012, two-way ANOVA). (**g**) AMPAR EPSCs (–70 mV) and AMPAR + NMDAR EPSCs (+50 mV) obtained from LHb$^{\rightarrow RMTg}$ neurons. (**h**) AMPA/NMDA ratios from sequentially recorded neighboring neurons (AAV-GluA1ct infected versus uninfected) after saline or cocaine (AMPA/NMDA; n = 9–11, 4 mice of 7–9 weeks; uninfected saline versus cocaine t_{18} = 2.9, $^{**}P$ = 0.008; infected saline versus cocaine t_{18} = 0.4, P = 0.7). Error bars represent s.e.m.

trafficking on LHb neuronal firing (**Supplementary Fig. 2i,j**). Consistently, we found that input resistance was larger following cocaine treatment, an effect that was prevented by GluA1ct expression. The cell input resistance was highly correlated with LHb$^{\rightarrow RMTg}$ neuronal excitability (**Fig. 2f,g**). To understand the cocaine-driven GluA1-dependent mechanisms causing LHb$^{\rightarrow RMTg}$ neuron hyperexcitability,

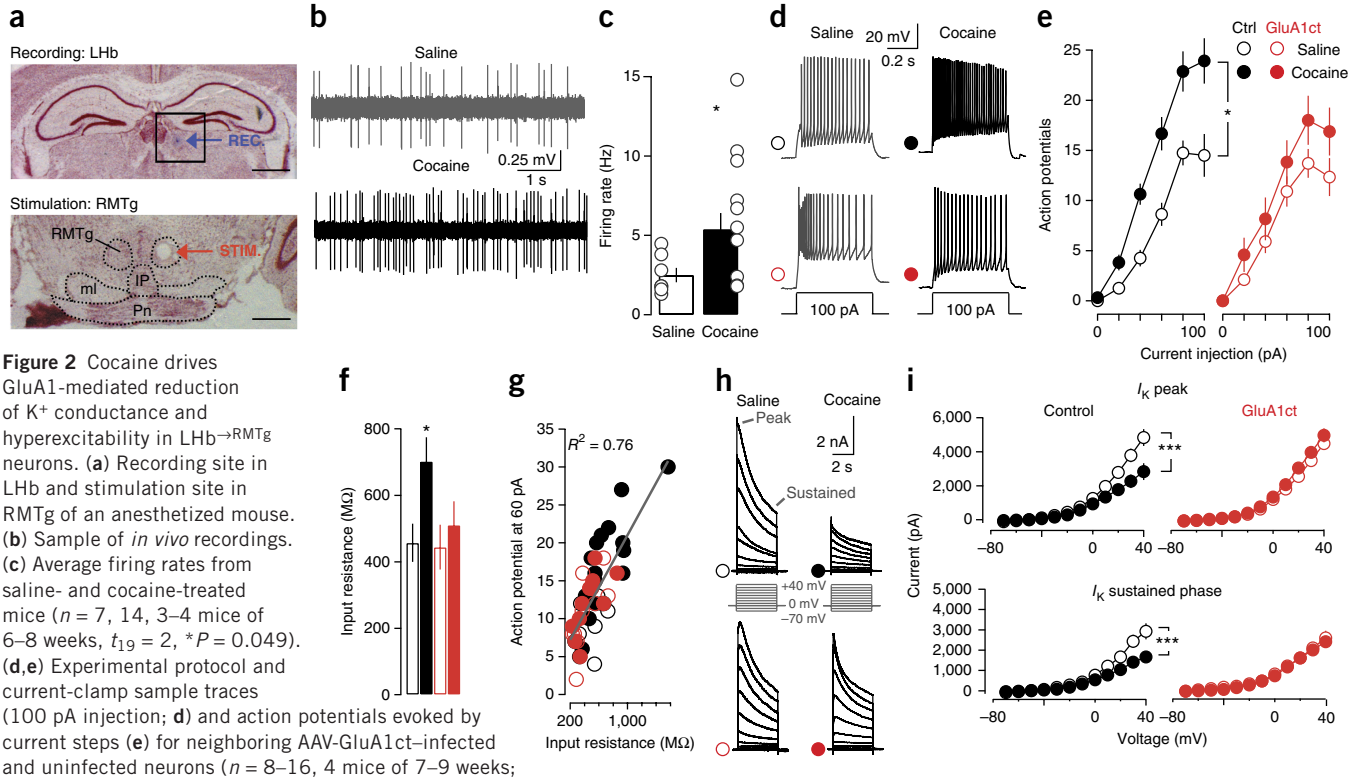

Figure 2 Cocaine drives GluA1-mediated reduction of K$^+$ conductance and hyperexcitability in LHb$^{\rightarrow RMTg}$ neurons. (**a**) Recording site in LHb and stimulation site in RMTg of an anesthetized mouse. (**b**) Sample of *in vivo* recordings. (**c**) Average firing rates from saline- and cocaine-treated mice (n = 7, 14, 3–4 mice of 6–8 weeks, t_{19} = 2, $^{*}P$ = 0.049). (**d**,**e**) Experimental protocol and current-clamp sample traces (100 pA injection; **d**) and action potentials evoked by current steps (**e**) for neighboring AAV-GluA1ct–infected and uninfected neurons (n = 8–16, 4 mice of 7–9 weeks; uninfected saline versus cocaine, interaction factor $F_{5,\,114}$ = 2.8, $^{*}P$ = 0.03 repeated-measures ANOVA; infected saline versus cocaine, interaction factor $F_{5,\,114}$ = 0.4, P = 0.14 repeated-measures ANOVA). (**f**) Bar graph for input resistance values obtained in the different experimental groups from neurons recorded in **e** (input resistance; n = 8–17, 6 mice of 7–9 weeks; uninfected saline versus cocaine t_{23} = 2.1, $^{*}P$ = 0.04; infected saline versus cocaine t_{20} = 0.6, P = 0.06). (**g**) Scatter plot for excitability versus input resistance. (**h**,**i**) K$^+$-mediated currents in response to increasing voltage steps of 10 mV, for neighboring AAV-GluA1ct–infected and uninfected neurons (n = 12–14, 6 mice of 7–8 weeks; peak current (top) uninfected saline versus cocaine, interaction factor $F_{11,\,558}$ = 5, $^{***}P$ = 0.00065 repeated-measures ANOVA; infected saline versus cocaine, interaction factor $F_{11,\,287}$ = 0.7, P = 0.7 repeated-measures ANOVA; sustained current (bottom) uninfected saline versus cocaine, interaction factor $F_{11,\,558}$ = 4.8, $^{***}P$ = 0.0059 repeated-measures ANOVA; infected saline versus cocaine, interaction factor $F_{11,\,287}$ = 0.1, P = 0.9 repeated-measures ANOVA). Error bars represent s.e.m.

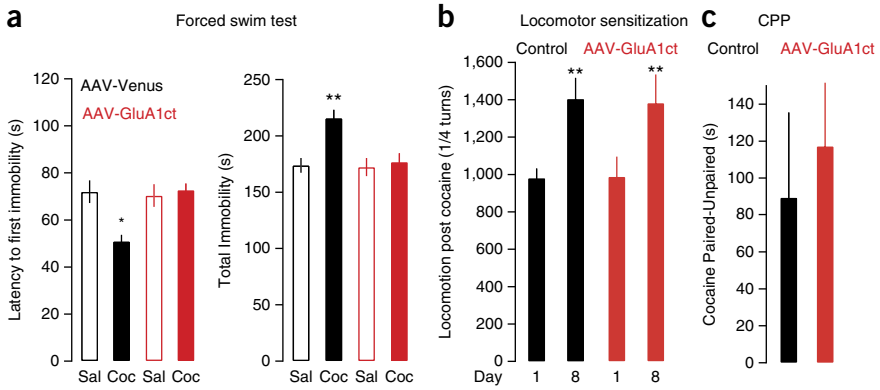

Figure 3 Cocaine-driven AMPAR trafficking in LHb serves for a cocaine-evoked depressive-like state in mice. (**a**) FST analysis after AAV-GluA1ct and AAV-control injection in LHb (n = 11–12 mice of 8–9 weeks; AAV-Venus; latency first immobility $F_{1,44}$ = 3.6, $^{*}P$ = 0.038; total immobility, interaction factor $F_{1,44}$ = 5.9, $^{**}P$ = 0.0011). (**b**) Quarter turns in control and AAV-GluA1ct–injected mice (n = 10 mice of 8–9 weeks; paired t test: t_9 = 3.7 $^{**}P$ = 0.0044 for cocaine on day 8 versus day 1 in AAV-control and t_9 = 3.9. $^{**}P$ = 0.003 cocaine on day 8 versus day 1 in AAV-GluA1ct–injected mice; P = 0.26 for locomotor response to cocaine on day 8 for AAV-GluA1ct versus control-injected mice). (**c**) Grouped data for conditioned place preference scores in saline and cocaine-treated animals (n = 10 mice of 8–9 weeks; t_{18} = 0.36 P = 0.42). Error bars represent s.e.m.

we focused on K^+ conductance, an inhibitory driving force that is critical for neuronal excitability[12]. $LHb^{\rightarrow RMTg}$ neurons from cocaine-exposed mice exhibited a marked reduction of K^+ channel–mediated peak and sustained currents, which are mediated by multiple K^+ channel subtypes (**Figs. 1f** and **2h**,**i**)[12]. Similar to the modifications described above, the reduction in K^+ currents was prevented by the expression of GluA1ct in $LHb^{\rightarrow RMTg}$ neurons. This suggests that cocaine triggers a GluA1-dependent synaptic potentiation, resulting in a functional reduction of K^+ conductance and $LHb^{\rightarrow RMTg}$ neuron hyperexcitability. Future studies will need to identify the specific K^+ component underlying cocaine-evoked adaptations of intrinsic excitability.

Is GluA1 trafficking–dependent plasticity in LHb a requirement for cocaine-driven behavioral phenotypes emerging during withdrawal? We employed the forced swim test (FST) and the tail suspension test (TST) to assess drug-evoked depressive-like states[13,14]. Exposing control mice (AAV-Venus) to five cocaine injections followed by a 2-week drug-free period resulted in depressive-like behaviors, with reduced latency to first immobility in the FST and increased total immobility in the FST and TST (**Fig. 3a** and **Supplementary Fig. 3a**,**c**). Notably, GluA1ct expression in the LHb prevented the cocaine-induced depressive-like phenotype (**Fig. 3a** and **Supplementary Fig. 3c**). Precluding GluA1 trafficking in the LHb specifically abolished the drug-mediated aversive component, as cocaine-induced locomotor sensitization or place preference remained intact following GluA1ct overexpression (**Fig. 3b**,**c** and **Supplementary Fig. 3b**,**d**,**e**).

We found that cocaine-evoked GluA1 trafficking mediated the potentiation of AMPAR transmission, reduction of K^+ conductance and hyperexcitability in the LHb. This ultimately contributes to the emergence of negative depressive-like symptoms during drug withdrawal. The GluA1-driven reduction in K^+ conductance provides a previously unidentified mechanism, potentially representing a common substrate for disorders characterized by LHb dysfunction[13]. The cocaine-driven hyperactivity of $LHb^{\rightarrow RMTg}$ neurons may provide an 'anti-reward' signal[1] that likely inhibits the dopamine (DA) system[15]. Indeed, cessation of cocaine intake diminishes striatal DA levels, and reduced DA neuron activity produces depressive-like behaviors[16,17]. Notably, deep-brain stimulation in the LHb rescues a depressive-like phenotype in the learned helplessness model by restoring the excitatory drive onto LHb[5]. Whether this intervention would also efficiently reverse the aversive component of cocaine remains an open question. In conclusion, our data provide mechanistic insights for cocaine-driven adaptations in the LHb. These findings support the idea that increased LHb output is instrumental for drug-evoked negative symptoms, potentially contributing to compulsive drug use.

METHODS

Methods and any associated references are available in the online version of the paper.

Note: Any Supplementary Information and Source Data files are available in the online version of the paper.

ACKNOWLEDGMENTS

We thank C. Bellone, M.T.C. Brown, C. Lüscher and J.C. Poncer for discussions and comments on the manuscript. This work was supported by funds from the INSERM Atip-Avenir, ERC StG SalienSy 335333 and the Paris School of Neuroscience Network (ENP) to M.M., and the Agence Nationale de la Recherche (ANR-12-bsv4-0022-01) to F. Georges. F.J.M. is supported by a postdoctoral fellowship from the Fyssen Foundation and K.V. is supported by a PhD fellowship from the French Ministry of Science (ESR).

AUTHOR CONTRIBUTIONS

F.J.M., K.V., S.L. and M.M. performed and analyzed all of the *in vitro* electrophysiological recordings. K.V., L.M.-P., and M.M. designed and performed the behavioral experiments. I.M. and M.J.M., prepared and tested the viral construct. S.M. and F. Gardoni performed the immunoblots. R.L.H. provided the phospho-mutant mice. F. Georges performed the *in vivo* recordings. M.M. designed the study and wrote the manuscript with the help of F.J.M., S.L. and K.V.

COMPETING FINANCIAL INTERESTS

The authors declare no competing financial interests.

1. Koob, G.F. & Le Moal, M. *Phil. Trans. R. Soc. Lond. B* **363**, 3113–3123 (2008).
2. Barr, A.M., Markou, A. & Phillips, A.G. *Trends Pharmacol. Sci.* **23**, 475–482 (2002).
3. Stamatakis, A.M. & Stuber, G.D. *Nat. Neurosci.* **15**, 1105–1107 (2012).
4. Jhou, T.C., Fields, H.L., Baxter, M.G., Saper, C.B. & Holland, P.C. *Neuron* **61**, 786–800 (2009).
5. Li, B. *et al. Nature* **470**, 535–539 (2011).
6. Maroteaux, M. & Mameli, M. *J. Neurosci.* **32**, 12641–12646 (2012).
7. Zuo, W., Chen, L., Wang, L. & Ye, J.H. *Neuropharmacology* **70**, 180–189 (2013).
8. Meye, F.J., Lecca, S., Valentinova, K. & Mameli, M. *Front. Hum. Neurosci.* **7**, 860 (2013).
9. Rumpel, S., LeDoux, J., Zador, A. & Malinow, R. *Science* **308**, 83–88 (2005).
10. Liu, B., Wang, S., Brenner, M., Paton, J.F. & Kasparov, S. *J. Gene Med.* **10**, 583–592 (2008).
11. Malinow, R. *Phil. Trans. R. Soc. Lond. B* **358**, 707–714 (2003).
12. Friedman, A.K. *et al. Science* **344**, 313–319 (2014).
13. Li, K. *et al. Science* **341**, 1016–1020 (2013).
14. Porsolt, R.D., Bertin, A. & Jalfre, M. *Arch. Int. Pharmacodyn. Ther.* **229**, 327–336 (1977).
15. Matsumoto, M. & Hikosaka, O. *Nature* **447**, 1111–1115 (2007).
16. Jhou, T.C. *et al. J. Neurosci.* **33**, 7501–7512 (2013).
17. Weiss, F., Markou, A., Lorang, M.T. & Koob, G.F. *Brain Res.* **593**, 314–318 (1992).

ONLINE METHODS

Surgery. C57Bl/6J wild-type mice, S845A knock-in mice and S831A knock-in mice (males of 4–9 weeks) were used in accordance with the guidelines of the French Agriculture and Forestry Ministry for handling animals. Animals were anesthetized with ketamine (90 mg per kg)/xylazine (15 mg per kg intraperitoneal) (Sigma-Aldrich) before bilateral injection with a herpes simplex virus (McGovern Institute) expressing enhanced GFP allowing for retrograde tracing, into the RMTg or VTA. Retrobeads (Lumafluor) were used for recordings performed 2 weeks after withdrawal[18]. The following coordinates were used (from bregma, in mm)[18]: RMTg: A-P, −2.9; M-L, ±0.5; D-V, −4.3; VTA: A-P, −2.5; M-L, ±0.8; D-V, −4.4. Recovery was allowed for 5–15 d. When indicated, an adeno-associated virus (AAV) coding for an 89 amino-acid sequence of the GluA1 carboxy-terminal tail was used (AAV-GluA1ct)[19]. The GluA1ct sequence is fused to mCherry and inserted under the control of a TET-ON system. AAV-GluA1ct-mCherry and AAV-Venus as a control were injected bilaterally in the LHb at a final volume of 300–500 nl. The following coordinates were used (from bregma, in mm): A-P, −1.7; M-L, ±0.45; D-V, −3.1. After 3 weeks, mice were subjected to doxycycline treatment that consisted of intragastric administrations of 5 mg per 100 µl twice per day for three consecutive days. The injection sites were carefully examined for all electrophysiology experiments and only animals with correct injections were used for recordings. Similarly, for behavioral studies only animals with correct injection sites were included in the analysis. Brain slices from mice injected with AAVs or HSV were directly examined under a fluorescent microscope.

Electrophysiology. Animals injected with saline or cocaine (20 mg per kg, intraperitoneal), once per day for 2 or 5 consecutive days, anesthetized (ketamine/xylazine; 50 mg/10 mg kg^{-1} intraperitoneal) 24 h, 7 d or 14 d after the last injection for preparation of LHb-containing brain slices. Slicing was done in bubbled ice-cold 95% O_2/5% CO_2-equilibrated solution containing (in mM): choline chloride 110; glucose 25; $NaHCO_3$ 25; $MgCl_2$ 7; ascorbic acid 11.6; sodium pyruvate 3.1; KCl 2.5; NaH_2PO_4 1.25; $CaCl_2$ 0.5. Coronal slices (250 µm) were stored at ~22 °C in 95% O_2/5% CO_2-equilibrated artificial cerebrospinal fluid (ACSF) containing (in mM): NaCl 124; $NaHCO_3$ 26.2; glucose 11; KCl 2.5; $CaCl_2$ 2.5; $MgCl_2$ 1.3; NaH_2PO_4 1. Recordings (flow rate of 2.5 ml min^{-1}) were made under an Olympus-BX51 microscope (Olympus) at 32 °C. Currents were amplified, filtered at 5 kHz and digitized at 20 kHz. Access resistance was monitored by a step of −4 mV (0.1 Hz). Experiments were discarded if the access resistance increased more than 20%. mEPSCs were recorded in voltage-clamp mode at −60 mV in presence of picrotoxin (100 µM) and tetrodotoxin (TTX, 1 µM) from retrogradely labeled RMTg-projecting LHb neurons. The internal solution contained (in mM): CsCl 130; NaCl 4; $MgCl_2$ 2; EGTA 1.1; HEPES 5; Na_2ATP 2; sodium creatine-phosphate 5; Na_3GTP 0.6; spermine 0.1. The liquid junction potential was −3 mV. Neighboring neurons positive for the EGFP retrograde labeling and negative or positive for the mCherry GluA1ct expression were recorded sequentially, counterbalancing the order of patching. EPSCs were evoked through glass electrodes placed 200 µm from the recording site. In the case of the sequential recording of neurons, the stimulation electrode was left in place using the same intensity. AMPA:NMDA ratios of evoked-EPSC were obtained by AMPA-EPSC −70 mV/NMDA-EPSCs at +50 mV as previously described, using the late component of the EPSC at 30 ms after the onset[18]. Rectification indexes were computed by AMPA-$EPSC_{-70}$/AMPA-$EPSC_{+50}$. Current-clamp recordings were obtained using an internal solution containing (in mM): potassium gluconate 140; KCl 5; HEPES 10; EGTA 0.2; $MgCl_2$ 2; Na_2ATP 4; Na_3GTP 0.3 mM; creatine phosphate 10. Current-clamp experiments were performed by a series of current steps (negative to positive) injected to induce action potentials (20-pA injection current per step, 500 ms). To isolate voltage-gated K^+ channel–mediated currents, 4-s incremental 10-mV voltage steps were given from −70 to +40 starting at −50 mV holding potential in ACSF containing 1 µM tetrodotoxin, 200 µM $CdCl_2$, 20 µM NBQX, 100 µM AP5 and 100 µM picrotoxin.

***In vivo* recordings in anesthetized mice.** Stereotaxic surgery for electrophysiology experiments was performed under isoflurane anesthesia as previously described[20]. Recording pipettes and stimulating electrodes were inserted into the LHb and RMTg, respectively.

A glass micropipette (tip diameter = 2–3 µm, 4–6 MΩ) filled with a 2% pontamine sky blue solution (wt/vol) in 0.5 M sodium acetate was lowered into the LHb. LHb neurons were identified according to recently established electrophysiological features[21], these include a broad triphasic extracellular spike (>3 ms), and a tonic regular, tonic irregular or bursting spontaneous activity. Through these electrodes, the extracellular potential was recorded with an Axoclamp2B amplifier in the bridge mode. The extracellular potential amplified tenfold by the Axoclamp2B amplifier was further amplified 100-fold and filtered (low-pass filter at 300 Hz and high-pass filter at 0.5 kHz) via a differential AC amplifier (model 1700, A-M Systems). Single neuron spikes were discriminated and digital pulses were collected on-line using a laboratory interface and software (CED 1401, SPIKE 2, Cambridge Electronic Design).

Electrical stimulation of the RMTg was used to test for antidromic activation of LHb neurons using high frequency following collision methods, as described previously[20]. A bipolar concentric stimulation electrode was inserted into the RMTg and driven impulses were considered antidromic if they met the following criteria: 1) constant latency of spike response, 2) driving by each paired stimulus pulses at frequencies of 100 Hz or greater, and 3) collision of driven spikes by spontaneous impulses occurring in a critical interval approximately equal to the sum of the refractory period plus the driving latency.

At the end of each recording experiment, the electrode placement was marked with an iontophoretic deposit of pontamine sky blue dye (−20 µA, continuous current for 12–15 min). To mark electrical stimulation sites, 10 µA of positive current was passed through the stimulation electrode for 1 min (**Fig. 3**). After the experimental procedures, the animals were deeply anesthetized with halothane (5%, vol/vol) and decapitated. Brains were removed and snap-frozen in a solution of isopentane at −70 °C. The tissue was sectioned into 25-µm-thick coronal slices, mounted, and stained with neutral red to enable histological determination of recording and stimulating electrodes sites.

Viral construct. To construct pAAV-TRE-GluA1ctmCherry-CMV-Tet-On3G, sequential subclonings were performed as described below. PCR primers and synthetic genes were purchased from Eurofins MWG Operon. TRE-GFP was PCR amplified with Phusion High Fidelity DNA Polymerase (ThermoScientific) using pTRE-GFP as template (Clontech). Product was digested with NsiI and SpeI enzyme (New England BioLabs) and cloned into NsiI/SpeI sites of the pCMV-Tet-On3G vector (Clontech) using T4 DNA ligase (Invitrogen), resulting in pTRE-GFP-CMV-Tet-On3G. GluAct DNA (was obtained by gene synthesis of mouse GluA1 nucleotides 2,425 to 2,667 corresponding to amino acids 809 to 889 (ref. 19). GluA1ct was cloned in pCMV-mCherry (kindly provided by X. Nicol, Institut de la Vision) in frame with N-terminal mCherry. GluA1ct-mCherry was then PCR amplified and digested with AgeI and EcoRV enzymes. pTRE-GFP-CMV-Tet-On3G was digested with AgeI and EcoRV enzymes and GluA1ct-mCherry was cloned in place of GFP to get pTRE-GluA1ct-mCherry-CMV-Tet-On3G. pAAV-hsyn-hChR2mcherry (Addgene) was cut with MluI and EcoRV to remove hSyn-hChR2mcherry and obtain pAAV empty vector. A linker sequence containing PpumI and AvrII sites was inserted into MluI and EcoRV sites by oligonucleotides annealing and ligation. pTRE-GluA1ct-mCherry-CMV-Tet-On3G was digested with PpumI and AvrII and the TRE-GluA1ctmCherry-CMV-Tet-On3G cassette was ligated into PpumI and AvrII sites of the pAAV vector. Then, the WPRE sequence was removed from 3′ of Tet-On3G by digestion with RsrII and ClaI, filling in and self-ligation of the vector. WPRE was finally cloned in 3′ of the GluA1ct-mCherry into NheI and SpeI sites to obtain pAAV-TRE-GluR1ctmCherry-CMV-Tet-On3G. All constructs were confirmed by restriction and sequence analysis. All of the AAV plasmids were made into recombinant AAV2/5 particles by the Vector Core Facility at the University of North Carolina, Chapel Hill, USA.

Immunoblotting. Treated and control LHb were initially microdissected and stored at −80 °C until processing. Tissue was homogenized by ten strokes in a Teflon-glass homogenizer in ice-cold 0.32 M sucrose containing 1 mM HEPES, 1 mM $MgCl_2$, 1 mM $NaHCO_3$, 0.5 mM NaF and 0.1 mM phenylmethylsulfonyl fluoride, in the presence of a complete set of protease inhibitors (Complete, Roche Diagnostic, Basel, Switzerland) and phosphatases inhibitors (Sigma Aldrich). Proteins were quantified using Bradford assay (Bio-Rad Laboratories) and 20 µg per sample were loaded on 7% SDS-PAGE gel and transferred to nitrocellulose membrane using Trans-Blot Turbo Transfer System (Bio-Rad Laboratories) to perform western blot analysis. Membranes were blocked with iBlock-TBS (Invitrogen, T2015) for at least 45 min and subsequently exposed to primary

doi:10.1038/nn.3923

antibody overnight at 4 °C in iBlock-TBS. The next day, membranes were washed in Tris-buffered saline/Tween 20 (TBST) three times for at least 10 min at ~22 °C, then incubated with horseradish peroxidase (HRP)-coupled secondary antibody (Bio-Rad Laboratories) for 1 h at ~22 °C and washed again as before. For detection, Clarity Western ECL Substrates (Bio-Rad Laboratories) were used, and chemiluminescence was exposed to trans-UV (302 nm) with Chemidoc MP System (Bio-Rad Laboratories). We used antibodies to phospho-GluA1 (Ser845) (Millipore, clone EPR2148, 1:1,000), phospho-GluA1 (Ser831) (Millipore, clone N453, 1:1,000) α-Tubulin (Sigma-Aldrich, clone DM1A, 1:10,000).

Behavioral assays. All behavioral tests were conducted during the light phase (8:00–19:00). Animals were randomly assigned to the saline or cocaine group after viral injection.

Locomotor sensitization. Procedure was done as described earlier[22]. The locomotor activity was measured in cylindrical locomotor activity boxes (Imetronics, Pessac, France) in a low luminosity environment. Mice previously injected with the AAV-GluA1ct-mcherry in the LHb, were treated with doxycycline as described above. 1 d after the last doxycycline exposure, experimental day 1, locomotor activity was recorded 30 min before and 1 h after cocaine injection (20 mg per kg, intraperitoneal). 1 week after (day 8), each mouse was injected as on day 1, in the same activity box. Locomotor activity was measured automatically as the number of consecutive beam breaks (one beam per quadrant).

Conditioned place preference. Conditioned place preference was performed in two compartments of the apparatus (Imetronic) with different visual cues and different wall textures, in a low luminosity environment. On day 1, mice were placed in the center of the apparatus and allowed to explore freely both compartments for 15 min. Then mice of each group were assigned with one or the other compartment in a counterbalanced way to avoid any initial bias in preference. On days 2, 4 and 6 mice were injected with cocaine 20 mg per kg and placed immediately in the assigned closed compartment for 20 min. On days 3, 5 and 7 the mice were placed in the other closed compartment after saline injection 10 ml kg^{-1}. Finally on day 8, mice were tested for preference during 15 min of free exploration and the time they spent in each compartment was automatically recorded. Offline analysis was performed blind to the animal treatments.

Forced swim test. Forced swim test was conducted under normal light condition as previously described[23]. Mice were placed in a cylinder of water (23–25 °C, 14 cm in diameter, 27 cm in height for mice) for 6 min. The depth of water was set to prevent animals from touching the bottom with their hind limbs. Animal behavior was videotracked from the top (Viewpoint). The latency to the first immobility event and the immobility time of each animal spent during the test was counted online by two independent observers blind to the animal treatments. Immobility was defined as floating or remaining motionless, which means absence of all movement except motions required to maintain the head above the water.

Tail suspension test. The tail suspension test was used to assess behavioral despair and conducted under normal light. Mice were suspended by their tails with adhesive tape for a single session of 6 min. Animal behavior was videotracked from the top/front (Viewpoint) and video recorded. Immobility time of each animal spent during the test was counted online by two independent observer blind of the animal treatments. Mice were considered immobile only when they hung passively and motionless.

Analysis and drugs. All drugs were obtained from Abcam and Tocris and dissolved in water, except for TTX (citric acid 1%, wt/vol) and cocaine HCl (NaCl 0.9%, vol/vol). Analysis for the electrophysiology data was performed in blocks depending on the experiment. Online/offline analysis were performed using IGOR-6 (Wavemetrics) and Prism (Graphpad). Data analysis for *in vivo* electrophysiology was performed off-line using Spike2 (CED) software. Sample size required for the experiment was empirically tested by running pilots experiments in the laboratory. Data distribution was assumed to be normal, and single data points are always plotted. Frequency histograms and mean firing rate were determined for each recorded cells. Compiled data are expressed as mean ± s.e.m. Significance was set at $P < 0.05$ using Student's t test, one- or two-way ANOVA with multiple comparison when applicable.

A **Supplementary Methods Checklist** is available.

18. Maroteaux, M. & Mameli, M. *J. Neurosci.* **32**, 12641–12646 (2012).
19. Rumpel, S., LeDoux, J., Zador, A. & Malinow, R. *Science* **308**, 83–88 (2005).
20. Glangetas, C. *et al. J. Neurosci.* **33**, 19657–19663 (2013).
21. Kowski, A.B., Veh, R.W. & Weiss, T. *Neuroscience* **161**, 1154–1165 (2009).
22. Valjent, E. *et al. Neuropsychopharmacology* **35**, 401–415 (2010).
23. Porsolt, R.D., Bertin, A. & Jalfre, M. *Arch. Int. Pharmacodyn. Ther.* **229**, 327–336 (1977).

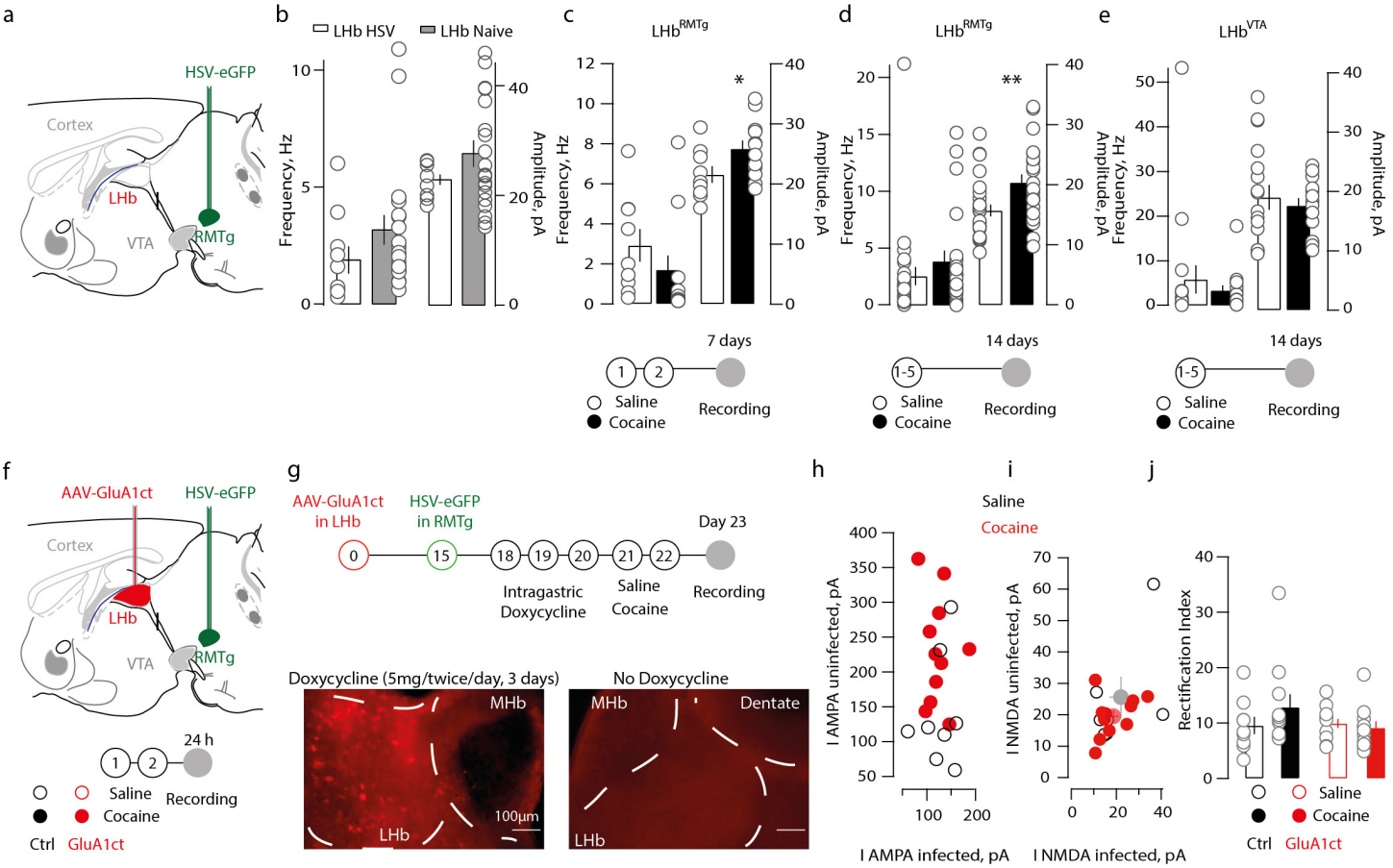

Supplementary Figure 1

Cocaine-evoked plasticity onto LHb$^{\rightarrow RMTg}$ neurons is long-lasting and is absent in LHb$^{\rightarrow VTA}$ neurons.

(a) Schematic indicating the injections of the HSV-eGFP in the RMTg. **(b)** Grouped data for recordings obtained from LHb neurons after HSV infusion or in naïve mice (n = 10-19; 8 mice of ~6 weeks; Frequency, HSV 1.8 ± 2.4 Hz; Naive 3.1 ± 1.8 Hz; $p > 0.05$ $t_{27} = 1.3$; Amplitude, HSV 22.8 ± 0.8 pA; Naive 27.6 ± 2.4 pA; $p > 0.05$ $t_{27} = 1.3$) **(c)** Grouped data for recordings obtained 7 days after the last injection of saline/cocaine (n = 9-12; 4 mice of 6 weeks; Frequency, Saline 2.9 ± 0.8 Hz; Cocaine 1.7 ± 0.7 Hz; $p > 0.05$ $t_{19} = 1.1$; Amplitude, Saline 21.5 ± 1.4 pA; Cocaine 25.8 ± 1.3 pA; *$p < 0.05$ $t_{19} = 2.1$). **(d)** Same as b but for recordings obtained 14 days after 5 cocaine injections (n = 22-26; 4 mice of 6-7 weeks; Frequency, Saline 2.6 ± 0.8 Hz; Cocaine 3.8 ± 0.9 Hz; $p > 0.05$ $t_{46} = 1$; Amplitude, Saline 15.7 ± 0.9 pA; Cocaine 20.3 ± 1.3 pA; **$p < 0.01$ $t_{46} = 2.8$). **(e)** Same as c but for recordings obtained in LHb$^{\rightarrow VTA}$ neurons (n = 15-17; 3 mice of 6-7 weeks; Frequency, Saline 5.8 ± 3.1 Hz; Cocaine 3.4 ± 1.1 Hz; $t_{30} = 0.7$ $p > 0.05$; Amplitude, Saline 19.1 ± 2.1 pA; Cocaine 17.7 ± 1.3 pA; $t_{30} = 0.5$ $p > 0.05$). **(f)** Schematic describing the AAV-GluA1ct injections in the LHb and parallel HSV-eGFP injections in the RMTg **(g)** Timeline for experimental procedures. Representative images obtained from mice injected with the AAV-GluA1ct in LHb, and treated (or not) with doxycycline (2 X 5 mg/day) intragastrically for three consecutive days. **(h, i)** Scatter plot representing the AMPA **(h)** and NMDA-EPSCs **(i)** from consecutively patched neighboring neurons (AAV-GluA1ct infected and uninfected) in saline and cocaine treated groups (n = 9-11; 4 mice of 7-9 weeks; NMDA EPSCs, Saline uninfected, 25.6 ± 6.5; Saline infected, 22.1 ± 0.7; Cocaine uninfected, 19.8 ± 1.9; Cocaine infected, 19 ± 2.4; Interaction factor $F_{(1,36)} = 0.09$, p□>□0.05 two way ANOVA). **(j)** Pooled data indicating the rectification index (RI = $EPSC_{-70}/EPSC_{+50}$) in AAV-GluA1ct infected and uninfected LHb-RMTg neurons in saline and cocaine treated groups (n = 9-11; 4 mice of 7-9 weeks; Saline uninfected, 9.5 ± 1.5; Cocaine uninfected, 12.8 ± 2.3; $p > 0.05$ $t_{18} = 1.1$; Saline infected, 9.9 ± 1.1; Cocaine infected, 9.1 ± 1.1; $t_{18} = 0.4$ $p > 0.05$).

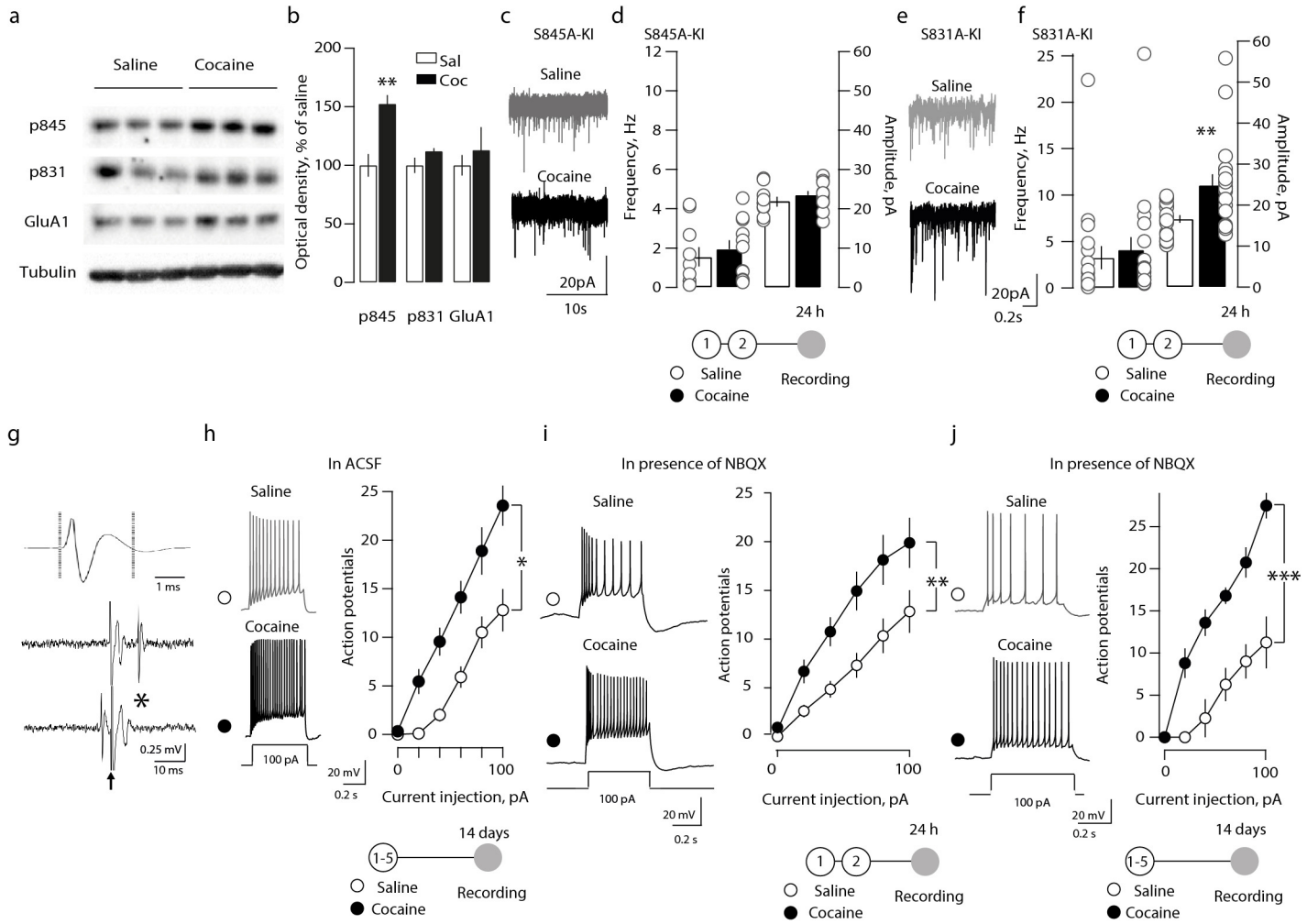

Supplementary Figure 2

Cellular mechanisms underlying cocaine-evoked plasticity in the LHb.

(a) Representative immunoblots for p845, and p831 and total GluA1 obtained from microdissected LHb in saline and cocaine groups. **(b)** Grouped data for immunoblots (n = 30 animals; n = 5 observations; p845, cocaine 152.8 ± 7.5%, t_8 = 4.3 **p < 0.01; p831, cocaine 112.1 ± 2.6%, t_8 = 1.7 p > 0.05; GluA1-total, cocaine 119.8 ± 22.8%; p > 0.05 t_8 = 1.3). **(c)** Sample traces of mEPSCs obtained in $LHb^{\rightarrow RMTg}$ neurons in S845A knock-in mice. **(d)** Scatter plot and grouped data for mEPSC frequency and amplitude from S845A knock-in mice (n = 10-11; 4 mice of 4-6 weeks; Frequency; Saline 1.5 ± 0.5 Hz; Cocaine 1.9 ± 0.4 Hz; t_{19} = 0.6 p > 0.05; Amplitude; Saline 21.9 ± 1.1 pA; Cocaine 23.2 ± 1 pA; t_{19} = 0.8 p > 0.05). **(e)** Sample traces of mEPSCs obtained in $LHb^{\rightarrow RMTg}$ neurons in S831A knock-in mice. **(f)** Scatter plot and grouped data for mEPSC frequency and amplitude in the saline and cocaine groups of S831A knock-in mice (n = 18; 4 mice of 4-6 weeks; Frequency; Saline 3.2 ± 1.2 Hz; Cocaine 4 ± 1.4 Hz; t_{34} = 0.4 p > 0.05; Amplitude; Saline 16.6 ± 0.9 pA; Cocaine 24.8 ± 2.6 pA; t_{34} = 2.9 p < 0.01). (**g**) Representative LHb neuron spike recorded in vivo, and sample antidromic collision test (*, erasure of antidromic spike; arrow, stimulus artifact). (**h**) Current-clamp sample traces (100 pA injection) and action potentials as function of current steps, for $LHb^{\rightarrow RMTg}$ neurons recorded 2 weeks after chronic treatment (n = 9–10; 4 mice of 8–9 weeks; saline versus cocaine, $F_{5, 85}$ = 6.05, *P < 0.05 repeated-measures ANOVA). **(i)** Current-clamp sample traces (100 pA injection) and action potentials as function of current steps, for $LHb^{\rightarrow RMTg}$ neurons recorded 24 hrs after 2 days of saline/cocaine treatment in the presence of NBQX (20 µM) in the ACSF (n = 12-16; 8 mice of 7-9 weeks Saline vs Cocaine, $F_{(5, 135)}$= 3.5, **p < 0.01 repeated measures ANOVA). **(j)** Same as g but for for $LHb^{\rightarrow RMTg}$ neurons recorded at 14 days of withdrawal after 5 days of cocaine treatment in the presence of NBQX (20 µM) in the ACSF (n = 5; 2 mice of 7-8 weeks Saline vs Cocaine, $F_{(5, 37)}$= 11.3, **p < 0.01 repeated measures ANOVA).

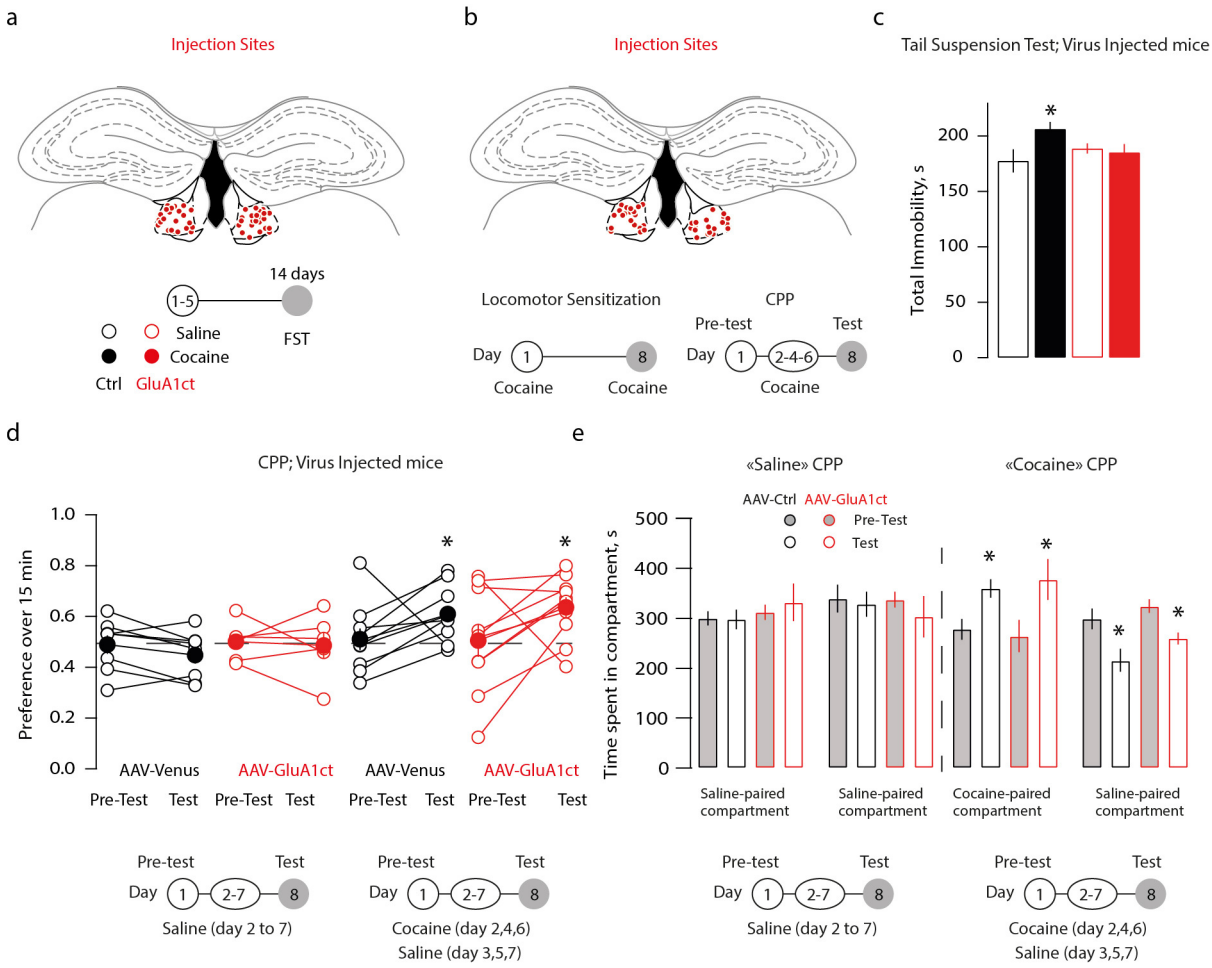

Supplementary Figure 3

Precluding cocaine-evoked GluA1 trafficking in LHb prevents a depressive-like behavior elicited by drug exposure.

(**a**,**b**) Injection sites in the LHb for AAV-GluA1ct for animals included in the behavioral analysis **(c)** Tail suspension test analysis after AAV-GluA1ct and AAV-control injection in LHb (n = 9-10 mice; 8-9 weeks; AAV-Venus; total immobility, Interaction factor $F_{(1,35)} = 4.6$, *p□<□0.05). **(d)** Scatter plot of cocaine-induced preference indicating no statistical differences between control and AAV-GluA1ct infused mice (See Figure 3) (n = 6-8 for saline CPP and n = 10 for cocaine CPP; mice of 8-9 weeks. Unpaired t-test, Pre-test vs Test, Saline-Saline, AAV-control $t_7 = 1.7$ $p > 0.05$; AAV-GluA1ct $t_5 = 1.3$ $p > 0.05$; Saline-Cocaine, AAV-control $t_9 = 1.9$ *$p < 0.05$; AAV-GluA1ct $t_9 = 1.9$ $p < 0.05$). **(e)** Same as (**d**) but indicating the total time spent by mice in the compartments for saline CPP and cocaine CPP (Saline CPP; Compartment #1 AAV-control $t_{14} = 0.05$ $p > 0.05$, AAV-GluA1ct $t_{14} = 0.3$ $p > 0.05$; Compartment #2 AAV-control $t_{12} = 1.48$ $p > 0.05$, AAV-GluA1ct $t_{12} = 0.8$ $p > 0.05$. Cocaine CPP; Compartment #1 AAV-control $t_{18} = 3.1$ $p < 0.01$, AAV-GluA1ct $t_{18} = 2.7$ $p < 0.05$; Compartment #2 AAV-control $t_{18} = 2.7$ $p < 0.05$, AAV-GluA1ct $t_{18} = 3.4$ $p < 0.01$).

Discussion

In the results section I presented two main pieces of work that have provided new insights on 1) how mGluR-dependent synaptic plasticity controls the firing activity of LHb neurons and 2) how cocaine-evoked synaptic and cellular adaptations in a specific LHb pathway contribute to depressive-like behaviors following cocaine withdrawal. These data describe detailed mechanisms underlying activity- or experience-dependent synaptic modifications and their repercussions on LHb neuronal output. Further we demonstrate a causal relationship between cocaine withdrawal-induced synaptic and cellular modifications in the LHb and subsequent depressive-like states. However several points arise following these studies.

Which inputs undergo mGluR-eLTD and iLTD?

The LHb is embedded in a highly interconnected circuit receiving multiple feedforward and feedback glutamatergic and GABAergic inputs. Here we show that low-frequency stimulation of axons within the *stria medullaris* triggers mGluR1-dependent LTD of excitatory synaptic transmission, while high frequency stimulation leads to mGluR1-dependent LTD of inhibitory transmission. We further show that mGluR-eLTD and iLTD bidirectionally contribute to LHb evoked firing. These findings raise the possibility that distinct inputs, capable to spike at low or high frequency ranges, may drive mGluR-eLTD or iLTD respectively. Indeed, when we monitored the effect of mGluR activation on EPSCs and IPSCs evoked from light stimulated EPN terminals we find that only inhibitory transmission undergoes mGluR-driven decrease in efficacy (Fig15C). Whether other afferents also express mGluR-iLTD, remains to be established. One plausible scenario is that other co-releasing inputs such as the VTA and potentially the LH may also be capable to trigger this form of plasticity given the close localization of excitatory and inhibitory postsynaptic structures (Fig15B) (Root et al., 2014b). Likewise HFS-induced glutamate release would trigger mGluR1 signaling in the vicinity of postsynaptic $GABA_A$ receptors allowing the interaction of PKC with the β2-$GABA_A$ receptor subunit. An electron microscopy investigation of the precise subcellular localization of mGluRs along the dendritic arborization of LHb

neurons as well as the identity and specific phenotype of the opposed inputs would be required to address this possibility.

Interestingly, LFS of the *stria medullaris* also induced an mGluR1-independent iLTD which occurred in the absence of presynaptic modifications. An alternative scenario is that other GPCRs activation may trigger this form of plasticity, the circuit specificity, molecular mechanisms and contribution to firing modulation of which remain unexplored. Consistently with this idea, results obtained in recombinant systems and cultured neurons demonstrate that the G_q-coupled muscarinic acetylcholine (mAChRs) and serotonin type 2C (5HT2C) receptors also reduce GABA transmission via PKC targeting of β1-$GABA_A$ and γ2-$GABA_A$ receptor subunits respectively (Feng et al., 2001; Brandon et al., 2002). 5HT2C receptors and mACh receptors are also expressed in the LHb (Pompeiano et al., 1994; Vilaró et al., 1990). These evidences raise therefore the possibility that subtypes of G_q-coupled GPCRs (i.e. mGluRs, 5HT-2C, mAChRs) throughout the CNS and potentially in the LHb may reduce synaptic inhibition via PKC phosphorylation of specific $GABA_A$ receptor subunits (β2, γ2, β1 respectively (Fig14) (Brandon et al., 2002; Feng et al., 2001; Kittler and Moss, 2003).

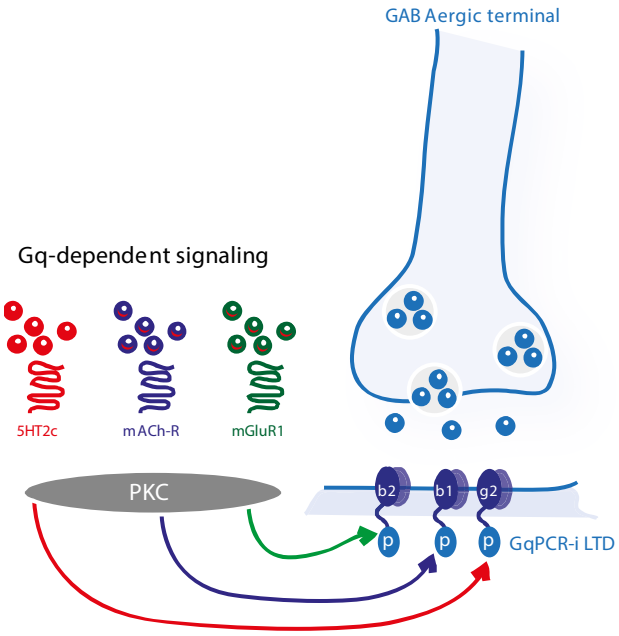

Figure 14 GqPCR model of inhibitory LTD

Different classes of Gq-coupled receptors such as the 5HT2C, mAChR and mGluR1 trigger PKC signaling and phosphorylate specific subunits of the $GABA_A$ receptor leading to reduced function of the receptor. 5HT2C signaling triggers PKC-dependent phosphorylation of the γ2 subunit (Feng et al., 2001) ;mACh signaling triggers PKC-dependent phosphorylation of the β1 subunit (Brandon et al., 2002) and mGluR1 triggers PKC-dependent reduction of β2-containing $GABA_A$ receptors function (Valentinova and Mameli, accepted).

Another open issue remaining to be explored is to assess which inputs express CB1 receptors and whether they undergo mGluR1-driven and CB1-dependent reduction in glutamate release (Fig15A). Notably, we have also noticed that inhibitory

transmission can undergo CB1 receptor agonist-induced reduction in efficacy (data not shown). However this does not require mGluR activation since mGluR-iLTD was not prevented in presence of CB1 receptor antagonist. The inhibitory inputs as well as the precise molecular determinants of this form of plasticity would require further investigation.

The potential input-specific expression of mGluR-eLTD and iLTD suggests that under physiologically relevant circumstances the contribution of specific inputs to LHb output firing can be tuned by mGluRs. It is therefore interesting to test whether light LFS or HFS of specific ChR2-expressing inputs, capable to trigger either mGluR-eLTD or iLTD, are able to decrease or increase evoked neuronal firing respectively.

Is there any output-specificity for mGluR-eLTD and iLTD?

Despite certain variability of the expression and magnitude of mGluR-eLTD and iLTD across recordings, we did not observe apparent medio-lateral or antero-posterior distinctions. We therefore conclude that the expression of mGluR-eLTD and iLTD could occur in different LHb neuronal populations independently of their output targets. However, we performed our recordings in the sagittal plane where the assessment of the medio-lateral axis is less precise. Moreover, different output-specific LHb populations may reside within close LHb subterritories (Fig6). A target-specific retrograde labeling of LHb neurons could help to identify projection-specific neurons and assess their ability to express mGluR-eLTD or iLTD (Fig15D, E, F).

What is the behavioral relevance of mGluR-LTD in the LHb?

Our data suggest that mGluR plasticity in the LHb occurs in an input- and frequency-specific manner. However we still lack information about the physiological conditions in which this might happen. Given that mGluR-eLTD contributes to decreased and mGluR-iLTD to increased neuronal output it is plausible that they may occur during persistent rewarding and aversive experience respectively (Matsumoto and Hikosaka, 2007). If this is the case one would expect that aversive experience (i.e. foot shock, restrained stress, predator odor exposure etc) would lead to mGluR-iLTD, but not eLTD in the LHb ultimately leading to increased neuronal activity. My prediction would be that mGluR-iLTD (DHPG or HFS), but not mGluR-eLTD (DHPG

or LFS) in slices from these animals would be occluded (Pascoli et al., 2012). In parallel the excitation/inhibition balance would be shifted towards more excitation compared to unexperienced animals. Similarly, if mGluR-eLTD and a subsequent firing decrease are triggered by reward experience (i.e. sucrose, enriched environment), LFS or DHPG application would fail to induce mGluR-eLTD in slices from these animals, without affecting the induction of mGluR-iLTD. Whether these potential scenarios hold true in the LHb, remains to be tested.

mGluR long term plasticity can be involved in learning mechanisms (Jörntell and Hansel, 2006; Riedel et al., 1996). Would it be possible that mGluR adaptations in the LHb engage any form of learning related to rewarding or aversive experience? While the activity of the LHb has been strongly associated to encoding aversive stimuli and in driving avoidance behaviors, much less is known about a potential control of the LHb on reward-related behaviors (Lammel et al., 2012; Matsumoto and Hikosaka, 2009a; Stamatakis and Stuber, 2012). In this regard, if LHb neurons undergo mGluR-dependent learning, it would be more plausible that they do so via mGluR-iLTD and increased neuronal output. A way to assess this issue would be to submit mice to aversive experience (i.e. predator odor) in a particular context and assess whether the animal learns to avoid the aversion-associated compartment. If we prevent mGluR-iLTD induction prior to experience (viral-based injection of a dominant negative peptide to block PKC and β2-$GABA_A$ receptor interaction) we would expect to abolish conditioned place avoidance.

Another alternative is that mGluR plasticity in the LHb could underlie pathological behaviors following drug exposure or stressful events leading to aberrant neuronal hyperactivity (Li et al., 2011; Meye et al., 2016; Shabel et al., 2014). Therefore a possibility is that also in these conditions mGluR-iLTD would be occluded. It would be interesting to examine what the role of mGluR-eLTD in such pathological conditions is and whether its induction is impaired (Kreitzer and Malenka, 2007). These scenarios are plausible, but still hypothetical and require further investigation.

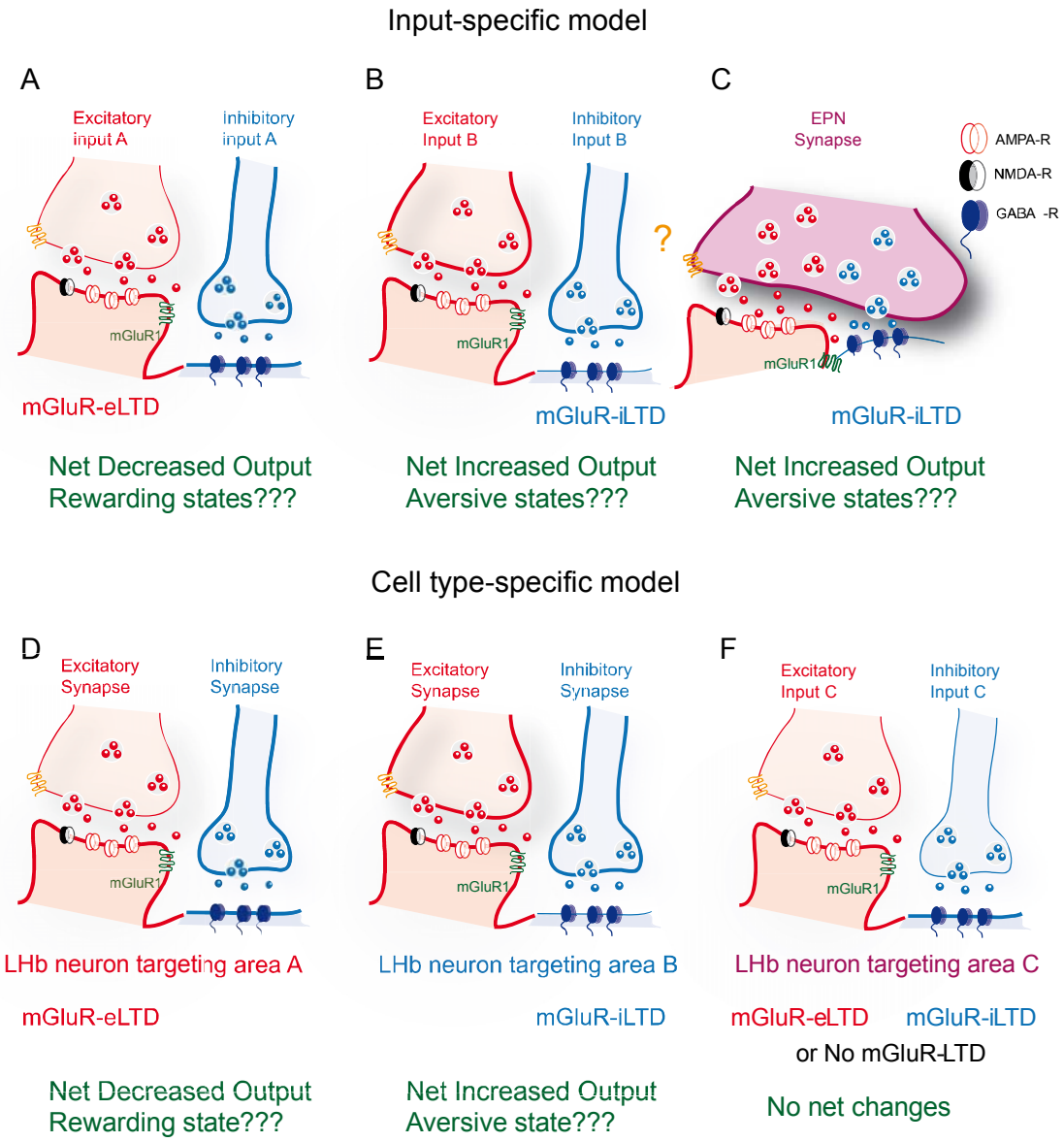

Figure 15 Input and cell type-specific model for mGluR-LTD in the LHb

(A). Input A expresses mGluRs postsynaptically and CB1 receptors presynaptically and undergoes eLTD, but not iLTD, overall decreasing the output of the LHb neuron and potentially driving rewarding states. (B). Input B undergoes iLTD, but not eLTD, overall increasing LHb neuronal output and potentially driving aversive states. (C). Mixed inputs such as EPN express iLTD, but not eLTD, potentially increasing LHb neuronal output and driving aversive states. (D). LHb neurons targeting area A undergo eLTD, but not iLTD, have decreased output and potentially drive rewarding states. (E). LHb neurons targeting area B undergo iLTD, but not eLTD, have increased output and drive aversive behaviors. (F). LHb neurons receiving input C or targeting area C undergo both eLTD and iLTD or do not express mGluR-LTD at all, therefore neuronal output is unchanged.

Induction mechanisms and circuit specificity of cocaine-evoked plasticity in the LHb

We have shown that five days of withdrawal period following chronic cocaine treatment leads to increased excitatory synaptic transmission specifically in LHb neurons projecting to the RMTg, but not to VTA. However, whether other target-specific LHb populations, such as the LHb-to-DRN, undergo similar changes remains to be addressed (Fig16).

An important question arising from our data is whether the induction of this form of drug-induced plasticity occurs locally via direct pharmacological action of cocaine in the LHb or whether other circuit adaptations are able to trigger it via specific synaptic input(s)? Given that cocaine inhibits the dopamine transporter thereby increasing dopamine concentration in the synaptic cleft (Amara and Sonders., 1998), a possible induction mechanism for cocaine-evoked plasticity in the LHb is via activation of dopamine receptors. Indeed, a direct cocaine application onto LHb-containing slices induces a transient D1 and D2 receptors-dependent potentiation of excitatory transmission occurring along with increased presynaptic release. Further, transient cocaine application also leads to synaptically driven acceleration of LHb firing (Zuo et al., 2013). These data demonstrate that the LHb is indeed a direct target of psychostimulants. Despite this, it is still not clear whether chronic cocaine exposure *in vivo* triggers locally the long-lasting synaptic adaptations observed in our study or whether other parallel circuit and synaptic modifications are also required.

We have collected data showing that pre-treating animals with the D2 receptor antagonist eticlopride, but not the D1 receptor antagonist SCH23390, prevented the increase of LHb mEPSCs amplitude recorded 24h following two days of cocaine treatment (data not shown). Whether this effect is driven by D2 receptors activation within the LHb or elsewhere remains unknown. Nevertheless, this evidence leaves open the possibility that specific glutamatergic input(s) could trigger the synaptic adaptations observed in our study (Fig16). This is particularly relevant in the light of a recent study from our laboratory showing that withdrawal from cocaine leads to diminished GABA vesicle packing at EPN-to-LHb co-releasing synapses as a result of decreased expression of Vgat, but without affecting the glutamatergic component. This ultimately leads to reduced inhibitory control over EPN-driven LHb firing activity and is instrumental for depressive like states and cocaine relapse (Fig16) (Meye et

al., 2016). This evidence together with our finding that LHb neurons activity is overall increased following cocaine withdrawal suggest that distinct synaptic adaptations occurring in parallel in the LHb increase neuronal output specifically to GABA neurons in the midbrain and are sufficient to drive negative emotional states (Fig16). Notably, a single LHb neuron may receive different inputs that undergo cocaine-induced modifications and the relative contribution of each may depend on the specific localization on the dendritic arbor as well as on its computational properties. Altogether these studies raise the hypothesis that regardless of the input and the synaptic mechanisms (increased excitatory transmission versus decreased inhibitory transmission) engaged after cocaine withdrawal, an increased excitability of LHb neurons is required for the establishment of depressive-like states. Although this hypothesis seems plausible, particularly in light of the evidence that LHb neurons can activate GABA neurons in the midbrain (Meye et al., 2016), it remains still to be tested whether LHb hyperactivity following cocaine withdrawal leads to dopamine neurons inhibition and reduces dopamine release (Fig16).

Synaptic adaptations after cocaine withdrawal

We have demonstrated that cocaine withdrawal induces GluA1-dependent synaptic potentiation of excitatory transmission and a reduction in potassium channels conductance. What could be the link between GluA1 trafficking and the decrease in potassium channels function? Several studies have suggested that activity-dependent LTP engages GluA1 trafficking together with endocytosis of small conductance Ca^{2+}-activated K^+ type 2 (SK2) channels or voltage-gated A-type K^+ channel Kv4.2 subunits (Kim et al., 2007; Lin et al., 2010). The insertion of the GluA1-containing AMPA receptors and the endocytosis of the SK channel seem to be functionally and unidirectionally coupled since selective inhibition of GluA1-containing AMPA receptors exocytosis blocks SK2-containing channel endocytosis, but the inverse manipulation does not affect AMPA receptor trafficking (Lin et al., 2010). Given that SK and A-type voltage gated channels trafficking can be coupled to AMPA receptors trafficking and the fact that they strongly regulate neuronal excitability (Adelman et al., 2012; Jerng and Pfaffinger, 2014) it is possible that these K^+ channels are the ones affected in the LHb following cocaine withdrawal. Although we did not identify the nature of these conductances their pattern of activation and

voltage dependence suggest that they might be rather of the A-type. It remains still unknown what is the precise sequence of circuit synaptic and cellular events following chronic cocaine exposure and whether the plasticity of AMPA receptors and K^+ channels in the LHb results from homeostatic adaptations.

A previous study in our laboratory has also shown that cocaine exposure induces metaplasticity in the LHb. Indeed, an anti-Hebbian type of protocol using relatively low frequency stimulation patterns (10Hz) together with somatic hyperpolarization induces LTD of EPSCs in LHb-to-RMTg neurons in saline treated animals but LTP in cocaine treated ones (Maroteaux and Mameli, 2012). These results demonstrate that the potentiation of these synapses following cocaine does not reach a ceiling effect, but rather opens a window for further plasticity to be expressed, the function of which as well as it's synaptic mechanisms remain elusive.

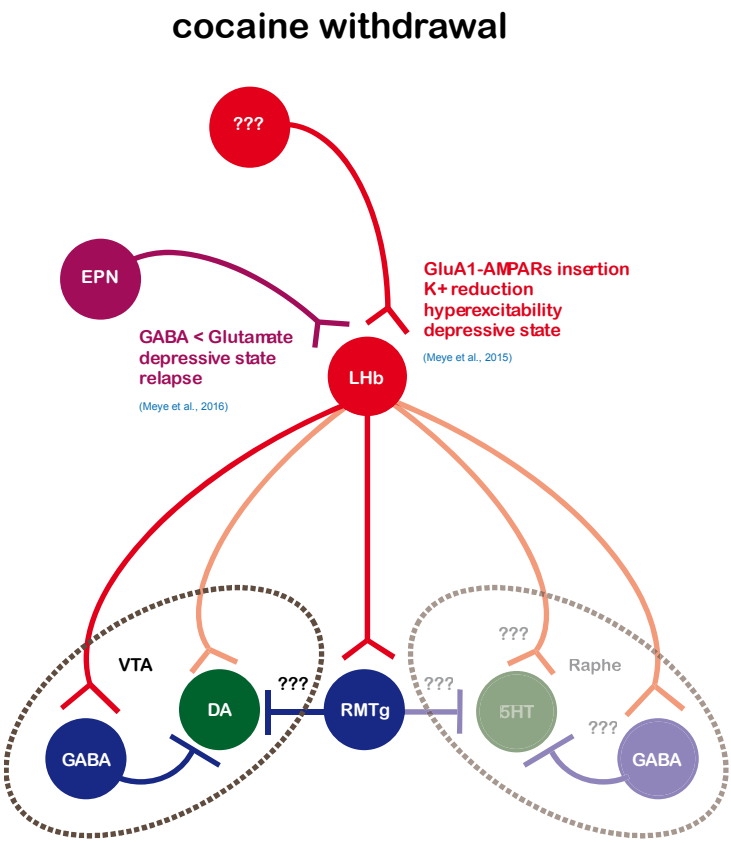

Figure 16 Effects of cocaine withdrawal in the LHb

Withdrawal from cocaine leads to decreased GABA component at EPN-to-LHb synapses likewise decreasing the inhibitory control on EPN-driven LHb firing, which is required for depressive-like states and stress-induced relapse (Meye et al., 2016). In parallel, GluA1-containg receptors are inserted at the membrane, while K^+ channels function is reduced specifically in LHb neurons projecting to the RMTg. The synaptic locus of this form of plasticity is unknown as well as whether other output-specific LHb populations are affected. This results in increased excitability of LHb-to-RMTg neurons. Altogether cocaine withdrawal shifts the balance of excitation/inhibition towards more excitation in LHb neurons projecting to GABA midbrain neurons. Whether dopamine neurons activity is reduced remains to be tested.

Distinct synaptic adaptations converge to increase LHb neuronal and behavioral output

In our study two or five consecutive days of cocaine exposure led to persistent synaptic potentiation of AMPA-mediated transmission. Two weeks of withdrawal following chronic regiment of cocaine resulted in increased LHb-to-RMTg output, sufficient to drive behavioral despair. We propose that these synaptic and cellular adaptations in the LHb underlie the emergence of drug-induced negative symptoms which are thought to be instrumental for the establishment of compulsive drug use (Koob and Le Moal, 2008; Koob, 2013). Indeed, it has been previously shown that prolonged cocaine administration (from 5 to 14 days) induces synaptic adaptations in VTA dopamine neurons, which persist even after long abstinence periods (up to 90 days) and are required for cocaine-seeking behaviors (Chen et al., 2008; Mameli et al., 2009). Notably the persistence of cocaine-induced synaptic changes depended on the cocaine administration procedure. Indeed, animals that self-administered cocaine presented more long-lasting plasticity compared to animals that were injected by the experimenter (Chen et al., 2008). Whether the cocaine-induced plasticity in the LHb persists more than two weeks and whether it triggers other long-term adaptations in downstream targets, such as the dopamine system require further investigation.

Meye et al., showed recently that shifting the balance of excitation and inhibition at EPN-to-LHb synapse after cocaine withdrawal is instrumental for the susceptibility to relapse following stressful events (Meye et al., 2016). This raises the question whether AMPA receptors and K^+ channels plasticity in the LHb also leads to such behavioral phenotype given its contribution to depressive-like symptoms. How does the plasticity of excitatory and inhibitory synaptic transmission occurring simultaneously, but at different synapses cooperate? Preventing the establishment of GluA1-dependent synaptic adaptations in the LHb was sufficient to prevent the depressive-like state. Similarly, rescuing Vgat expression at EPN-to-LHb synapses restored the behavioral performance in the forced-swim test and precluded the stress-induced relapse. These data suggest that the induction of the two mechanisms is either interdependent or alternatively they are required to occur simultaneously in order to shift LHb neuronal activity towards a hyperexcitable state. A possible

strategy to address this issue would be to test whether preventing GluA1-dependent plasticity would also prevent Vgat-dependent adaptations at EPN synapses or alternatively, whether overexpression of Vgat at these synapses would restore excitatory transmission.

Concluding remarks

In this thesis I attempted to provide an overview on lateral habenula function in motivational processing. Indeed, the LHb encodes aversive-related stimuli and drives motivated behaviors via its connection to monoaminergic systems. Dysfunction of the LHb leads to pathologies of motivation, including addiction and depression characterized by LHb neuronal hyperexcitability. However, information about precise synaptic and cellular mechanisms controlling LHb neuronal activity and motivational states is still scarce.

The work presented here tackled this general question and has provided novel mechanistic insights on how LHb synapses can undergo distinct forms of synaptic plasticity in physiological and pathological conditions. Moreover, we show that these different pre- and postsynaptic mechanisms can control LHb neuronal output. Finally we demonstrate a causal relationship between aberrant synaptic plasticity as well as neuronal activity in a discrete LHb circuit and the expression of negative emotional states. Our results could represent important cellular corollary for LHb-driven motivated behaviors in physiology and pathology.

These studies open new avenues for the investigation of the pathophysiology of the lateral habenula. In the future it would be necessary to assess the specificity of mGluR-eLTD and iLTD within distinct LHb microcircuits as well as their relative input-specific contribution for single LHb neuronal activity. Indeed, the specific locus and integration properties of LHb neurons could impact on mGluR-dependent control on firing. Given that activity of specific LHb populations drive motivational states and that mGluRs control neuronal output, it would be further interesting to probe the behavioral relevance of this plasticity for reward and aversive behaviors or alternatively in pathological states. Following our study and others, the LHb is now emerging as a target of drugs of abuse and drug-driven behavioral maladaptations.

Therefore the data here presented raises the possibility that the LHb could represent a general substrate for drug-induced withdrawal symptoms. Future studies could lead to the identification of alternative and novel mechanisms contributing to withdrawal-dependent behaviors.

These and other questions require further studies that will allow us to understand the precise circuit, synaptic and cellular substrates controlling LHb-driven behaviors. This knowledge may ultimately permit to develop interventions capable to prevent or reverse pathological plasticity and behaviors.

Publications and contributions

- Tchenio A,* *Valentinova K* *and* Mameli M **Can the lateral habenula crack the serotonin code?** *Under Review at Front Syn Neurosci*

- *Valentinova K and* Mameli M. **mGluR-LTD at excitatory and inhibitory synapses tunes lateral habenula output**. *Accepted at Cell Rep.*

- Glangetas C, Fois GR, Jalabert M, Lecca S, *Valentinova K*, Meye FJ, Diana M, Faure P, Mameli M, Caille S, Georges F, **Ventral Subiculum Stimulation Promotes Persistent Hyperactivity of Dopamine Neurons and Facilitates Behavioral Effects of Cocaine.** Cell Rep, 2015; 13

- *Valentinova K*, Tchenio A, Meye FJ, Lecca S, Mameli M, **[Hell after the pleasure: drug-induced negative symptoms involve lateral habenula].** Med Sci (Paris), 2015; 31

- Meye FJ*, *Valentinova K**, Lecca S*, Marion-Poll L, Maroteaux MJ, Musardo S, Moutkine I, Gardoni F, Huganir RL, Georges F, Mameli M, **Cocaine-evoked negative symptoms require AMPA receptor trafficking in the lateral habenula.** Nat Neurosci, 2015; 18

- Meye FJ, Lecca S, *Valentinova K*, Mameli M, **Synaptic and cellular profile of neurons in the lateral habenula.** Front Hum Neurosci, 2013; 7

*equally contributed

Reference list

Abercrombie, E.D., Keefe, K.A., DiFrischia, D.S., Zigmond, M.J., 1989. Differential effect of stress on in vivo dopamine release in striatum, nucleus accumbens, and medial frontal cortex. J. Neurochem. 52, 1655–8.

Adamantidis, A.R., Tsai, H.-C., Boutrel, B., Zhang, F., Stuber, G.D., Budygin, E.A., Touriño, C., Bonci, A., Deisseroth, K., de Lecea, L., 2011. Optogenetic interrogation of dopaminergic modulation of the multiple phases of reward-seeking behavior. J. Neurosci. 31, 10829–35.

Adelman, J.P., Maylie, J., Sah, P., 2012. Small-conductance Ca2+-activated K+ channels: form and function. Annu. Rev. Physiol. 74, 245–69.

Aghajanian, G.K., Wang, R.Y., 1977. Habenular and other midbrain raphe afferents demonstrated by a modified retrograde tracing technique. Brain Res. 122, 229–42.

Aizawa, H., Amo, R., Okamoto, H., 2011. Phylogeny and ontogeny of the habenular structure. Front. Neurosci. 5, 138.

Aizawa, H., Kobayashi, M., Tanaka, S., Fukai, T., Okamoto, H., 2012. Molecular characterization of the subnuclei in rat habenula. J. Comp. Neurol. 520, 4051–66.

Amara SG and Sonders MS., 1998. Neurotransmitter transporters as molecular targets for addictive drugs. Drug Alcohol Depend. 51, 87–96.

Amo, R., Aizawa, H., Takahoko, M., Kobayashi, M., Takahashi, R., Aoki, T., Okamoto, H., 2010. Identification of the zebrafish ventral habenula as a homolog of the mammalian lateral habenula. J. Neurosci. 30, 1566–74.

Andres, K.H., von Düring, M., Veh, R.W., 1999. Subnuclear organization of the rat habenular complexes. J. Comp. Neurol. 407, 130–50.

Anwyl, R., 1999. Metabotropic glutamate receptors: electrophysiological properties and role in plasticity. Brain Res. Brain Res. Rev. 29, 83–120.

Araki, M., McGeer, P.L., McGeer, E.G., 1984. Retrograde HRP tracing combined with a pharmacohistochemical method for GABA transaminase for the identification of presumptive GABAergic projections to the habenula. Brain Res. 304, 271–7.

Balcita-Pedicino, J.J., Omelchenko, N., Bell, R., Sesack, S.R., 2011. The inhibitory influence of the lateral habenula on midbrain dopamine cells: ultrastructural evidence for indirect

mediation via the rostromedial mesopontine tegmental nucleus. J. Comp. Neurol. 519, 1143–64.

Banke, T.G., Bowie, D., Lee, H., Huganir, R.L., Schousboe, A., Traynelis, S.F., 2000. Control of GluR1 AMPA receptor function by cAMP-dependent protein kinase. J. Neurosci. 20, 89–102.

Barbon, A., Barlati, S., 2011. Glutamate receptor RNA editing in health and disease. Biochem. Biokhimiia 76, 882–9.

Barria, A., Derkach, V., Soderling, T., 1997. Identification of the Ca2+/calmodulin-dependent protein kinase II regulatory phosphorylation site in the alpha-amino-3-hydroxyl-5-methyl-4-isoxazole-propionate-type glutamate receptor. J. Biol. Chem. 272, 32727–30.

Bellone, C., Lüscher, C., 2006. Cocaine triggered AMPA receptor redistribution is reversed in vivo by mGluR-dependent long-term depression. Nat. Neurosci. 9, 636–41.

Bellone, C., Lüscher, C., Mameli, M., 2008. Mechanisms of synaptic depression triggered by metabotropic glutamate receptors. Cell. Mol. Life Sci. 65, 2913–23.

Bernard, R., Veh, R.W., 2012. Individual neurons in the rat lateral habenular complex project mostly to the dopaminergic ventral tegmental area or to the serotonergic raphe nuclei. J. Comp. Neurol. 520, 2545–58.

Berridge, K.C., Robinson, T.E., 1998. What is the role of dopamine in reward: Hedonic impact, reward learning, or incentive salience? Brain Res. Rev. 28, 309–369.

Berton, O., McClung, C.A., Dileone, R.J., Krishnan, V., Renthal, W., Russo, S.J., Graham, D., Tsankova, N.M., Bolanos, C.A., Rios, M., Monteggia, L.M., Self, D.W., Nestler, E.J., 2006. Essential role of BDNF in the mesolimbic dopamine pathway in social defeat stress. Science 311, 864–8.

Bianco, I.H., Wilson, S.W., 2009. The habenular nuclei: a conserved asymmetric relay station in the vertebrate brain. Philos. Trans. R. Soc. Lond. B. Biol. Sci. 364, 1005–20.

Birnir, B., Korpi, E.R., 2007. The impact of sub-cellular location and intracellular neuronal proteins on properties of GABA(A) receptors. Curr. Pharm. Des. 13, 3169–77.

Björklund, A., Dunnett, S.B., 2007. Dopamine neuron systems in the brain: an update. Trends Neurosci. 30, 194–202.

Brandon, N.J., Jovanovic, J.N., Smart, T.G., Moss, S.J., 2002. Receptor for activated C

kinase-1 facilitates protein kinase C-dependent phosphorylation and functional modulation of GABA(A) receptors with the activation of G-protein-coupled receptors. J. Neurosci. 22, 6353–61.

Brinschwitz, K., Dittgen, a., Madai, V.I., Lommel, R., Geisler, S., Veh, R.W., 2010. Glutamatergic axons from the lateral habenula mainly terminate on GABAergic neurons of the ventral midbrain. Neuroscience 168, 463–476.

Brischoux, F., Chakraborty, S., Brierley, D.I., Ungless, M. a, 2009. Phasic excitation of dopamine neurons in ventral VTA by noxious stimuli. Proc. Natl. Acad. Sci. U. S. A. 106, 4894–9.

Bromberg-Martin, E.S., Matsumoto, M., Hikosaka, O., 2010. Dopamine in Motivational Control: Rewarding, Aversive, and Alerting. Neuron 68, 815–834.

Brown, R.M., Short, J.L., Lawrence, A.J., 2010. Identification of brain nuclei implicated in cocaine-primed reinstatement of conditioned place preference: a behaviour dissociable from sensitization. PLoS One 5, e15889.

Burnashev, N., Monyer, H., Seeburg, P.H., Sakmann, B., 1992. Divalent ion permeability of AMPA receptor channels is dominated by the edited form of a single subunit. Neuron 8, 189–98.

Cao, J.-L., Covington, H.E., Friedman, A.K., Wilkinson, M.B., Walsh, J.J., Cooper, D.C., Nestler, E.J., Han, M.-H., 2010. Mesolimbic dopamine neurons in the brain reward circuit mediate susceptibility to social defeat and antidepressant action. J. Neurosci. 30, 16453–8.

Chang, S., Kim, U., 2004. Ionic mechanism of long-lasting discharges of action potentials triggered by membrane hyperpolarization in the medial lateral habenula. J. Neurosci. 24, 2172–81.

Chaudhury, D., Walsh, J.J., Friedman, A.K., Juarez, B., Ku, S.M., Koo, J.W., Ferguson, D., Tsai, H.-C., Pomeranz, L., Christoffel, D.J., Nectow, A.R., Ekstrand, M., Domingos, A., Mazei-Robison, M.S., Mouzon, E., Lobo, M.K., Neve, R.L., Friedman, J.M., Russo, S.J., Deisseroth, K., Nestler, E.J., Han, M.-H., 2013. Rapid regulation of depression-related behaviours by control of midbrain dopamine neurons. Nature 493, 532–6.

Chen, B.T., Bowers, M.S., Martin, M., Hopf, F.W., Guillory, A.M., Carelli, R.M., Chou, J.K., Bonci, A., 2008. Cocaine but not natural reward self-administration nor passive cocaine infusion produces persistent LTP in the VTA. Neuron 59, 288–97.

Chevaleyre, V., Castillo, P.E., 2004. Endocannabinoid-mediated metaplasticity in the hippocampus. Neuron 43, 871–81.

Chevaleyre, V., Takahashi, K.A., Castillo, P.E., 2006. Endocannabinoid-mediated synaptic plasticity in the CNS. Annu. Rev. Neurosci. 29, 37–76.

Christoph, G.R., Leonzio, R.J., Wilcox, K.S., 1986. Stimulation of the lateral habenula inhibits dopamine-containing neurons in the substantia nigra and ventral tegmental area of the rat. J. Neurosci. 6, 613–9.

Clem, R.L., Barth, A., 2006. Pathway-specific trafficking of native AMPARs by in vivo experience. Neuron 49, 663–70.

Clem, R.L., Huganir, R.L., 2010. Calcium-permeable AMPA receptor dynamics mediate fear memory erasure. Science 330, 1108–12.

Comenencia-Ortiz, E., Moss, S.J., Davies, P.A., 2014. Phosphorylation of GABAA receptors influences receptor trafficking and neurosteroid actions. Psychopharmacology (Berl). 231, 3453–65.

Day, J.J., Roitman, M.F., Wightman, R.M., Carelli, R.M., 2007. Associative learning mediates dynamic shifts in dopamine signaling in the nucleus accumbens. Nat. Neurosci. 10, 1020–8.

DeLong, M.R., 1971. Activity of pallidal neurons during movement. J. Neurophysiol. 34, 414–27.

Derkach, V., Barria, A., Soderling, T.R., 1999. Ca2+/calmodulin-kinase II enhances channel conductance of alpha-amino-3-hydroxy-5-methyl-4-isoxazolepropionate type glutamate receptors. Proc. Natl. Acad. Sci. U. S. A. 96, 3269–74.

Di Chiara, G., Imperato, A., 1988. Drugs abused by humans preferentially increase synaptic dopamine concentrations in the mesolimbic system of freely moving rats. Proc. Natl. Acad. Sci. U. S. A. 85, 5274–8.

Díaz, E., Bravo, D., Rojas, X., Concha, M.L., 2011. Morphologic and immunohistochemical organization of the human habenular complex. J. Comp. Neurol. 519, 3727–47.

Donevan, S.D., Rogawski, M.A., 1995. Intracellular polyamines mediate inward rectification of Ca(2+)-permeable alpha-amino-3-hydroxy-5-methyl-4-isoxazolepropionic acid receptors. Proc. Natl. Acad. Sci. U. S. A. 92, 9298–302.

Dorocic, I.P., Fu, D., Xuan, Y., Johansson, Y., Pozzi, L., Silberberg, G., Carle, M., 2014. Article A Whole-Brain Atlas of Inputs to Serotonergic Neurons of the Dorsal and Median Raphe Nuclei 663–678.

Ehlers, M.D., 2000. Reinsertion or degradation of AMPA receptors determined by activity-dependent endocytic sorting. Neuron 28, 511–25.

Esteban, J.A., Shi, S.-H., Wilson, C., Nuriya, M., Huganir, R.L., Malinow, R., 2003. PKA phosphorylation of AMPA receptor subunits controls synaptic trafficking underlying plasticity. Nat. Neurosci. 6, 136–43.

Ettenberg, A., 2009. The runway model of drug self-administration. Pharmacol. Biochem. Behav. 91, 271–7.

Ettenberg, A., Geist, T.D., 1993. Qualitative and quantitative differences in the operant runway behavior of rats working for cocaine and heroin reinforcement. Pharmacol. Biochem. Behav. 44, 191–8.

Ettenberg, A., Raven, M.A., Danluck, D.A., Necessary, B.D., 1999. Evidence for opponent-process actions of intravenous cocaine. Pharmacol. Biochem. Behav. 64, 507–12.

Farrant, M., Nusser, Z., 2005. Variations on an inhibitory theme: phasic and tonic activation of GABA(A) receptors. Nat. Rev. Neurosci. 6, 215–29.

Feng, J., Cai, X., Zhao, J., Yan, Z., 2001. Serotonin Receptors Modulate GABA A Receptor Channels through Activation of Anchored Protein Kinase C in Prefrontal Cortical Neurons 21, 6502–6511.

Ferster, C.B., 1957. Withdrawal of positive reinforcement as punishment. Science 126, 509.

Fiorillo, C.D., Tobler, P.N., Schultz, W., 2003. Discrete coding of reward probability and uncertainty by dopamine neurons. Science 299, 1898–902.

Fiorino, D.F., Coury, A., Fibiger, H.C., Phillips, A.G., 1993. Electrical stimulation of reward sites in the ventral tegmental area increases dopamine transmission in the nucleus accumbens of the rat. Behav. Brain Res. 55, 131–41.

Freed, C., Revay, R., Vaughan, R.A., Kriek, E., Grant, S., Uhl, G.R., Kuhar, M.J., 1995. Dopamine transporter immunoreactivity in rat brain. J. Comp. Neurol. 359, 340–9.

Friedman, A., Lax, E., Dikshtein, Y., Abraham, L., Flaumenhaft, Y., Sudai, E., Ben-Tzion, M., Ami-Ad, L., Yaka, R., Yadid, G., 2010. Electrical stimulation of the lateral habenula

produces enduring inhibitory effect on cocaine seeking behavior. Neuropharmacology 59, 452–9.

Geisler, S., Andres, K.H., Veh, R.W., 2003. Morphologic and cytochemical criteria for the identification and delineation of individual subnuclei within the lateral habenular complex of the rat. J. Comp. Neurol. 458, 78–97.

Geist, T.D., Ettenberg, A.,. Concurrent positive and negative goalbox events produce runway behaviors comparable to those of cocaine-reinforced rats. Pharmacol. Biochem. Behav. 57, 145–50.

George, O., Koob, G.F., Vendruscolo, L.F., 2014. Negative reinforcement via motivational withdrawal is the driving force behind the transition to addiction 3911–3917.

Gerber, G.J., Sing, J., Wise, R.A., 1981. Pimozide attenuates lever pressing for water reinforcement in rats. Pharmacol. Biochem. Behav. 14, 201–5.

Gifuni, A.J., Jozaghi, S., Gauthier-Lamer, A.-C., Boye, S.M., 2012. Lesions of the lateral habenula dissociate the reward-enhancing and locomotor-stimulant effects of amphetamine. Neuropharmacology 63, 945–57.

Gill, M.J., Ghee, S.M., Harper, S.M., See, R.E., 2013. Inactivation of the lateral habenula reduces anxiogenic behavior and cocaine seeking under conditions of heightened stress. Pharmacol. Biochem. Behav. 111, 24–9.

Gonçalves, L., Sego, C., Metzger, M., 2012. Differential projections from the lateral habenula to the rostromedial tegmental nucleus and ventral tegmental area in the rat. J. Comp. Neurol. 520, 1278–1300.

González, J.A., Iordanidou, P., Strom, M., Adamantidis, A., Burdakov, D., 2016. Awake dynamics and brain-wide direct inputs of hypothalamic MCH and orexin networks. Nat. Commun. 7, 11395.

Good, C.H., Wang, H., Chen, Y.-H., Mejias-Aponte, C. a, Hoffman, A.F., Lupica, C.R., 2013. Dopamine D4 receptor excitation of lateral habenula neurons via multiple cellular mechanisms. J. Neurosci. 33, 16853–64.

Gruber, C., Kahl, A., Lebenheim, L., Kowski, A., Dittgen, A., Veh, R.W., 2007. Dopaminergic projections from the VTA substantially contribute to the mesohabenular pathway in the rat. Neurosci. Lett. 427, 165–70.

Hearing, M., Kotecki, L., Marron Fernandez de Velasco, E., Fajardo-Serrano, A., Chung,

H.J., Luján, R., Wickman, K., 2013. Repeated cocaine weakens GABA(B)-Girk signaling in layer 5/6 pyramidal neurons in the prelimbic cortex. Neuron 80, 159–70.

Heifets, B.D., Castillo, P.E., 2009. Endocannabinoid signaling and long-term synaptic plasticity. Annu. Rev. Physiol. 71, 283–306.

Henley, J.M., Wilkinson, K.A., 2016. Synaptic AMPA receptor composition in development, plasticity and disease. Nat. Rev. Neurosci. advance on, 337–50.

Hennigan, K., D'Ardenne, K., McClure, S.M., 2015. Distinct Midbrain and Habenula Pathways Are Involved in Processing Aversive Events in Humans. J. Neurosci. 35, 198–208.

Herkenham, M., Nauta, W.J., 1979. Efferent connections of the habenular nuclei in the rat. J. Comp. Neurol. 187, 19–47.

Herkenham, M., Nauta, W.J., 1977. Afferent connections of the habenular nuclei in the rat. A horseradish peroxidase study, with a note on the fiber-of-passage problem. J. Comp. Neurol. 173, 123–46.

Hernandez, L., Hoebel, B.G., 1988. Food reward and cocaine increase extracellular dopamine in the nucleus accumbens as measured by microdialysis. Life Sci. 42, 1705–12.

Herring, D., Huang, R., Singh, M., Dillon, G.H., Leidenheimer, N.J., 2005. PKC modulation of GABA A receptor endocytosis and function is inhibited by mutation of a dileucine motif within the receptor b 2 subunit 48, 181–194.

Hikosaka, O., 2010. The habenula: from stress evasion to value-based decision-making. Nat. Rev. Neurosci. 11, 503–513.

Hnasko, T.S., Hjelmstad, G.O., Fields, H.L., Edwards, R.H., 2012. Ventral tegmental area glutamate neurons: electrophysiological properties and projections. J. Neurosci. 32, 15076–85.

Hollerman, J.R., Schultz, W., 1998. Dopamine neurons report an error in the temporal prediction of reward during learning. Nat. Neurosci. 1, 304–9.

Hong, S., Hikosaka, O., 2013. Diverse sources of reward value signals in the basal ganglia nuclei transmitted to the lateral habenula in the monkey. Front. Hum. Neurosci. 7, 778.

Hong, S., Hikosaka, O., 2008. The globus pallidus sends reward-related signals to the lateral

habenula. Neuron 60, 720–9.

Hong, S., Jhou, T.C., Smith, M., Saleem, K.S., Hikosaka, O., 2011. Negative reward signals from the lateral habenula to dopamine neurons are mediated by rostromedial tegmental nucleus in primates. J. Neurosci. 31, 11457–71.

Hörtnagl, H., Tasan, R.O., Wieselthaler, A., Kirchmair, E., Sieghart, W., Sperk, G., 2013. Patterns of mRNA and protein expression for 12 GABAA receptor subunits in the mouse brain. Neuroscience 236, 345–72.

Huganir, R.L., Nicoll, R.A., 2013. Perspective AMPARs and Synaptic Plasticity : The Last 25 Years. Neuron 80, 704–717.

Huguenard, J.R., Gutnick, M.J., Prince, D.A., 1993. Transient Ca2+ currents in neurons isolated from rat lateral habenula. J. Neurophysiol. 70, 158–66.

Hyman, S.E., 2005. Addiction: a disease of learning and memory. Am. J. Psychiatry 162, 1414–22.

Ikemoto, S., 2007. Dopamine reward circuitry: two projection systems from the ventral midbrain to the nucleus accumbens-olfactory tubercle complex. Brain Res. Rev. 56, 27–78.

Ikemoto, S., Yang, C., Tan, A., 2015. Basal ganglia circuit loops, dopamine and motivation: A review and enquiry. Behav. Brain Res. 290, 17–31.

Jörntell, H., Hansel, C., 2006. Synaptic Memories Upside Down: Bidirectional Plasticity at Cerebellar Parallel Fiber-Purkinje Cell Synapses. Neuron.

James, M.H., Charnley, J.L., Flynn, J.R., Smith, D.W., Dayas, C. V, 2011. Propensity to “relapse” following exposure to cocaine cues is associated with the recruitment of specific thalamic and epithalamic nuclei. Neuroscience 199, 235–42.

Jennings, J.H., Sparta, D.R., Stamatakis, A.M., Ung, R.L., Pleil, K.E., Kash, T.L., Stuber, G.D., 2013. Distinct extended amygdala circuits for divergent motivational states. Nature 496, 224–228.

Jerng, H.H., Pfaffinger, P.J., 2014. Modulatory mechanisms and multiple functions of somatodendritic A-type K (+) channel auxiliary subunits. Front. Cell. Neurosci. 8, 82.

Jhou, T.C., Fields, H.L., Baxter, M.G., Saper, C.B., Holland, P.C., 2009a. The rostromedial tegmental nucleus (RMTg), a GABAergic afferent to midbrain dopamine neurons,

encodes aversive stimuli and inhibits motor responses. Neuron 61, 786–800.

Jhou, T.C., Geisler, S., Marinelli, M., Degarmo, B.A., Zahm, D.S., 2009b. The mesopontine rostromedial tegmental nucleus: A structure targeted by the lateral habenula that projects to the ventral tegmental area of Tsai and substantia nigra compacta. J. Comp. Neurol. 513, 566–96.

Jhou, T.C., Good, C.H., Rowley, C.S., Xu, S.-P., Wang, H., Burnham, N.W., Hoffman, A.F., Lupica, C.R., Ikemoto, S., 2013. Cocaine drives aversive conditioning via delayed activation of dopamine-responsive habenular and midbrain pathways. J. Neurosci. 33, 7501–12.

Ji, H., Shepard, P.D., 2007. Lateral habenula stimulation inhibits rat midbrain dopamine neurons through a GABA(A) receptor-mediated mechanism. J. Neurosci. 27, 6923–30.

Kalivas, P.W., Duffy, P., 1995. Selective activation of dopamine transmission in the shell of the nucleus accumbens by stress. Brain Res. 675, 325–8.

Kasanetz, F., Deroche-Gamonet, V., Berson, N., Balado, E., Lafourcade, M., Manzoni, O., Piazza, P.V., 2010. Transition to addiction is associated with a persistent impairment in synaptic plasticity. Science 328, 1709–12.

Kaufling, J., Veinante, P., Pawlowski, S.A., Freund-Mercier, M.-J., Barrot, M., 2009. Afferents to the GABAergic tail of the ventral tegmental area in the rat. J. Comp. Neurol. 513, 597–621.

Keiflin, R., Janak, P.H., 2015. Review Dopamine Prediction Errors in Reward Learning and Addiction : From Theory to Neural Circuitry. Neuron 88, 247–263.

Kelly, L., Farrant, M., Cull-Candy, S.G., 2009. Synaptic mGluR activation drives plasticity of calcium-permeable AMPA receptors. Nat. Neurosci. 12, 593–601.

Kiening, K., Sartorius, A., 2013. A new translational target for deep brain stimulation to treat depression. EMBO Mol. Med. 5, 1151–3.

Kim J, Jung SC, Clemens AM, Petralia RS, H.D., 2007. Regulation of dendritic excitability by activity-dependent trafficking of the A-type K+ channel subunit Kv4.2 in hippocampal neurons. Neuron 54, 933–47.

Kim, C.H., Lee, J., Lee, J.-Y., Roche, K.W., 2008. Metabotropic glutamate receptors: phosphorylation and receptor signaling. J. Neurosci. Res. 86, 1–10.

Kim, U., Chang, S.-Y., 2005. Dendritic morphology, local circuitry, and intrinsic electrophysiology of neurons in the rat medial and lateral habenular nuclei of the epithalamus. J. Comp. Neurol. 483, 236–50.

Kim, U., Lee, T., 2012. Topography of descending projections from anterior insular and medial prefrontal regions to the lateral habenula of the epithalamus in the rat. Eur. J. Neurosci. 35, 1253–69.

Kittler, J.T., Moss, S.J., 2003. Modulation of GABAA receptor activity by phosphorylation and receptor trafficking: implications for the efficacy of synaptic inhibition. Curr. Opin. Neurobiol. 13, 341–7.

Knackstedt, L.A., Samimi, M.M., Ettenberg, A., 2002. Evidence for opponent-process actions of intravenous cocaine and cocaethylene. Pharmacol. Biochem. Behav. 72, 931–6.

Koob, G.F., 2013. Negative reinforcement in drug addiction : the darkness within. Curr. Opin. Neurobiol. 23, 559–563.

Koob, G.F., Le Moal, M., 2008. Review. Neurobiological mechanisms for opponent motivational processes in addiction. Philos. Trans. R. Soc. Lond. B. Biol. Sci. 363, 3113–23.

Kowski, a B., Veh, R.W., Weiss, T., 2009. Dopaminergic activation excites rat lateral habenular neurons in vivo. Neuroscience 161, 1154–65.

Kowski, A.B., Geisler, S., Krauss, M., 2008. Differential Projections from Subfields in the Lateral Preoptic Area to the Lateral Habenular Complex of the Rat 1478, 1465–1478.

Kreitzer, A.C., Malenka, R.C., 2007. Endocannabinoid-mediated rescue of striatal LTD and motor deficits in Parkinson's disease models. Nature 445, 643–7.

Kreitzer, A.C., Malenka, R.C., 2005. Dopamine modulation of state-dependent endocannabinoid release and long-term depression in the striatum. J. Neurosci. 25, 10537–45.

Krishnan, V., Han, M.-H., Graham, D.L., Berton, O., Renthal, W., Russo, S.J., Laplant, Q., Graham, A., Lutter, M., Lagace, D.C., Ghose, S., Reister, R., Tannous, P., Green, T. a, Neve, R.L., Chakravarty, S., Kumar, A., Eisch, A.J., Self, D.W., Lee, F.S., Tamminga, C. a, Cooper, D.C., Gershenfeld, H.K., Nestler, E.J., 2007. Molecular adaptations underlying susceptibility and resistance to social defeat in brain reward regions. Cell 131, 391–404.

Lammel, S., Elizabeth, E., Luo, L., Robert, C., Wall, N.R., Beier, K., Luo, L., 2015. Diversity of Transgenic Mouse Models for Selective Targeting of Midbrain Dopamine Neurons Matters Arising Diversity of Transgenic Mouse Models for Selective Targeting of Midbrain Dopamine Neurons 429–438.

Lammel, S., Ion, D.I., Roeper, J., Malenka, R.C., 2011. Projection-Specific Modulation of Dopamine Neuron Synapses by Aversive and Rewarding Stimuli. Neuron 70, 855–862.

Lammel, S., Lim, B.K., Malenka, R.C., 2014. Reward and aversion in a heterogeneous midbrain dopamine system. Neuropharmacology 76 Pt B, 351–9.

Lammel, S., Lim, B.K., Ran, C., Huang, K.W., Betley, M.J., Tye, K.M., Deisseroth, K., Malenka, R.C., 2012. Input-specific control of reward and aversion in the ventral tegmental area. Nature 491, 212–7.

Lamsa, K.P., Heeroma, J.H., Somogyi, P., Rusakov, D.A., Kullmann, D.M., 2007. Anti-Hebbian long-term potentiation in the hippocampal feedback inhibitory circuit. Science 315, 1262–6.

Lawson, R.P., Nord, C.L., Seymour, B., Thomas, D.L., Dayan, P., Pilling, S., Roiser, J.P., 2016. Disrupted habenula function in major depression. Mol. Psychiatry.

Lawson, R.P., Seymour, B., Loh, E., Lutti, A., Dolan, R.J., Dayan, P., Weiskopf, N., Roiser, J.P., 2014. The habenula encodes negative motivational value associated with primary punishment in humans. Proc. Natl. Acad. Sci. U. S. A. 111, 11858–63.

Le Roux, N., Cabezas, C., Böhm, U.L., Poncer, J.C., 2013. Input-specific learning rules at excitatory synapses onto hippocampal parvalbumin-expressing interneurons. J. Physiol. 591, 1809–22.

Lecca, S., Melis, M., Luchicchi, A., Muntoni, A.L., Pistis, M., 2012. Inhibitory inputs from rostromedial tegmental neurons regulate spontaneous activity of midbrain dopamine cells and their responses to drugs of abuse. Neuropsychopharmacology 37, 1164–76.

Lecca, S., Meye, F.J., Mameli, M., 2014. The lateral habenula in addiction and depression: an anatomical, synaptic and behavioral overview. Eur. J. Neurosci. 39, 1170–8.

Lecca, S., Pelosi, A., Tchenio, A., Moutkine, I., Lujan, R., Hervé, D., Mameli, M., 2016. Rescue of GABA B and GIRK function in the lateral habenula by protein phosphatase 2A inhibition ameliorates depression-like phenotypes in mice.

Lecourtier, L., DeFrancesco, A., Moghaddam, B., 2008. Differential tonic influence of lateral

habenula on prefrontal cortex and nucleus accumbens dopamine release. Eur. J. Neurosci. 27, 1755–1762.

LeDoux, J.E., 2000. Emotion circuits in the brain. Annu. Rev. Neurosci. 23, 155–84.

Lee HK, Barbarosie M, Kameyama K, Bear MF, H.R., 2000. Regulation of distinct AMPA receptor phosphorylation sites during bidirectional synaptic plasticity. Nature 405, 955–9.

Li, B., Piriz, J., Mirrione, M., Chung, C., Proulx, C.D., Schulz, D., Henn, F., Malinow, R., 2011. Synaptic potentiation onto habenula neurons in the learned helplessness model of depression. Nature 470, 535–9.

Li, K., Zhou, T., Liao, L., Yang, Z., Wong, C., Henn, F., Malinow, R., Yates, J.R., Hu, H., 2013. βCaMKII in lateral habenula mediates core symptoms of depression. Science 341, 1016–20.

Lim, L.W., Prickaerts, J., Huguet, G., Kadar, E., Hartung, H., Sharp, T., Temel, Y., 2015. Electrical stimulation alleviates depressive-like behaviors of rats: investigation of brain targets and potential mechanisms. Transl. Psychiatry 5, e535.

Lin, M.T., Luján, R., Watanabe, M., Frerking, M., Maylie, J., Adelman, J.P., 2010. Coupled activity-dependent trafficking of synaptic SK2 channels and AMPA receptors. J. Neurosci. 30, 11726–34.

Liu, S.J., Zukin, R.S., 2007. Ca2+-permeable AMPA receptors in synaptic plasticity and neuronal death. Trends Neurosci. 30, 126–34.

Lomeli, H., Mosbacher, J., Melcher, T., Höger, T., Geiger, J.R., Kuner, T., Monyer, H., Higuchi, M., Bach, A., Seeburg, P.H., 1994. Control of kinetic properties of AMPA receptor channels by nuclear RNA editing. Science 266, 1709–13.

Lujan, R., Nusser, Z., Roberts, J.D., Shigemoto, R., Somogyi, P., 1996. Perisynaptic location of metabotropic glutamate receptors mGluR1 and mGluR5 on dendrites and dendritic spines in the rat hippocampus. Eur. J. Neurosci. 8, 1488–500.

Luscher, B., Fuchs, T., Kilpatrick, C.L., 2011. GABAA receptor trafficking-mediated plasticity of inhibitory synapses. Neuron 70, 385–409.

Lüscher, C., 2016. The Emergence of a Circuit Model for Addiction. Annu. Rev. Neurosci.

Lüscher, C., Huber, K.M., 2010. Group 1 mGluR-dependent synaptic long-term depression:

mechanisms and implications for circuitry and disease. Neuron 65, 445–59.

Lüscher, C., Malenka, R.C., 2011. Drug-evoked synaptic plasticity in addiction: from molecular changes to circuit remodeling. Neuron 69, 650–63.

Lüscher, C., Slesinger, P.A., 2010. Emerging roles for G protein-gated inwardly rectifying potassium (GIRK) channels in health and disease. Nat. Rev. Neurosci. 11, 301–15.

Madsen, H.B., Brown, R.M., Short, J.L., Lawrence, A.J., 2012. Investigation of the neuroanatomical substrates of reward seeking following protracted abstinence in mice. J. Physiol. 590, 2427–42.

Maejima, T., Hashimoto, K., Yoshida, T., Aiba, A., Kano, M., 2001. Presynaptic inhibition caused by retrograde signal from metabotropic glutamate to cannabinoid receptors. Neuron 31, 463–75.

Mahler, S. V, Aston-Jones, G.S., 2012. Fos activation of selective afferents to ventral tegmental area during cue-induced reinstatement of cocaine seeking in rats. J. Neurosci. 32, 13309–26.

Malenka, R.C., Bear, M.F., 2004. LTP and LTD: an embarrassment of riches. Neuron 44, 5–21.

Malinow, R., Malenka, R.C., 2002. AMPA receptor trafficking and synaptic plasticity. Annu. Rev. Neurosci. 25, 103–26.

Mameli, M., Balland, B., Luján, R., Lüscher, C., 2007. Rapid synthesis and synaptic insertion of GluR2 for mGluR-LTD in the ventral tegmental area. Science 317, 530–3.

Mameli, M., Bellone, C., Brown, M.T.C., Lüscher, C., 2011. Cocaine inverts rules for synaptic plasticity of glutamate transmission in the ventral tegmental area. Nat. Neurosci. 14, 414–6.

Mameli, M., Halbout, B., Creton, C., Engblom, D., Parkitna, J.R., Spanagel, R., Lüscher, C., 2009. Cocaine-evoked synaptic plasticity: persistence in the VTA triggers adaptations in the NAc. Nat. Neurosci. 12, 1036–41.

Mammen AL, Kameyama K, Roche KW, H.R., 1997. Phosphorylation of the alpha-amino-3-hydroxy-5-methylisoxazole4-propionic acid receptor GluR1 subunit by calcium/calmodulin-dependent kinase II. J. Biol. Chem. 272, 32528–33.

Maroteaux, M., Mameli, M., 2012. Cocaine evokes projection-specific synaptic plasticity of

lateral habenula neurons. J. Neurosci. 32, 12641–6.

Matsui, A., Williams, J.T., 2011. Opioid-sensitive GABA inputs from rostromedial tegmental nucleus synapse onto midbrain dopamine neurons. J. Neurosci. 31, 17729–35.

Matsumoto, M., Hikosaka, O., 2009a. Representation of negative motivational value in the primate lateral habenula. Nat. Neurosci. 12, 77–84.

Matsumoto, M., Hikosaka, O., 2009b. Two types of dopamine neuron distinctly convey positive and negative motivational signals. Nature 459, 837–41.

Matsumoto, M., Hikosaka, O., 2007. Lateral habenula as a source of negative reward signals in dopamine neurons. Nature 447, 1111–5.

McClure, S.M., Daw, N.D., Montague, P.R., 2003. A computational substrate for incentive salience. Trends Neurosci. 26, 423–8.

McCutcheon, J.E., Wang, X., Tseng, K.Y., Wolf, M.E., Marinelli, M., 2011a. Calcium-permeable AMPA receptors are present in nucleus accumbens synapses after prolonged withdrawal from cocaine self-administration but not experimenter-administered cocaine. J. Neurosci. 31, 5737–43.

McCutcheon, J.E., Loweth, J.A., Ford, K.A., Marinelli, M., Wolf, M.E., Tseng, K.Y., 2011b. Group I mGluR Activation Reverses Cocaine-Induced Accumulation of Calcium-Permeable AMPA Receptors in Nucleus Accumbens Synapses via a Protein Kinase C-Dependent Mechanism 31, 14536–14541.

Meng, H., Wang, Y., Huang, M., Lin, W., Wang, S., Zhang, B., 2011. Chronic deep brain stimulation of the lateral habenula nucleus in a rat model of depression. Brain Res. 1422, 32–8.

Meye, F.J., Lecca, S., Valentinova, K., Mameli, M., 2013. Synaptic and cellular profile of neurons in the lateral habenula. Front. Hum. Neurosci. 7, 860.

Meye, F.J., Soiza-Reilly, M., Smit, T., Diana, M.A., Schwarz, M.K., Mameli, M., 2016. Shifted pallidal co-release of GABA and glutamate in habenula drives cocaine withdrawal and relapse. Nat. Neurosci.

Meye, F.J., Valentinova, K., Lecca, S., Marion-poll, L., Maroteaux, M.J., Musardo, S., Moutkine, I., Gardoni, F., Huganir, R.L., Georges, F., Mameli, M., 2015. Cocaine-evoked negative symptoms require AMPA receptor trafficking in the lateral habenula.

Mirenowicz, J., Schultz, W., 1996. Preferential activation of midbrain dopamine neurons by appetitive rather than aversive stimuli. Nature 379, 449–51.

Mirrione, M.M., Schulz, D., Lapidus, K. a B., Zhang, S., Goodman, W., Henn, F. a, 2014. Increased metabolic activity in the septum and habenula during stress is linked to subsequent expression of learned helplessness behavior. Front. Hum. Neurosci. 8, 29.

Mogenson, G.J., Jones, D.L., Yim, C.Y., 1980. From motivation to action: functional interface between the limbic system and the motor system. Prog. Neurobiol. 14, 69–97.

Morris, J.S., Smith, K.A., Cowen, P.J., Friston, K.J., Dolan, R.J., 1999. Covariation of activity in habenula and dorsal raphé nuclei following tryptophan depletion. Neuroimage 10, 163–72.

Nagy, J.I., Carter, D.A., Lehmann, J., Fibiger, H.C., 1978. Evidence for a GABA-containing projection from the entopeduncular nucleus to the lateral habenula in the rat. Brain Res. 145, 360–4.

Nestler, E.J., Carlezon, W.A., 2006. The mesolimbic dopamine reward circuit in depression. Biol. Psychiatry 59, 1151–9.

Neumann, P.A., Ishikawa, M., Otaka, M., Huang, Y.H., Schlüter, O.M., Dong, Y., 2015. Increased excitability of lateral habenula neurons in adolescent rats following cocaine self-administration. Int. J. Neuropsychopharmacol. 18.

Nicoll, R.A., Tomita, S., Bredt, D.S., 2006. Auxiliary subunits assist AMPA-type glutamate receptors. Science 311, 1253–6.

Nieh, E.H., Kim, S.-Y., Namburi, P., Tye, K.M., 2013. Optogenetic dissection of neural circuits underlying emotional valence and motivated behaviors. Brain Res. 1511, 73–92.

Olsen, R.W., Sieghart, W., 2009. GABA A receptors: subtypes provide diversity of function and pharmacology. Neuropharmacology 56, 141–8.

Omelchenko, N., Bell, R., Sesack, S.R., 2009. Lateral habenula projections to dopamine and GABA neurons in the rat ventral tegmental area. Eur. J. Neurosci. 30, 1239–50.

Padgett, C.L., Lalive, A.L., Tan, K.R., Terunuma, M., Munoz, M.B., Pangalos, M.N., Martínez-Hernández, J., Watanabe, M., Moss, S.J., Luján, R., Lüscher, C., Slesinger, P.A., 2012. Methamphetamine-evoked depression of GABA(B) receptor signaling in GABA neurons of the VTA. Neuron 73, 978–89.

Paoletti, P., Bellone, C., Zhou, Q., 2013. NMDA receptor subunit diversity: impact on receptor properties, synaptic plasticity and disease. Nat. Rev. Neurosci. 14, 383–400.

Parent, A., Gravel, S., Boucher, R., 1981. The origin of forebrain afferents to the habenula in rat, cat and monkey. Brain Res. Bull. 6, 23–38.

Pascoli, V., Turiault, M., Lüscher, C., 2012. Reversal of cocaine-evoked synaptic potentiation resets drug-induced adaptive behaviour. Nature 481, 71–5.

Perrotti, L.I., Bolaños, C.A., Choi, K.-H., Russo, S.J., Edwards, S., Ulery, P.G., Wallace, D.L., Self, D.W., Nestler, E.J., Barrot, M., 2005. DeltaFosB accumulates in a GABAergic cell population in the posterior tail of the ventral tegmental area after psychostimulant treatment. Eur. J. Neurosci. 21, 2817–24.

Phillipson, O.T., Pycock, C.J., 1982. Dopamine neurones of the ventral tegmentum project to both medial and lateral habenula. Some implications for habenular function. Exp. brain Res. 45, 89–94.

Pignatelli, M., Bonci, A., 2015. Role of Dopamine Neurons in Reward and Aversion: A Synaptic Plasticity Perspective. Neuron 86, 1145–57.

Pirker, S., Schwarzer, C., Wieselthaler, A., Sieghart, W., Sperk, G., 2000. GABA(A) receptors: immunocytochemical distribution of 13 subunits in the adult rat brain. Neuroscience 101, 815–50.

Poller, W.C., Bernard, R., Derst, C., Weiss, T., Madai, V.I., Veh, R.W., 2011. Lateral habenular neurons projecting to reward-processing monoaminergic nuclei express hyperpolarization-activated cyclic nucleotid-gated cation channels. Neuroscience 193, 205–16.

Poller, W.C., Madai, V.I., Bernard, R., Laube, G., Veh, R.W., 2013. A glutamatergic projection from the lateral hypothalamus targets VTA-projecting neurons in the lateral habenula of the rat. Brain Res. 1507, 45–60.

Pompeiano, M., Palacios, J.M., Mengod, G., 1994. Distribution of the serotonin 5 - H T 2 receptor family mRNAs : comparison between 5-HT2A and 5-HT2c receptors 23, 163–178.

Porrino, L.J., Domer, F.R., Crane, A.M., Sokoloff, L., 1988. Selective alterations in cerebral metabolism within the mesocorticolimbic dopaminergic system produced by acute cocaine administration in rats. Neuropsychopharmacology 1, 109–18.

Proulx, C.D., Hikosaka, O., Malinow, R., 2014. Reward processing by the lateral habenula in normal and depressive behaviors. Nat. Neurosci. 17, 1146–1152.

Riedel, G., Wetzel, W., Reymann, K.G., 1996. Comparing the role of metabotropic glutamate receptors in long-term potentiation and in learning and memory. Prog. Neuro-Psychopharmacology Biol. Psychiatry 20, 761–789.

Robbins, T.W., Everitt, B.J., 1996. Neurobehavioural mechanisms of reward and motivation. Curr. Opin. Neurobiol. 6, 228–36.

Roche KW, O'Brien RJ, Mammen AL, Bernhardt J, H.R., 1996. Characterization of multiple phosphorylation sites on the AMPA receptor GluR1 subunit. Neuron 16, 1179–88.

Root, D.H., Mejias-Aponte, C. a., Qi, J., Morales, M., 2014a. Role of Glutamatergic Projections from Ventral Tegmental Area to Lateral Habenula in Aversive Conditioning. J. Neurosci. 34, 13906–13910.

Root, D.H., Mejias-Aponte, C. a, Zhang, S., Wang, H.-L., Hoffman, A.F., Lupica, C.R., Morales, M., 2014b. Single rodent mesohabenular axons release glutamate and GABA. Nat. Neurosci. 17.

Rumpel, S., LeDoux, J., Zador, A., Malinow, R., 2005. Postsynaptic receptor trafficking underlying a form of associative learning. Science 308, 83–8.

Russo, S.J., Nestler, E.J., 2013. The brain reward circuitry in mood disorders. Nat. Rev. Neurosci. 14, 609–25.

Saal, D., Dong, Y., Bonci, A., Malenka, R.C., 2003. Drugs of abuse and stress trigger a common synaptic adaptation in dopamine neurons. Neuron 37, 577–82.

Sartorius, A., Henn, F. a, 2007. Deep brain stimulation of the lateral habenula in treatment resistant major depression. Med. Hypotheses 69, 1305–8.

Sartorius, A., Kiening, K.L., Kirsch, P., von Gall, C.C., Haberkorn, U., Unterberg, A.W., Henn, F. a, Meyer-Lindenberg, A., 2010. Remission of major depression under deep brain stimulation of the lateral habenula in a therapy-refractory patient. Biol. Psychiatry 67, e9–e11.

Schultz, W., 2007a. Behavioral dopamine signals. Trends Neurosci. 30, 203–10.

Schultz, W., 2007b. Multiple dopamine functions at different time courses. Annu. Rev. Neurosci. 30, 259–88.

Schultz, W., 1998. Predictive reward signal of dopamine neurons. J. Neurophysiol. 80, 1–27.

Schultz, W., Dayan, P., Montague, P.R., 1997. A neural substrate of prediction and reward. Science (80-.). 275, 1593–1599.

Sego, C., Gonçalves, L., Lima, L., Furigo, I.C., Donato, J., Metzger, M., 2014. Lateral habenula and the rostromedial tegmental nucleus innervate neurochemically distinct subdivisions of the dorsal raphe nucleus in the rat. J. Comp. Neurol. 522, 1454–1484.

Self, D.W., Nestler, E.J.,. Relapse to drug-seeking: neural and molecular mechanisms. Drug Alcohol Depend. 51, 49–60.

Shabel, S.J., Proulx, C.D., Piriz, J., Malinow, R., 2014. Mood regulation. GABA/glutamate co-release controls habenula output and is modified by antidepressant treatment. Science 345, 1494–8.

Shabel, S.J., Proulx, C.D., Trias, A., Murphy, R.T., Malinow, R., 2012. Input to the lateral habenula from the basal ganglia is excitatory, aversive, and suppressed by serotonin. Neuron 74, 475–81.

Shen, X., Ruan, X., Zhao, H., 2012. Stimulation of midbrain dopaminergic structures modifies firing rates of rat lateral habenula neurons. PLoS One 7, e34323.

Shumake, J., Gonzalez-Lima, F., 2003. Brain systems underlying susceptibility to helplessness and depression. Behav. Cogn. Neurosci. Rev. 2, 198–221.

Sinha, R., 2008. Chronic stress, drug use, and vulnerability to addiction. Ann. N. Y. Acad. Sci. 1141, 105–30.

Skagerberg, G., Lindvall, O., Björklund, A., 1984. Origin, course and termination of the mesohabenular dopamine pathway in the rat. Brain Res. 307, 99–108.

Smith, Y., Séguéla, P., Parent, A., 1987. Distribution of GABA-immunoreactive neurons in the thalamus of the squirrel monkey (Saimiri sciureus). Neuroscience 22, 579–91.

Stamatakis, A.M., Jennings, J.H., Ung, R.L., Blair, G. a, Weinberg, R.J., Neve, R.L., Boyce, F., Mattis, J., Ramakrishnan, C., Deisseroth, K., Stuber, G.D., 2013. A unique population of ventral tegmental area neurons inhibits the lateral habenula to promote reward. Neuron 80, 1039–53.

Stamatakis, A.M., Stuber, G.D., 2012. Activation of lateral habenula inputs to the ventral midbrain promotes behavioral avoidance. Nat. Neurosci. 15, 1105–1107.

Stamatakis, A.M., Van Swieten, M., Basiri, M.L., Blair, G.A., Kantak, P., Stuber, G.D., 2016. Lateral Hypothalamic Area Glutamatergic Neurons and Their Projections to the Lateral Habenula Regulate Feeding and Reward. J. Neurosci. 36, 302–11.

Stuber, G.D., Klanker, M., de Ridder, B., Bowers, M.S., Joosten, R.N., Feenstra, M.G., Bonci, A., 2008. Reward-predictive cues enhance excitatory synaptic strength onto midbrain dopamine neurons. Science 321, 1690–2.

Stuber, G.D., Stamatakis, A.M., Kantak, P.A., 2015. Considerations when using cre-driver rodent lines for studying ventral tegmental area circuitry. Neuron 85, 439–45.

Stuber, G.D., Wise, R.A., 2016. Lateral hypothalamic circuits for feeding and reward. Nat. Neurosci. 19, 198–205.

Sutherland, R.J., 1982. The dorsal diencephalic conduction system: a review of the anatomy and functions of the habenular complex. Neurosci. Biobehav. Rev. 6, 1–13.

Swanson, G.T., Kamboj, S.K., Cull-Candy, S.G., 1997. Single-channel properties of recombinant AMPA receptors depend on RNA editing, splice variation, and subunit composition. J. Neurosci. 17, 58–69.

Swanson, L.W.,. The projections of the ventral tegmental area and adjacent regions: a combined fluorescent retrograde tracer and immunofluorescence study in the rat. Brain Res. Bull. 9, 321–53.

Swope, S.L., Moss, S.J., Raymond, L.A., Huganir, R.L., 1999. Regulation of ligand-gated ion channels by protein phosphorylation. Adv. Second Messenger Phosphoprotein Res. 33, 49–78.

Tan, K.R., Yvon, C., Turiault, M., Mirzabekov, J.J., Doehner, J., Labouèbe, G., Deisseroth, K., Tye, K.M., Lüscher, C., 2012. GABA neurons of the VTA drive conditioned place aversion. Neuron 73, 1173–83.

Terunuma, M., Pangalos, M.N., Moss, S.J., 2010. Functional modulation of GABAB receptors by protein kinases and receptor trafficking. Adv. Pharmacol. 58, 113–22.

Thierry, A.M., Tassin, J.P., Blanc, G., Glowinski, J., 1976. Selective activation of mesocortical DA system by stress. Nature 263, 242–4.

Tian, J., Uchida, N., 2015. Habenula Lesions Reveal that Multiple Mechanisms Underlie Dopamine Prediction Errors Article Habenula Lesions Reveal that Multiple Mechanisms Underlie Dopamine Prediction Errors. Neuron 87, 1304–1316.

Tobler, P.N., Dickinson, A., Schultz, W., 2003. Coding of predicted reward omission by dopamine neurons in a conditioned inhibition paradigm. J. Neurosci. 23, 10402–10.

Tripathi, A., Prensa, L., Mengual, E., 2013. Axonal branching patterns of ventral pallidal neurons in the rat. Brain Struct. Funct. 218, 1133–57.

Tsai, H.-C., Zhang, F., Adamantidis, A., Stuber, G.D., Bonci, A., de Lecea, L., Deisseroth, K., 2009. Phasic firing in dopaminergic neurons is sufficient for behavioral conditioning. Science 324, 1080–4.

Tzschentke, T.M., 2007. Measuring reward with the conditioned place preference (CPP) paradigm: update of the last decade. Addict. Biol. 12, 227–462.

Ullsperger, M., von Cramon, D.Y., 2003. Error monitoring using external feedback: specific roles of the habenular complex, the reward system, and the cingulate motor area revealed by functional magnetic resonance imaging. J. Neurosci. 23, 4308–14.

Ungerstedt, U., 1971. Adipsia and aphagia after 6-hydroxydopamine induced degeneration of the nigro-striatal dopamine system. Acta Physiol. Scand. Suppl. 367, 95–122.

Ungless, M. a, Magill, P.J., Bolam, J.P., 2004. Uniform inhibition of dopamine neurons in the ventral tegmental area by aversive stimuli. Science (80-.). 303, 2040–2042.

Ungless, M.A., Whistler, J.L., Malenka, R.C., Bonci, A., 2001. Single cocaine exposure in vivo induces long-term potentiation in dopamine neurons. Nature 411, 583–7.

Valenstein, E.S., Valenstein, T., 1964. Interaction of positive and negative reinforcing neural systems. Science 145, 1456–8.

van Zessen, R., Phillips, J.L., Budygin, E.A., Stuber, G.D., 2012. Activation of VTA GABA neurons disrupts reward consumption. Neuron 73, 1184–94.

Vaughan, R.A., Foster, J.D., 2013. Mechanisms of dopamine transporter regulation in normal and disease states. Trends Pharmacol. Sci. 34, 489–96.

Vilaró, M.T., Palacios, J.M., Mengod, G., 1990. Localization of m5 muscarinic receptor mRNA in rat brain examined by in situ hybridization histochemistry. Neurosci. Lett. 114, 154–9.

Vitek, J.L., 2002. Mechanisms of deep brain stimulation: excitation or inhibition. Mov. Disord. 17 Suppl 3, S69–72.

Volman, S.F., Lammel, S., Margolis, E.B., Kim, Y., Richard, J.M., Roitman, M.F., Lobo, M.K.,

2013. New insights into the specificity and plasticity of reward and aversion encoding in the mesolimbic system. J. Neurosci. 33, 17569–17576.

Wagner, F., Stroh, T., Veh, R.W., 2014. Correlating habenular subnuclei in rat and mouse by using topographic, morphological, and cytochemical criteria. J. Comp. Neurol. 522, 2650–62.

Wang, J.Q., Arora, A., Yang, L., Parelkar, N.K., Zhang, G., Liu, X., Choe, E.S., Mao, L., 2005. Phosphorylation of AMPA receptors: mechanisms and synaptic plasticity. Mol. Neurobiol. 32, 237–49.

Warden, M.R., Selimbeyoglu, A., Mirzabekov, J.J., Lo, M., Thompson, K.R., Kim, S.-Y., Adhikari, A., Tye, K.M., Frank, L.M., Deisseroth, K., 2012. A prefrontal cortex-brainstem neuronal projection that controls response to behavioural challenge. Nature 492, 428–32.

Weiss, T., Veh, R.W., 2011. Morphological and electrophysiological characteristics of neurons within identified subnuclei of the lateral habenula in rat brain slices. Neuroscience 172, 74–93.

Weissbourd, B., Ren, J., Deloach, K.E., Guenthner, C.J., Miyamichi, K., 2014. Article Presynaptic Partners of Dorsal Raphe Serotonergic and GABAergic Neurons. Neuron 83, 645–662.

Wilcox, K.S., Gutnick, M.J., Christoph, G.R., 1988. Electrophysiological properties of neurons in the lateral habenula nucleus: an in vitro study. J. Neurophysiol. 59, 212–25.

Winter, C., Vollmayr, B., Djodari-Irani, a, Klein, J., Sartorius, a, 2011. Pharmacological inhibition of the lateral habenula improves depressive-like behavior in an animal model of treatment resistant depression. Behav. Brain Res. 216, 463–5.

Wise, R. a., 2005. Forebrain substrates of reward and motivation. J. Comp. Neurol. 493, 115–121.

Wise, R.A., Rompre, P.P., 1989. Brain dopamine and reward. Annu. Rev. Psychol. 40, 191–225.

Wise, R.A., Spindler, J., deWit, H., Gerberg, G.J., 1978. Neuroleptic-induced “anhedonia” in rats: pimozide blocks reward quality of food. Science 201, 262–4.

Yang, H., Yang, J., Xi, W., Hao, S., Luo, B., He, X., Zhu, L., Lou, H., Yu, Y., Xu, F., Duan, S., Wang, H., 2016. Laterodorsal tegmentum interneuron subtypes oppositely regulate

olfactory cue-induced innate fear. Nat. Neurosci.

Yang, L.-M., Hu, B., Xia, Y.-H., Zhang, B.-L., Zhao, H., 2008. Lateral habenula lesions improve the behavioral response in depressed rats via increasing the serotonin level in dorsal raphe nucleus. Behav. Brain Res. 188, 84–90.

Zahm, D.S., Becker, M.L., Freiman, A.J., Strauch, S., Degarmo, B., Geisler, S., Meredith, G.E., Marinelli, M., 2010. Fos after single and repeated self-administration of cocaine and saline in the rat: emphasis on the Basal forebrain and recalibration of expression. Neuropsychopharmacology 35, 445–63.

Zhang, C.-X., Zhang, H., Xu, H.-Y., Li, M.-X., Wang, S., 2013. The lateral habenula is a common target of cocaine and dexamethasone. Neurosci. Lett. 555, 12–7.

Zhang, F., Zhou, W., Liu, H., Zhu, H., Tang, S., Lai, M., Yang, G., 2005. Increased c-Fos expression in the medial part of the lateral habenula during cue-evoked heroin-seeking in rats. Neurosci. Lett. 386, 133–7.

Zhang, L., Hernández, V.S., Vázquez-Juárez, E., Chay, F.K., Barrio, R.A., 2016. Thirst Is Associated with Suppression of Habenula Output and Active Stress Coping: Is there a Role for a Non-canonical Vasopressin-Glutamate Pathway? Front. Neural Circuits 10, 13.

Zhu, Y., Wienecke, C.F.R., Nachtrab, G., Chen, X., 2016. A thalamic input to the nucleus accumbens mediates opiate dependence. Nature 530, 219–22.

Zuo, W., Chen, L., Wang, L., Ye, J., 2013a. Neuropharmacology Cocaine facilitates glutamatergic transmission and activates lateral habenular neurons. Neuropharmacology 70, 180–189.